6. EXHALATIVE BASE METAL SULPHIDES

Introduction

Stratiform exhalative sulphide deposits are generally concordant, massive to semi-massive accumulations of sulphide (primarily iron sulphide) – sulphate minerals (barite, anhydrite) that formed on or immediately below the seafloor penecontemporaneously with their host rocks. They range in age from those that are actively forming within modern oceanic spreading ridges and back-arc basins, to those preserved in ca. 2.0 Ga sedimentary basins, and in ca. 3.4 Ga oceanic crust. Canada is particularly well endowed with classical examples of all subtypes, as well as with deposits that may be regarded as hybrid or of mixed character between the different subtypes. Four subtypes are identified:

Subtype 6.1, Sedimentary exhalative sulphides (Sedex) occur in terranes dominated by sedimentary strata. Volcanic rocks (lava, tuff) may be a minor component of the associated strata, and penecontemporaneous intrusions (mafic sills, dykes) may be present regionally. Zinc, lead, and silver are the primary metals recovered from the subtype; copper is generally a minor product. Barite may be abundant (deposits of mainly Phanerozoic age) or minor (deposits of mainly Proterozoic age); many deposits have none at all. Iron sulphide (pyrite, pyrrhotite) content is also highly variable.

Subtype 6.2, Sedimentary nickel sulphides occur in basinal sedimentary terranes similar to those that host Sedex deposits, and in fact have much in common with them in terms of physical characteristics and genesis. However the primary metals available from this subtype are nickel, zinc, molybdenum, and platinum group elements (PGEs).

Subtype 6.3, Volcanic-associated massive sulphide base metals. All volcanic-associated deposits occur in terranes dominated by volcanic rocks. The deposits may occur in volcanic or sedimentary strata that are integral parts of a volcanic complex. Volcanic-associated massive sulphide deposits may be divided into two compositional groups: base metal enriched (subtype 6.3) and auriferous (subtype 6.4). Deposits of the first group contain highly variable amounts of economically-recoverable copper, lead, zinc, silver, and gold. Minor elements such as tin, cadmium, bismuth, and selenium may also be important smelter byproducts; however base metals are the *primary* commodities recovered. Some deposits are dominated by iron sulphide (up to 90% pyrite) and have been mined primarily for iron and sulphur.

Subtype 6.4, Volcanic-associated massive sulphide gold. In deposits of this group, gold is the *primary* commodity, with copper, zinc, silver, and lead being of lesser economic importance. Mineralization may be massive, disseminated, or in stockworks.

Contents

6.1. SEDIMENTARY EXHALATIVE SULPHIDES (SEDEX)

John W. Lydon

INTRODUCTION

The term "Sedex" is an acronym for "sedimentary exhalative" that was proposed by Carne and Cathro (1982) as a short and convenient name for a class of deposits that was referred to by a variety of terms, including "sediment-hosted stratiform Zn-Pb", "shale-hosted", and "sedimentary-exhalative" deposits. The deposit class includes important producers of zinc and lead ores, such as Broken Hill and Mount Isa in Australia, Sullivan in Canada, Red Dog in Alaska, and Navan in Ireland.

A working definition of the deposit class is *a sulphide deposit formed in a sedimentary basin by the submarine venting of hydrothermal fluids and whose principal ore minerals are sphalerite and galena*. This definition is deliberately loose because more explicit definitions tend to exclude examples that should be included in the class. However, the definition serves to distinguish Sedex deposits from other seafloor metalliferous deposits related to hydrothermal venting, of which volcanogenic massive sulphides (VMS), Besshi-type, iron-formations, manganese formations, and bedded baritite deposits are the most important examples (see "Definitive characteristics", below).

This definition requires a knowledge of the processes by which a deposit has been formed. In highly metamorphosed or intensely deformed terranes, primary textural evidence for genetic processes may not be preserved. Under these conditions, it may be difficult to distinguish Mississippi Valley-type (MVT) deposits from Sedex-type deposits, because both have similar hydrothermal mineralogy and bulk composition (Sangster, 1990), and a MVT deposit that has been structurally transposed into geometric conformity with its host rocks may assume an overall morphology comparable to a Sedex deposit. Even for well preserved deposits, the distinction between the two types may be unclear. Considering that the subsurface deposition of sulphides (with its resultant epigenetic textures) is an important component of the ore-forming process of most Sedex deposits, those hosted in carbonate rocks may only be distinguished from MVT deposits by evidence that the ores were emplaced below a submarine hydrothermal vent field. Similarly, there is a continuum between Sedex deposits and VMS deposits in both depositional environment and deposit characteristics, and again it is more a matter of prejudice than of verifiable fact, that certain deposits are classified as one type instead of the other.

Lydon, J.W.
1996: Sedimentary exhalative sulphides (Sedex); in Geology of Canadian Mineral Deposit Types, (ed.) O.R. Eckstrand, W.D. Sinclair, and R.I. Thorpe; Geological Survey of Canada, Geology of Canada, no. 8, p. 130-152 (also Geological Society of America, The Geology of North America, v. P-1).

IMPORTANCE

Sedex deposits are a major source of zinc and lead, and an important source of silver. A compilation by Tikkannen (1986) indicates that, on the global scale, Sedex deposits accounted for about 40% of zinc production and about 60% of lead production. For known resources that are not being mined, the proportions are considerably greater, though no accurate statistics are available. In Canada, most production of zinc and lead from Sedex-type deposits has been obtained from the Sullivan mine, British Columbia, and the Faro and Vangorda deposits of the Anvil district in Yukon Territory (Fig. 6.1-1). Over the last decade, this has accounted for about 15% and 20% of primary Canadian zinc and lead production respectively (Fig. 6.1-2).

Despite their importance in terms of proportion of metal production and reserves, Sedex deposits are a comparatively rare type of deposit. A compilation of known Sedex deposits (Table 6.1-1) contains only about 70 examples, of which only 24 have been, or are being mined. The list is not exhaustive, especially for deposits in Asia, South America, and Eastern Europe, for which the literature is not sufficiently informative for accurate compilation. However, even if the list contained twice the number, it would not change the basic facts that: i) Sedex deposits are comparatively rare; ii) the majority of Sedex deposits are uneconomic because the ores are of too low a grade or because they are too fine grained for high beneficiation recoveries; and iii) a minority of Sedex deposits constitutes the greatest individual concentrations of zinc and lead ores known.

The positive aspect of this third fact outweighs the negative considerations of the other two, and makes Sedex deposits the most attractive targets for zinc and lead exploration.

SIZE AND GRADE OF DEPOSITS

The average size and grade of 62 deposits classified here as of the Sedex type (exclusive of Howards Pass deposits) is 41.3 Mt grading 6.8% Zn, 3.5% Pb, and 50 g/t Ag. The size of Sedex deposits range up to 120 Mt, with a few, the giant Sedex deposits, containing reserves in excess of this figure (Fig. 6.1-3C). Grades of zinc and lead range up to 18% and 9% respectively (Fig. 6.1-3A, B). Exclusive of the giant Sedex deposits, the amount of contained metal ranges up to 20 Mt of combined zinc and lead (Fig. 6.1-3F) and up to 10 million kilograms silver (Fig. 6.1-3E).

The Zn:Pb ratios of Sedex deposits, expressed as (Zn x 100)/(Zn+Pb), range from 15 to 100 (Fig. 6.1-3F), a seemingly nonsystematic spread. However, there seems to be some geological significance to the ratios.

Contents

i) The (Zn x 100)/(Zn+Pb) ratio of aqueous chloride solutions saturated with respect to sphalerite and galena varies from 75 to 85, depending on temperature and chlorinity. This would be the ratio expected of a Sedex deposit if the upflowing ore fluids (see "Genetic models", below) were saturated with metals and all the metal were precipitated and preserved in the deposit. About 30% of Sedex deposits are in this range of ratios.

ii) Sedex deposits are typically zoned, with the bulk of the galena being concentrated in the highest grade ores close to the upflow zone. Most of the deposits plotting between 40 and 70 are those for which mining, and not geological reserves, are reported. Thus, to varying degrees, the grades of the ore reserves do not include the zinc-dominant lower grade outer margins of the geological sulphide body. For example, drill indicated 1975 reserves for the Tom deposit were calculated at 15.7 Mt at 7.0% Zn and 4.61% Pb (Zn x 100)/(Zn+Pb)=60 but these figures do not include the known 600 m northward low grade extension to the West zone. Using a cut-off of Zn+Pb=7% for the "geological reserves", mining reserves are reported as 9.2 Mt at 7.49% Zn and 6.19% Pb (Zn x 100)/(Zn+Pb)=55 (McClay and Bidwell, 1986).

iii) Those deposits with (Zn x 100)/(Zn+Pb) values of less than 40 include those that have been subjected to oxidative weathering during their history. The oxidative weathering of a sphalerite-galena body may lead to the preferential removal of zinc; sphalerite is solubilized as the sulphate but galena develops a protective rind of insoluble cerussite. The effect can be seen by comparing the compositions of the sulphide protore and secondary

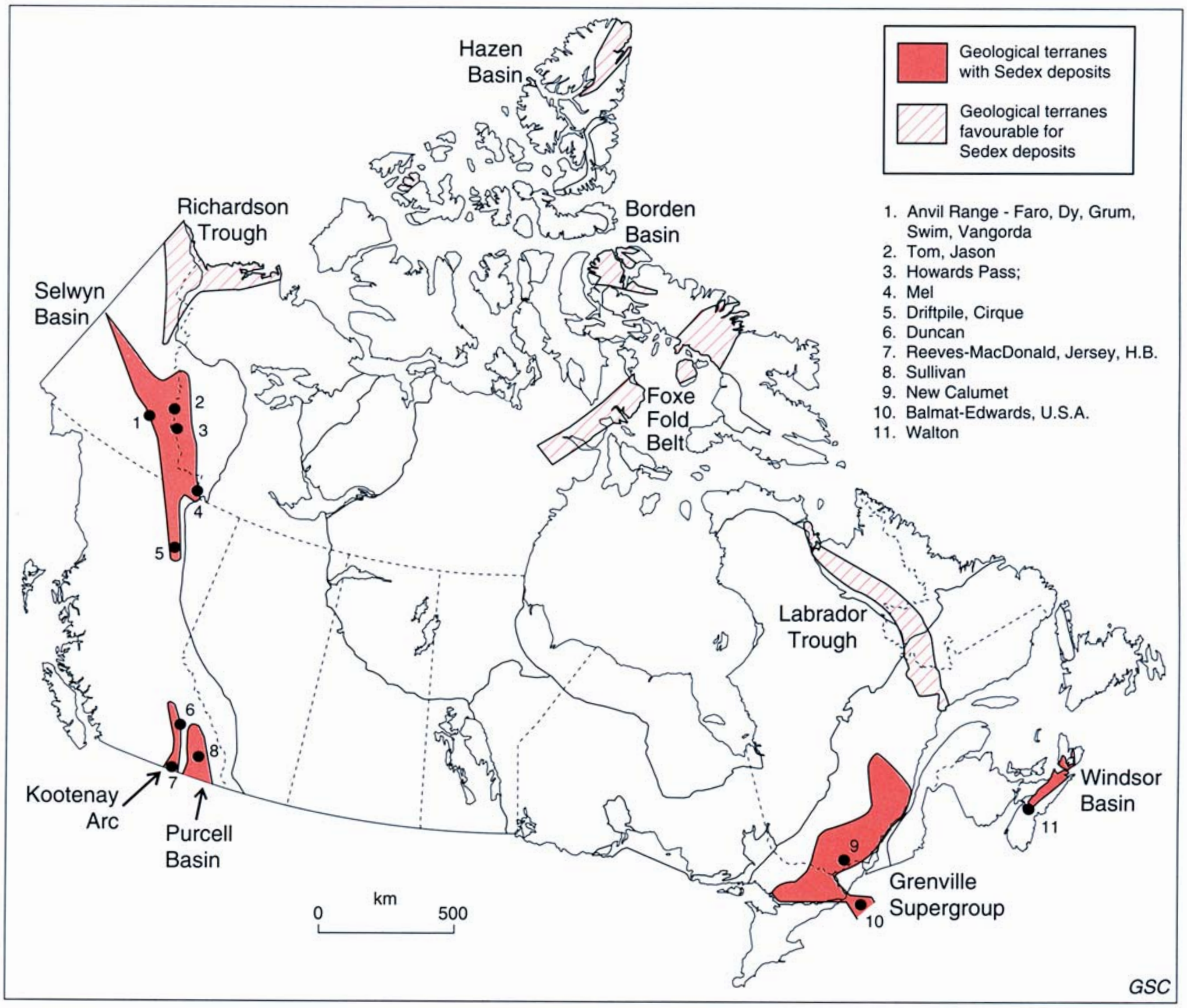

Figure 6.1-1. Distribution of Sedex deposits and geological terranes with potential for the occurrence of Sedex deposits in Canada.

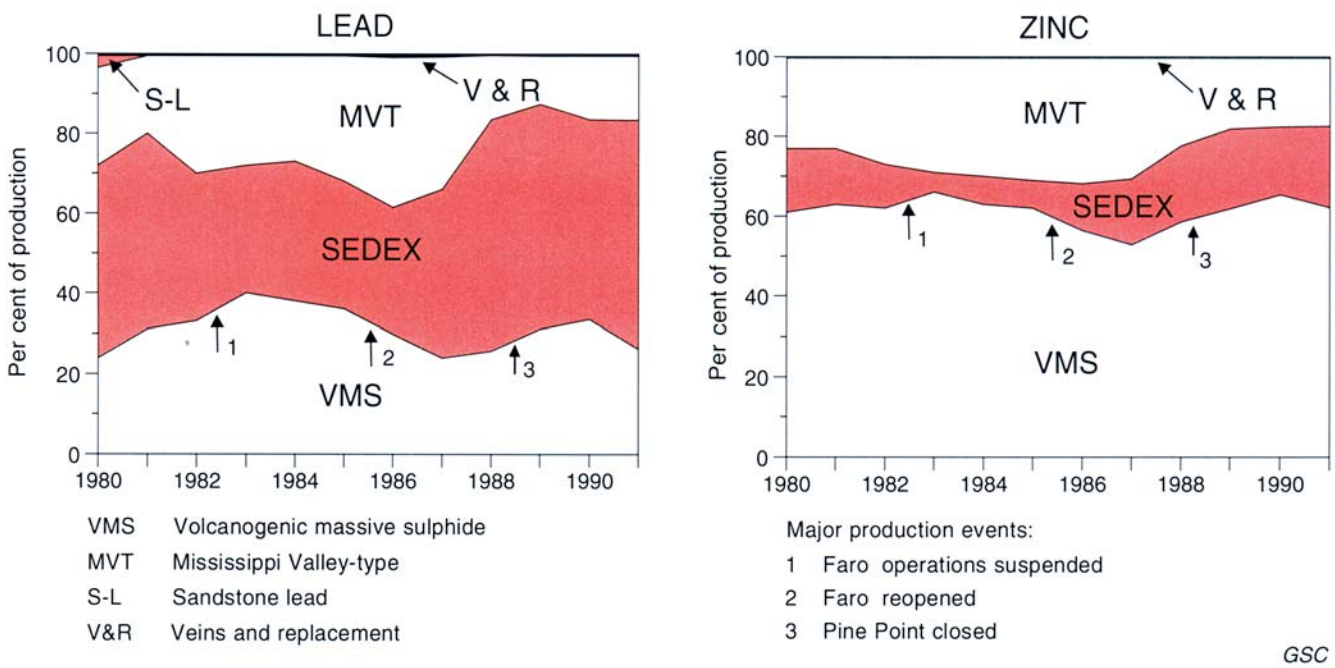

Figure 6.1-2. Canadian mine production of zinc and lead by deposit type for the period 1980-1991.

ore at Dariba (Table 6.1-1). The Tynagh ores also largely consist of the insoluble residue of subaerial weathering. It is interesting to note that the Broken Hill and Big Syn deposits of the Aggeneys area, other lead-dominant examples, are associated with magnetite iron-formation and baritite, both products of an oxidative environment, and it may well be that these deposits represent the remains of sulphide deposits that were partially oxidized while on the seafloor.

GEOLOGICAL FEATURES

Morphology and architecture of deposits

The idealized characteristics of a Sedex deposit are schematically illustrated in Figure 6.1-4. Sedex deposits usually comprise a conformable to semiconformable stratiform lens or lenses of sulphide and associated hydrothermal products (Fig. 6.1-4). The stratiform lens typically has an aspect ratio (the ratio of maximum lateral extent to maximum thickness) of 20, and maximum thicknesses are most commonly in the range 5 to 20 m.

Typically the stratiform lens can be divided into three distinct facies: i) vent complex; ii) bedded ores; and iii) distal hydrothermal products. In some deposits, discordant vein and replacement mineralization stratigraphically below the vent complex is significant enough to warrant a fourth facies type being distinguished: iv) feeder zone.

Vent complex

The vent complex part of the deposit lies within the upflow zone of the hydrothermal fluids, and consists of hydrothermal products that formed immediately below and within the submarine vent field. Ore textures (see Fig. 6.1-5A, D, G) typically reflect recurrent cycles of hydrofracturing, hydrothermal cementation, and replacement. The vent complex usually contains the highest grade mineralization, and for some deposits is the only part that is of ore grade.

Bedded ores

The bedded ores facies is a compositionally layered apron of hydrothermal products, which may or may not be interlayered with host rock lithologies, that is usually asymmetrically distributed around the vent complex. Examples are illustrated in Figure 6.1-5B, C, F. The thickness of individual compositional layers of hydrothermal products ranges from the scale of millimetres to the scale of metres. Individual layers are commonly very persistent laterally, and they decrease in thickness only very gradually away from the vent complex. The layers of hydrothermal products in most deposits are internally laminated. Their appearance, which is varve-like, has led to their interpretation as products of brine pool sedimentation or fallout from a hydrothermal plume that has accumulated in a low energy environment. In some deposits, the bedded ores contain fragmental, graded, or massive layers of hydrothermal products that have been interpreted to be debris flows, turbidites, and mudflows, respectively, and whose source area was a topographically elevated vent complex. Other schools of thought interpret sedimentary textures of the bedded ores to represent pseudomorphs of precursor lithologies formed by selective replacement of the host sediments by hydrothermal metasomatism just below the seafloor. In most deposits, the sphalerite and galena contents of the bedded ores gradually decrease with increasing distance from the vent complex.

Contents

Table 6.1-1. List of Sedex deposits for which there are sufficient published data for their classification.

Deposit	Location	Zn %	Pb %	Cu %	Ag (g/t)	Au (g/t)	$BaSO_4$	Size (Mt)	Age (Ma)	References
Santa Lucia	Cuba	5.7	1.8	0.0	30.0	0.0	Yes	19.4	150	Valdes-Nodarse et al., 1993; Mining Journal, Sept. 3, 1993
Gunga	Pakistan	5.0	1.0	0.0	0.0	0.0	Yes	10.0	150	Anderson and Lydon, 1990
Duddar	Pakistan	16.4	3.9	0.0	0.0	0.0	Yes	1.0	150	Anderson and Lydon, 1990
Filizchai	Azerbaijan	7.0	1.0	2.1	0.0	0.0	?	5.0	175	Laznicka, 1981
Lik	Alaska	8.8	3.0	0.0	28.0	0.0	Yes	25.0	340	Forrest and Sawkins, 1984
Galmoy	Ireland	10.9	1.0	0.0	0.0	0.0	?	6.7	340	Mining Journal, Sept. 1990, p. 231
Lisheen	Ireland	12.0	1.5	0.0	32.0	0.0	?	20.0	340	Shearley et al., 1992
Navan	Ireland	10.1	2.6	0.0	0.0	0.0	No	69.9	340	Andrew and Ashton, 1985
Silvermines	Ireland	6.4	2.5	0.0	23.0	0.0	Yes	17.7	340	Hitzman and Large, 1986
Tynagh	Ireland	4.5	4.8	0.4	46.5	0.0	Yes	13.6	340	Morrissey et al., 1971
Walton	Canada	1.4	4.3	0.6	305.0	0.0	Yes	0.7	340	Patterson, 1988
Red Dog	U.S.A.	17.1	5.0	0.0	82.3	0.0	Yes	77.0	350	Moore et al., 1986
Tom	Canada	7.0	4.6	0.0	49.1	0.0	Yes	15.7	350	McClay and Bidwell, 1986; Goodfellow and Rhodes, 1990
Elura	Australia	8.4	5.6	0.0	139.0	0.0	Yes	27.0	370	Schmidt, 1990
Cirque	Canada	8.0	2.0	0.0	0.0	0.0	Yes	52.2	370	Jefferson et al., 1983; Canadian Mines Handbook 1991-2, p. 127
Driftpile	Canada	11.9	3.1	0.0	0.0	0.0	Yes	2.4	370	MacIntyre, 1983; Teck Corporation, 1994 (circular)
Jason	Canada	7.4	6.5	0.0	79.9	0.0	Yes	10.1	370	Turner, 1990; Northern Miner, May 28, 1990, p. 21
Meggen	Germany	7.0	1.0	0.1	14.0	0.0	Yes	50.0	370	Krebs, 1981
Rammelsberg	Germany	16.4	7.8	1.0	103.0	0.0	Yes	27.2	370	Hannak, 1981; Krebs, 1981
Zhairem	Khazakhstan	5.0	2.0	0.5	0.0	0.0	Yes	N/A	370	Smirnov and Gorzhersky, 1977; Laznicka, 1981
Tekeli	Khazakhstan	6.0	5.0	1.0	0.0	0.0	Yes	6.0	380	Smirnov and Gorzhersky, 1977; Laznicka, 1981
Howards Pass	Canada	5.0	2.0	0.0	9.0	0.0	No	476.0	435	Goodfellow and Jonasson, 1986; Placer Dev., Annual Report 1982
Peary Land	Greenland	8.0	1.0	0.0	?	?		12.0	435	Northern Miner, Oct. 10, 1994, p. 3
El Aguilar	Argentina	8.5	6.5	0.1	100.0	0.0	No	30.0	450	Sureda and Martin, 1990; Gemmell et al., 1992
Bleikvassli	Norway	7.5	3.0	0.4	0.0	0.0	No	6.0	460	Skauli et al., 1992
Mofjellet	Norway	4.7	1.0	0.4	0.0	0.0	No	4.2	460	Laznicka, 1981
Dy	Canada	6.7	5.5	0.1	84.0	1.0	Yes	21.1	510	Jennings and Jilson, 1986
Faro	Canada	5.7	3.4	0.0	36.0	0.0	Yes	57.6	510	Jennings and Jilson, 1986
Grum	Canada	4.9	3.1	0.0	49.0	0.0	Yes	31.0	510	Jennings and Jilson, 1986
Swim	Canada	4.7	3.8	0.0	42.0	0.0	Yes	4.3	510	Jennings and Jilson, 1986
Vangorda	Canada	4.9	3.8	0.3	54.0	0.8	Yes	7.5	510	Jennings and Jilson, 1986; Canadian Mines Handbook 1988-89, p. 135
Koushk	Iran	15.0	3.0	0.0	0.0	0.0	?	5.0	510	Mining Journal, June 14, 1991, p. 454
Portel	Portugal	1.4	0.2	0.0	0.0	0.0	Yes	35.0	510	J.W. Lydon, unpub. data, 1968
Fuenteheridos	Spain	2.0	0.2	0.0	0.0	0.0	Yes	100.0	510	J.W. Lydon, unpub. data, 1968
Duncan	Canada	3.1	3.3	0.0	0.0	0.0	?	2.8	550	Höy, 1982
H.B.	Canada	4.1	0.8	0.0	4.8	0.0	?	6.5	550	Höy, 1982
Jersey	Canada	3.5	1.7	0.0	3.1	0.0	?	7.7	550	Höy, 1982
Mel	Canada	5.6	2.1	0.0	0.0	0.0	Yes	4.8	550	Miller and Wright, 1983
Reeves-MacDonald	Canada	3.5	1.0	0.0	3.4	0.0	?	5.8	550	Höy, 1982
Aberfeldy	Scotland	1.2	0.4	0.0	0.0	0.0	Yes	N/A	600	Coates et al., 1980; Willan and Coleman, 1983
Kholodnina	Russia	7.0	1.5	0.0	0.0	0.0	?	N/A	1075	Smirnov and Gorzhersky, 1977; Laznicka, 1981
Rosh Pinah	Namibia	7.0	2.0	0.1	0.0	0.0	Yes	17.4	1100	Page and Watson, 1976; VanVuuren, 1986
Jiashengpan	China	3.8	1.3	0.0	0.0	0.0	No	N/A	1300	Lang and Xingjun, 1987
Balmat-Edwards	U.S.A.	10.1	0.3	0.0	0.0	0.0	No	17.4	1300	Lea and Dill, 1968
New Calumet	Canada	8.8	2.8	0.2	0.0	0.1	No	1.3	1300	McLarsn, 1946
Sullivan	Canada	5.5	5.8	0.0	59.0	0.0	No	170.0	>1468	Hamilton et al., 1982; H.E. Anderson, D. Davis, and R.R. Parrish,
Sargipali	India	0.4	2.0	0.0	65.0	0.0	?	N/A	1600	Sarkar, 1974
Big Syn	South Africa	2.5	1.0	0.1	12.9	0.0	Yes	101.0	1650	Ryan et al., 1986; Reid et al., 1987
Black Mtn.	South Africa	0.6	2.7	0.8	29.8	0.0	Yes	81.6	1650	Reid et al., 1987; Ryan et al., 1986
Broken Hill	South Africa	1.8	3.6	0.3	48.1	0.0	Yes	85.0	1650	Reid et al., 1987; Ryan et al., 1986
Gamsberg	South Africa	7.1	0.5	0.0	6.0	0.0	Yes	150.0	1650	Reid et al., 1987; Ryan et al., 1986
Century	Australia	10.0	1.5	0.0	30.0	0.0	?	120.0	1670	Mining Magazine, Oct. 1991, p. 233-237
Hilton	Australia	10.2	6.5	0.0	137.9	0.0	No	72.0	1670	Forrestal, 1990
Lady Loretta	Australia	14.0	8.0	0.0	110.0	0.0	Yes	9.0	1670	Australian Mining Yearbook, 1988, p. 20; Louden et al., 1975
Mt. Isa	Australia	6.0	7.0	0.1	160.0	0.0	No	125.0	1670	Mathias and Clark, 1975; Forrestal, 1990
Dugald River	Australia	15.0	2.0	0.0	62.0	0.0	No	12.0	1670	Whitcher, 1975; Mining Journal, May 4 1990, p. 352
H.Y.C.	Australia	9.5	4.1	0.0	40.0	0.0	No	227.0	1690	Lambert, 1976; Logan et al., 1990
Broken Hill	Australia	12.0	13.0	0.2	175.0	0.0	No	300.0	1690	Both and Rutland, 1976; Wright et al., 1987
Balaria(Zawar)	India	5.6	1.1	0.0	0.0	0.0	No	19.0	1700	Deb et al., 1989
Baroi magra	India	1.2	4.3	0.0	0.0	0.0	No	11.0	1700	Deb et al., 1989
Mochia(Zawar)	India	3.8	1.7	0.0	0.0	0.0	No	27.0	1700	Deb et al., 1989
Zarwarmala(Zawar)	India	3.7	2.1	0.0	0.0	0.0	No	18.0	1700	Deb et al., 1989
Dariba	India	7.3	2.0	1.0	5.0	0.0	No	13.0	1800	Nandan et al., 1981; Deb and Bhattacharya, 1980
Dariba(secondary)	India	1.2	4.0	0.3	200.0	0.0	No	31.6	1800	Nandan et al., 1981; Deb and Bhattacharya, 1980
Dariba-Rajpura	India	5.1	1.2	1.1	122.0	0.0	No	51.0	1800	Nandan et al., 1981; Deb and Bhattacharya, 1980
Rampura-Agucha	India	13.5	1.6	0.0	45.0	0.0	No	61.1	1800	Nandan et al., 1981; Deb and Bhattacharya, 1980
Saladipura	India	1.0	0.0	0.0	0.0	0.0	No	115.0	1800	Deb et al., 1989
Sindesar	India	2.1	0.5	0.0	0.0	0.0	No	70.0	1800	Deb, 1982; Deb et al., 1989

Distal hydrothermal products

The lateral lithological equivalents of the bedded ores, outside the economic limits of the Sedex orebody, are termed here "distal hydrothermal products", reflecting their greater distance from the vent complex than the bedded ores themselves. Although the boundary between the bedded ores and distal hydrothermal products is primarily an economic one, in some deposits it may also have geological significance, separating two distinct sedimentological or metasomatic facies.

Feeder zone

Though not documented for most deposits, the vent complex is rooted in a feeder zone of discordant vein and/or replacement-type mineralization. The fracture systems of the feeder zone may either be due to tectonism, and related to movement on synsedimentary faults with which many Sedex deposits are spatially associated, and/or may be due to hydrofracturing accompanying hydrothermal eruption. In contrast to VMS deposits, the feeder zone of Sedex deposits rarely contributes any significant ore reserves. There are two main reasons for this.

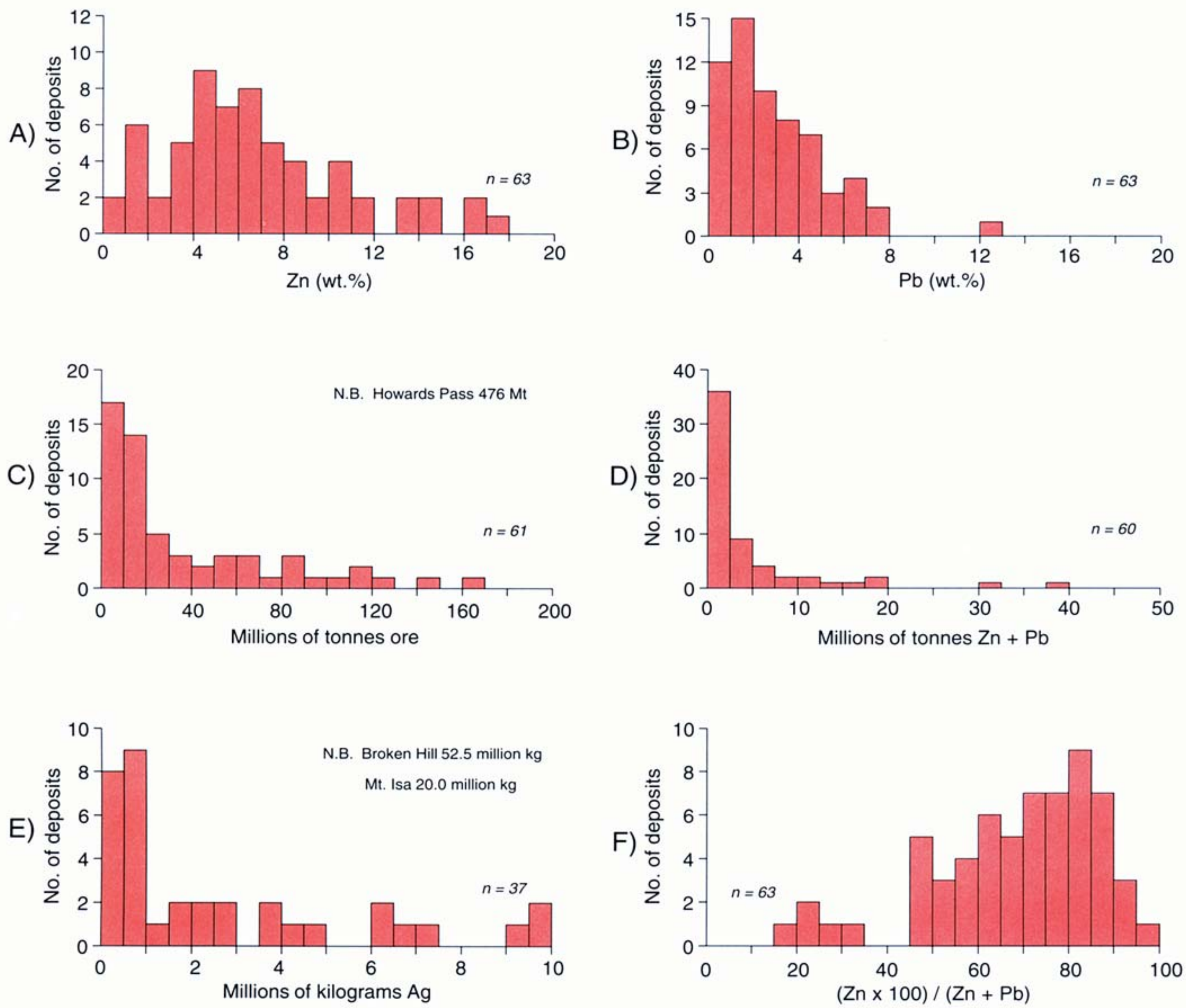

Figure 6.1-3. Grade and tonnage statistics for Sedex deposits listed in Table 6.1- 1. Note that for deposits that have not been mined, the figures reported are usually geological reserves; for deposits that have been or are being mined, the figures are mining reserves plus production. **A)** Grade of zinc in ore; **B)** grade of lead in ore; **C)** tonnage of ore (production plus reserves); **D)** tonnes of contained zinc plus lead per deposit; **E)** kilograms of contained silver per deposit (note that silver grades are not reported for a majority of deposits); **F)** Average Zn:Pb ratio of deposit expressed as (Zn x 100)/(Zn + Pb).

GSC

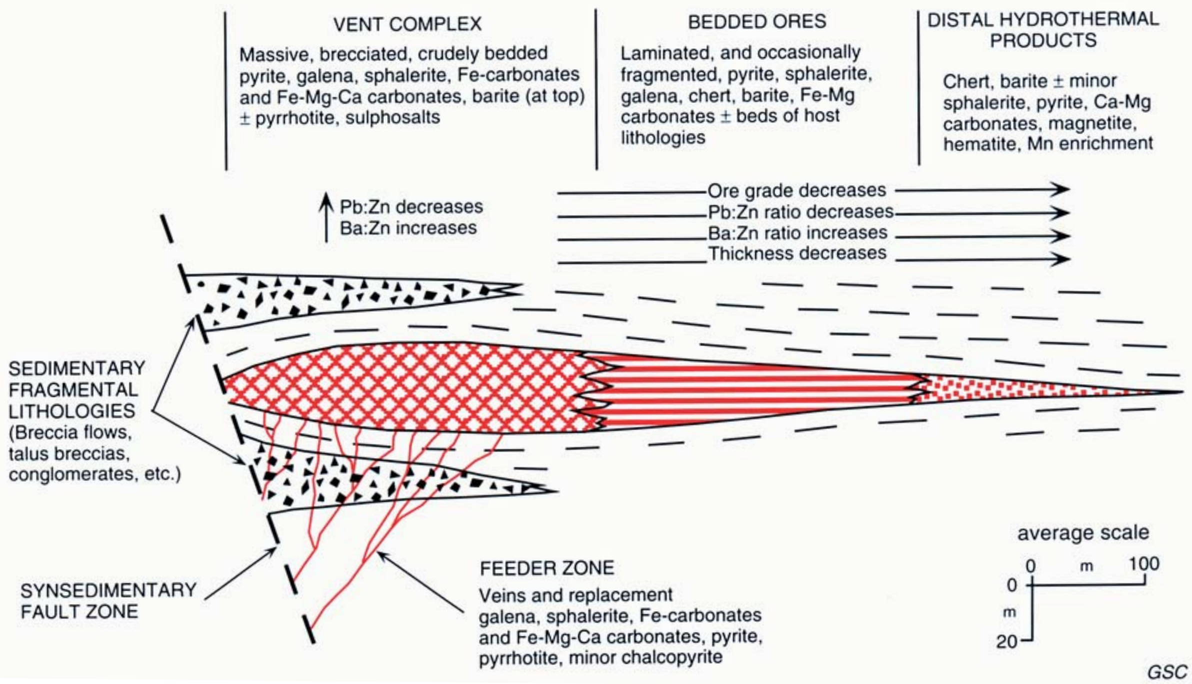

Figure 6.1-4. Schematic illustration of the characteristic features of the idealized Sedex deposit.

1. The formation of high grade vein networks and mineralized breccias of feeder zone ores requires a rock with sufficient mechanical strength to brecciate and form rigid clasts that can support a high fracture porosity. In contrast to volcanic rocks, which attain a high mechanical strength immediately upon cooling on the seafloor, unconsolidated sediments have such low mechanical strength that they tend to flow rather than brecciate when subjected to differential pore fluid pressures. Fault breccias, hydrothermal vent breccias, and hydrothermal eruption breccias may readily form in a substrate of volcanic rocks to provide the host for typical feeder zone mineralization. In unconsolidated sediments, however, the equivalent expressions of tectonic movement or hydrothermal eruption are zones of disrupted sediment, discordant columns of turbated sediment and concordant mud flows, none of which have a significantly higher porosity than surrounding undisturbed sediments, and hence do not provide a host for preferential subsurface hydrothermal precipitation.
2. The main economic mineral in feeder zone ores of VMS deposits is chalcopyrite which, because of its higher economic value compared to sphalerite and galena, lowers the concentration of ore minerals required to achieve ore grade. The average relative proportion of copper in Sedex deposits (Table 6.1-1) is very much less than in VMS deposits, so that even though in Sedex deposits chalcopyrite tends to be concentrated in feeder zone mineralization, it rarely attains absolute concentrations of economic significance.

Mineralogy

Primary hydrothermal minerals

Typical hydrothermal products of Sedex deposits include sulphides, carbonates, quartz, and barite. Pyrite is usually the most abundant sulphide, and commonly is the only iron sulphide in the deposit. However, in some Proterozoic deposits, such as Mt. Isa (Mathias and Clark, 1975), pyrrhotite is common, and in the Sullivan deposit is more abundant than pyrite (Hamilton et al., 1982). At the Duddar deposit, Pakistan, which is one of the youngest fossil Sedex deposit known, marcasite is the dominant primary iron sulphide.

Sphalerite and galena are invariably the main economic minerals. Chalcopyrite is usually a very minor constituent, although it was abundant enough in the Rammelsberg deposit to be economically recoverable (Hannak, 1981). Antimony, arsenic, and bismuth, particularly in the sulphosalts tetrahedrite, freibergite, and boulangerite, are typically concentrated in and around the vent complex, and in cases are the host minerals for much of the silver content of the ores.

Carbonates are much more important constituents of Sedex deposits than VMS deposits. Siderite and ankerite may occur as veins in the feeder zone, as replacive masses in the vent complex and as beds or laminations in the bedded ores, as, for example, in the Tom deposit, Yukon Territory (Goodfellow and Rhodes, 1990), and at Silvermines, Ireland (Taylor, 1984; Andrew, 1986). Calcite is relatively common as veins, interstitial cement, and laminations in

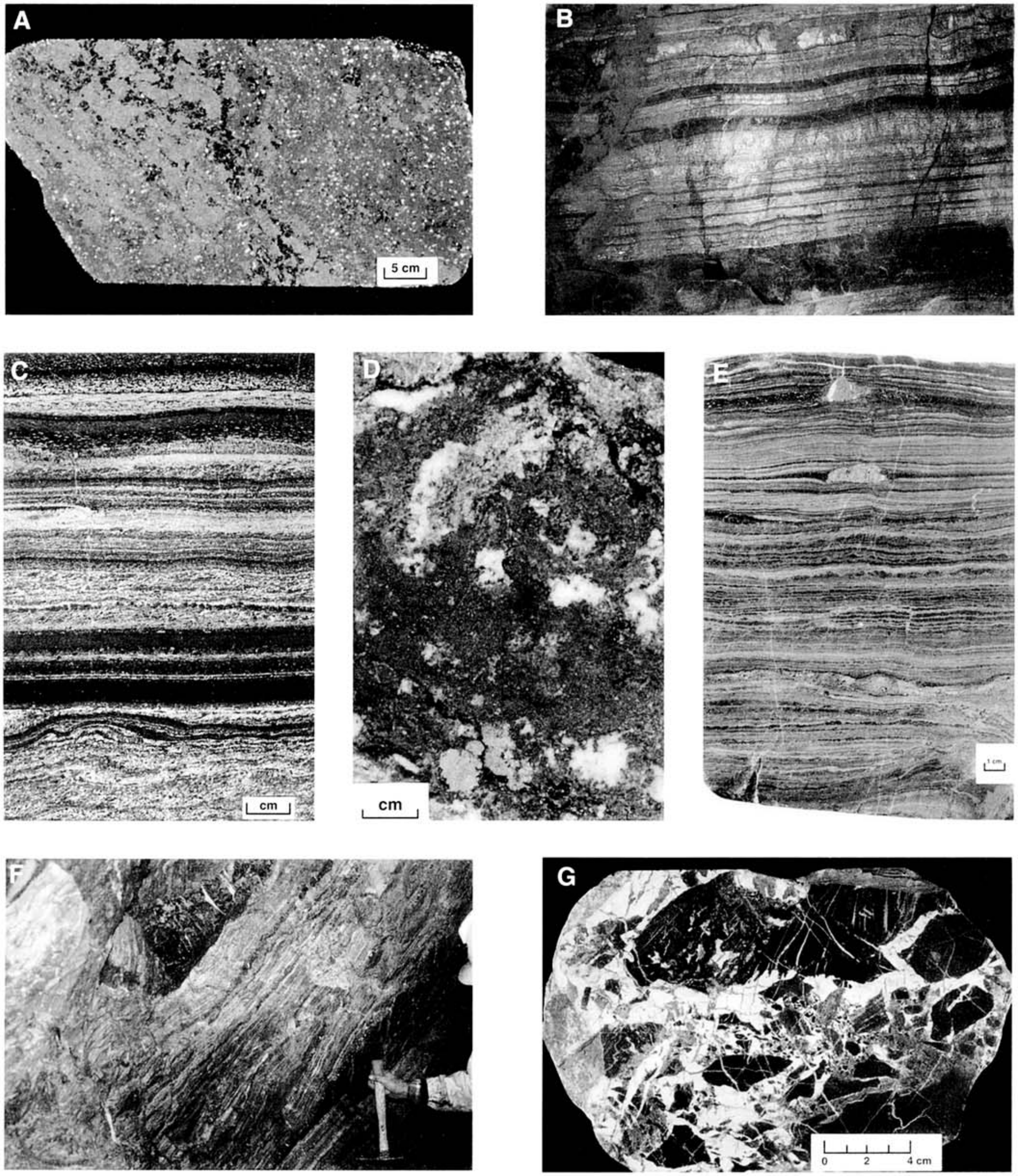
A
5 cm
B
C
cm
D
cm
E
F
G
0
2
4 cm

both the vent complex and bedded ores of the Sullivan deposit (Hamilton et al., 1982). Abundant bedded calcium carbonate is restricted to the ore zone of the XY deposit at Howards Pass (Goodfellow and Jonasson, 1986). Calcite nodules are a common hydrothermally induced feature of unconsolidated sediment surrounding the modern metalliferous hydrothermal vents of Middle Valley (Goodfellow et al., 1994). Dolomite, either as a precipitate or hydrothermal alteration product, is common around Sedex deposits in carbonate rocks (e.g., Tynagh and Silvermines, Ireland: Hitzman and Large, 1986; Fuenteheridos, Spain). Secondary dolomite is co-extensive with the stratiform sulphide mineralization of the McArthur River deposits, Australia (Williams, 1978a), but there is debate whether the widespread silica dolomite alteration at Mt. Isa is genetically related to the Zn-Pb mineralization. Quartz, as chert, is abundant in many Sedex deposits (e.g. Tom, Silvermines), but is conspicuously absent in others (e.g. Sullivan). Where it is present, the proportion of quartz, relative to other hydrothermal products, increases with increasing distance from the vent complex. Barite, notably as bedded baritite in the bedded ores and distal hydrothermal facies, is a common constituent of most Paleozoic and younger Sedex deposits, but is much less common in Proterozoic deposits. Notable exceptions are the Howards Pass and Navan deposits of Paleozoic age which do not contain significant barite, and the Proterozoic deposits of the Aggeneys area, South Africa, which do. Tourmaline is spatially associated with several Sedex deposits, including Sullivan, where it is the major component in the footwall feeder zone (Hamilton et al., 1982), Broken Hill, Australia (Slack et al., 1993), and the Rampura-Agucha deposits, India (Ranawat and Sharma, 1990). Because tourmaline is not readily recognizable, especially in a fine grained form, it may be more common in Sedex deposits than has been recognized.

Figure 6.1-5. Photographs of some macroscopic textures and relationships in Sedex deposits
A) Vent complex ore, Sullivan deposit. Polished drill core (dark grey with white flecks – galena; light grey – pyrrhotite; black – silicates). GSC 1994-640C
B) Bedded ore, Sullivan deposit. Interlayered sulphides (light grey) and argillite (dark grey), "A" ore band. Height of photograph about 2 m. GSC 1994-640H
C) Bedded ore, Sullivan deposit. Interlaminated light grey sulphides (pyrrhotite, sphalerite, galena) and dark grey to black argillite, "B-Triplet" ore band. Light grey flecks in argillite are pyrrhotite laths. Note both tectonic low strain (well laminated) and high strain (turbated) sulphide layers; polished slab. GSC 1994-640F
D) Vent complex mineralization, Tom deposit. Polished slab; dark grey – pyrite; medium grey – ankerite; white – calcite. GSC 1994-640A
E) Bedded ore, Tom deposit. Polished slab; dark grey - chert; medium grey – sphalerite and siderite; light grey – barite. GSC 1994-640I
F) Bedded ore, Tom deposit. Height of photo about 1 m. Laminated barite and sphalerite (light grey) interlayered with siliceous argillite (black). GSC 1994-640D
G) Vent complex mineralization, Tom deposit. Polished slab, black – brecciated siliceous argillite; medium grey – pyrite; white – ankerite. GSC 1994-640G

Metamorphic minerals

The effect of high temperature and pressure metamorphism on mineral assemblages typical of Sedex deposits does not generally obscure recognition of the original mineralogy of the deposit, even though some significant mineralogical changes may be produced. Pyrite may be converted to pyrrhotite by reaction with ferrous silicate minerals or by the degassing of sulphur from the sulphide body during metamorphism. At least some of the pyrrhotite at Broken Hill, Australia, in the Aggeneys district, South Africa, and in the Rampura-Agucha (Ranawat and Sharma, 1990) and Rajpura-Dariba (Deb, 1990) deposits of India, is probably of metamorphic origin. During metamorphic retrogression, pyrrhotite may react to form pyrite and magnetite, although the quantities of pyrite and magnetite so formed would be minor unless a source of oxygen were available. At least some of the pyrite-magnetite assemblage at the Sullivan deposit appears to have formed by this mechanism.

Sphalerite may react with aluminosilicates to form gahnite ($ZnAl_2O_4$) at amphibolite facies and higher metamorphic grades. It is a common though minor mineral at Broken Hill, Australia (Mackenzie and Davies, 1990; van de Hayden and Edgecombe, 1990) and in the deposits of the Aggeneys area, South Africa (Spry, 1987).

Barite may react with aluminosilicates at greenschist facies to form cymrite, celsian, or hyalophane. At the Aberfeldy deposit, Scotland, a cherty layer of rock several metres thick, and composed largely of celsian, forms an envelope around the distal parts of the deposit (Coates et al., 1980).

Zonation

Sedex deposits exhibit compositional zonation in both lateral and vertical directions.

Lateral zonation

Characteristic of most Sedex deposits is a lateral mineralogical, chemical, and thickness zonation with respect to the vent complex. Fundamentally this zonation can be attributed to two main effects:

1. A decrease in the relative proportion of hydrothermal products with respect to intercalated or admixed indigenous sediment with increasing lateral distance from the vent complex. This effect can be ascribed to mechanisms of hydrothermal dispersal as a function of distance from the local hydrothermal upflow zone.
2. A zonation due to systematic changes in the relative proportion of different hydrothermal products with lateral distance from the vent complex. This effect can be ascribed to the different chemical behaviour of different components during dispersal from their local source in the hydrothermal upflow zone.

The first effect largely determines the morphology of the deposit, in the sense that the deposit is defined as that volume of rock containing hydrothermal products. The second effect largely determines the compositional architecture of the deposit, especially its mineralogical zonation. Grades of individual hydrothermal ore components are a function of both effects, because the concentration of any one hydrothermal component may be diluted both by indigenous sediment and by other hydrothermal products.

However, such a simple and consistent zonation pattern reflecting steady state dispersal and accumulation processes is rarely exhibited by most Sedex deposits. The theoretically simple zonation patterns that should result are usually disrupted by various unpredictable events, such as:

1. Dilution of hydrothermal products by locally derived terrigenous sediments. Sedimentary fragmental rocks are a common feature of most Sedex deposits and include talus breccias and debris flows from the wasting of synsedimentary fault scarps, hydrothermal eruption breccias, and mud volcano extrusions.
2. Mass transportation of hydrothermal products, particularly as slide sheets and debris flows, from topographically elevated portions of the deposit.
3. Mass removal of hydrothermal and terrigenous accumulations from the hydrothermal upflow zone by hydrothermal eruption.
4. Preferential chemical removal of previously accumulated hydrothermal components from the upflow zone during the zone refinement process. The removal of barite from the vent complex is perhaps the most outstanding example. Barite, which is formed by hydrothermal barium combining with water column sulphate, is easily solubilized by reduced hydrothermal fluids in the upflow zone and may be recycled to be reprecipitated in more oxidized parts of the deposit.

Notwithstanding these complications, which produce zonation patterns whose details are unique for each Sedex deposit, there are trends that are common to a high proportion of the class as a whole:

1. There is a zonation from reduced mineral facies (e.g., sulphides, ferroan carbonates) within the hydrothermal upflow zone to more oxidized facies (e.g., barite, iron oxides, calcic carbonates) at the periphery of the deposit. Chemically, this trend may be reflected, for example, in decreasing ratios of Zn:Ba and Zn:Mn.
2. Amongst the sulphides, there is a general zonation outwards from the core of the upflow zone in the sequence chalcopyrite, pyrrhotite, galena, sphalerite, and pyrite. The zonation from chalcopyrite via galena to sphalerite, as in VMS deposits, largely reflects a thermal gradient. Chalcopyrite rarely attains significant concentrations in most Sedex deposits because the temperature of the hydrothermal fluids (<300°C) is too low to transport copper in reduced sulphidic fluids. The Rammelsberg deposit (Hannak, 1981), which contains 1.0% Cu, is the notable exception. Primary pyrrhotite is common in only a few Sedex deposits, notably of Proterozoic age (e.g. Sullivan, Mt. Isa). If primary iron monosulphide was a common quenching product in Sedex deposits, as it is in modern black smoker buoyant plumes, then most of it has been sulphidized to pyrite. In terms of metal ratios the most consistent zonation is an increase in Zn:Pb ratios outwards from the vent complex. In deposits in which most of the iron is contained in pyrite, ratios of Fe:Pb and Fe:Zn also generally increase with increasing distance from the vent complex. The polarity of the normal upward and outward increase in Fe:Pb and Fe:Zn ratios is reversed in the core of the Sullivan deposit by the replacement of sphalerite and galena by pyrrhotite, upward and outward from the base of the vent complex.
3. Tin, bismuth, arsenic, and mercury tend to be concentrated in the vent complex in sulphosalt minerals and arsenopyrite. Silver, an important economic constituent in most Sedex deposits, is frequently hosted by sulphosalts as well as being held in solid solution in galena. Consequently, the highest grades of silver are typically in the vent complex. A significant proportion of the trace copper content of Sedex deposits may also be contained in sulphosalts (e.g., Tynagh, Tom).
4. Carbonates are probably an integral hydrothermal component of most Sedex deposits, but their importance may have been overlooked in many cases. It might be expected that carbonates are more abundant in Phanerozoic deposits than in Proterozoic deposits, because of the increased abundance of marine calcareous faunal remains in the younger terrigenous source rocks for the hydrothermal fluids. For example, the Tom deposits contains 15-20% CO_2 in the vent complex (Goodfellow and Rhodes, 1990), whereas the Sullivan deposits contains 0.2-1.0% CO_2 (Hamilton et al., 1982). The carbonates tend to be zoned from ferruginous, in the core of the upflow zone, to calcic at the periphery of the deposit, and occur both as subsurface infillings and replacements in the upflow zone, as well as layers in the stratified part of the deposit. For example, siderite, occurs as vein fillings and as an interstitial cement of discordant mineralization at Jason deposit (Bailes et al., 1986; Turner, 1990), and as a basal layer to the massive bedded sulphides in the Mogul B deposit, Silvermines, Ireland (Taylor, 1984; Andrew, 1986).
5. Sulphide grades, especially for Zn and Pb, generally systematically decrease towards the periphery of the deposit from maxima in the vent complex. Elemental ratios diagnostic of the gradual dilution of hydrothermal sulphide by indigenous sediment (e.g. Zn:Al_2O_3; S(sulphide):Al_2O_3) or by other hydrothermal products (e.g., Zn:Ba) gradually decrease towards the periphery of the deposit.
6. Manganese tends to be concentrated at the margins of the deposit in carbonates, iron oxides or, in the case of more highly metamorphosed deposits, in garnet. A manganese enrichment in carbonates surrounding the Meggen deposit may be detected several kilometres away from the deposit (Gwosdz and Krebs, 1977). At Tynagh, Ireland, manganese is concentrated in the hematite iron-formation which constitutes a distal hydrothermal products facies, but also forms a halo of manganese enrichment in the host carbonates for a distance of 7 km around the deposit (Russell, 1974, 1975). At Sullivan, manganese garnets are concentrated in the bedded ores, particularly at the margins of the deposit, and in the footwall conglomerate.
7. The thickness of the deposit generally decreases towards its periphery, though its maximum thickness may not be coincident with the central part of the vent complex.

8. Maximal Zn or Pb grade may or may not coincide with the thickest part of the deposit. This is particularly true where there has been dichotomy of processes that produced maximum thicknesses of hydrothermal products on the one hand (e.g., sedimentation, tectonic deformation) and maximum zinc and lead concentrations on the other (e.g., zone refinement). The Tom deposit (McClay and Bidwell, 1986; Goodfellow and Rhodes, 1990) and the Cirque (Stronsay) deposit (Jefferson et al., 1983; Pigage, 1986; MacIntyre, 1992) are examples in which the thickest part of the deposit occurs in the bedded ores, but the highest Zn and Pb grades occur in the vent complex. The Sullivan deposit is an example where both the highest grades and the thickest part of the deposit occur in the vent complex.

Vertical zonation

In most deposits, especially in the vent complex, the vertical zonation of mineral assemblages and chemistry mimics the lateral zonation. This upward and outward zonation is similar to that observed above the feeder zone in VMS deposits, and would seem to be most logically interpreted to be the result of a subsurface zone refinement process.

The sequence of vertical zonation within the bedded part of the deposit need not necessarily duplicate that observed in the vent complex portion, nor is there a consistency in zonal order of mineral facies from deposit to deposit. For example, baritite, which usually is most abundant towards the periphery of the deposit e.g., Silvermines deposit (Taylor, 1984; Andrew, 1986), Tom deposit (McClay and Bidwell, 1986), and Jason deposit (Bailes et al., 1986), may be concentrated near the stratigraphic top of the bedded part of the deposit, for example, Rammelsberg (Hannak, 1981) or at the stratigraphic base, for example, Duddar deposit. The variation of metal ratios as a function of stratigraphic position in the bedded portion of Sedex deposits has been examined by Lydon (1983). Lead:zinc ratio generally decreases stratigraphically upwards in some deposits (e.g., Tom, Sullivan), decreases downwards in others (Rammelsberg, Broken Hill) whereas in others there is no discernible trend (H.Y.C. and Howards Pass [according to Lydon, 1983]). Silver:lead ratios generally decrease stratigraphically upward in most deposits (e.g., Tom, Sullivan, Broken Hill), although a Ag enrichment in the stratigraphically highest ores is apparent in some deposits. Stratigraphically upward Zn:Fe ratios may increase overall (e.g., Sullivan), decrease overall (e.g., Rammelsberg), or not show any discernible trend (e.g., H.Y.C.).

Fluid inclusions

There are few published data on fluid inclusions from Sedex deposits. At the Tom (Gardner and Hutcheon, 1985) and nearby Jason (Ansdell et al., 1989) deposits of the Selwyn Basin, homogenization temperatures average about 260°C and salinities average about 9 wt.% NaCl equivalent (i.e. 2 to 3 times sea water salinity). At the Silvermines deposit, Ireland, homogenization temperatures range between 50°C and 260°C and salinities between 8 and 28 wt.% NaCl equivalent (Samson and Russell, 1987). A negative correlation between homogenization temperature and salinity in quartz was interpreted by Samson and Russell (1987) to indicate the mixing of higher temperature, lower salinity, hydrothermal fluids with either lower temperature high salinity brines of a seafloor brine pool or shallow pore fluids formed by contemporaneous evaporitic processes. At the Sullivan deposit, Leitch (1992) reported homogenization temperatures that range from 150°C to 320°C and salinities that range from 8 to 36 wt.% NaCl equivalent but no prima facie evidence to link the values to the ore fluids.

GEOLOGICAL SETTING

Sedex deposits occur in sedimentary basins that are controlled by tectonic subsidence associated with major intracratonic or epicratonic rift systems. Most commonly, Sedex deposits occur within rift-cover sequences as opposed to the rift-fill sequences (Fig. 6.1-6). That is, they occur in that sequence of sediments that covers the coarse clastic sediments, turbidites, and/or volcanic rocks which were deposited within the rift during its most active stages of extension and subsidence. The rift-cover sequence, which commonly consists of shallow water sedimentary facies, is deposited during the thermal subsidence or rift sag stage (of rifting) and covers both the buried site of the rift and its adjacent platformal shoulders.

The time lapse between initiation of rifting and deposition of Sedex deposits may be as much as 400 million years. For example, in the Mount Isa area, the initiation of rifting and infilling of the Leichhardt River Fault Trough was at about 1800 Ma. Infilling of the rapidly subsiding rift zone with about 16 km of fluviatile to shallow marine clastics and mafic volcanics was completed by about 1740 Ma. A rift-cover sequence, 2.5 km thick, dominated by quartzites and carbonates, but with subaerial felsic volcanic rocks at it base, is overlain by a marine transgressive sequence that is 6 km thick. The transgressive sequence consists of basal arenites, siltites, and shales and overlying fine grained terrigenous and dolomitic sediments that form the host rocks to Sedex deposits. Tuff beds in the ore host have been dated at about 1670 Ma (Page, 1981), indicating for the Mount Isa, Hilton, and H.Y.C. deposits a time lapse of about 130 Ma between initiation of rift-fill and the formation of Sedex deposits.

Similarly, the Cambrian to Devonian basinal rocks hosting Sedex deposits in the Selwyn Basin of Canada can be viewed as a rift-cover sequence to Upper Proterozoic rift-fill clastics of the Windermere Supergroup. Windermere deposition began along a newly rifted margin of western North America at about 770 Ma (Abbott et al., 1986; Gabrielse and Campbell, 1991). Although only the eastern margin of the westward thickening rift-fill sequence is exposed, at least 3 km of coarse feldspathic turbidites occur beneath the lowest calcareous rift-cover strata of Cambrian age (Eisbacher, 1981). Sedex deposits in Cambrian to Mississippian host rocks therefore postdate rift initiation by between 200 and 400 Ma.

In Ireland, extensional basins were initiated during the Lower Devonian, either in response to crustal extension or as pull-apart basins along transcurrent faults. More than 6 km of conglomerate, sandstone, and mudstone fill the Munster Basin (Phillips and Sevastopulo, 1986). The Irish deposits of middle Dinantian age were thus formed only about 40 Ma after initiation of rift-controlled subsidence.

The major exception to the generalization that Sedex deposits occur in a rift-cover sequence is the Sullivan deposit of the middle Proterozoic Belt-Purcell Supergroup.

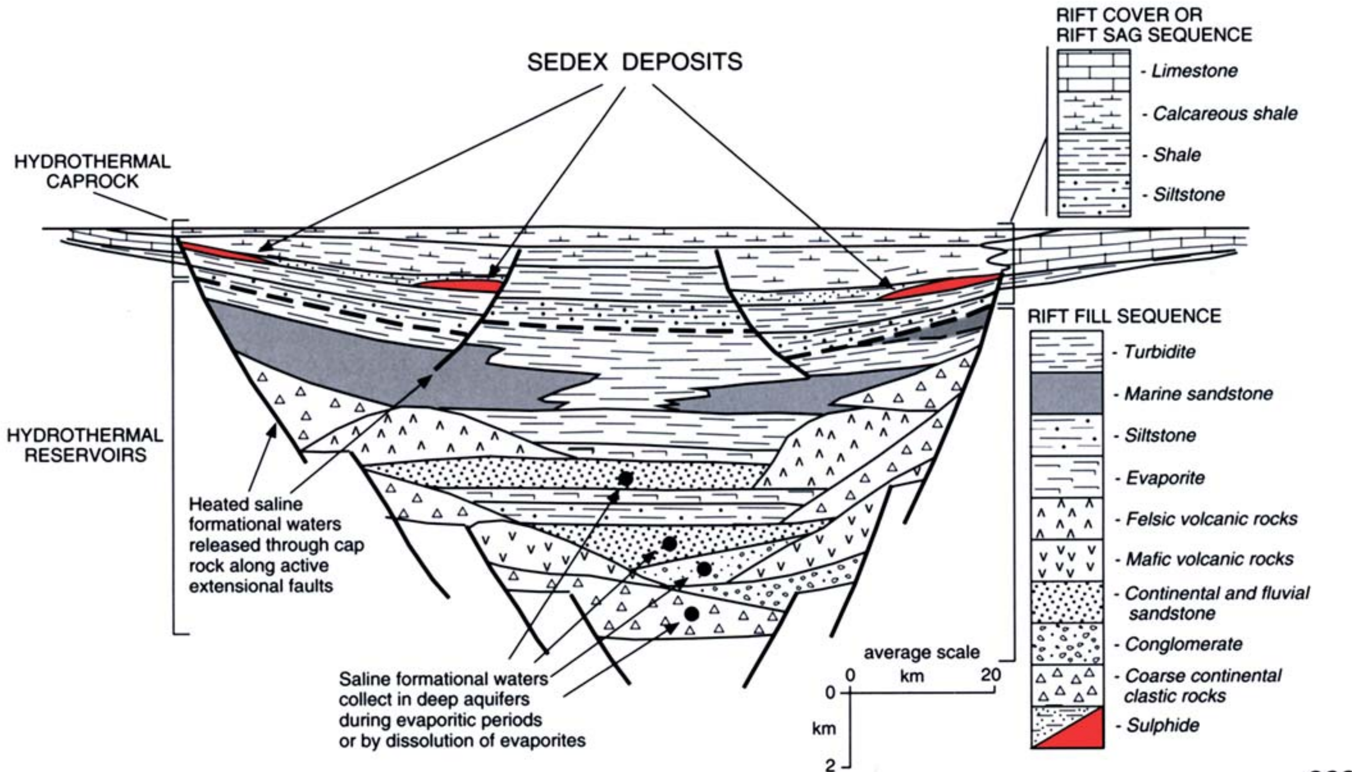

Figure 6.1-6. Schematic representation of the geological setting of Sedex deposits. Sedex deposits are hosted by the cover sequence to an intracontinental rift system that has been filled by continental clastics, volcanics, and/or marine clastics. Chloride brines, formed during an evaporitic period of rift filling or by the later subsurface dissolution of the evaporites, collect in the deep part of the rift fill sequence. The rift cover sequence acts as a hydrothermal caprock (base marked by bold dashed line) to the brines during heating by burial or deep magmatism. The heated brines flow to the contemporaneous surface of the cover sequence when the caprock is ruptured by renewed extensional tectonism.

The deposit occurs in a rift-fill sequence of turbidites and tholeiitic sills of the Aldridge Formation in the lower part of the exposed stratigraphy. However, some exploration potential can be inferred from the presence of a few relatively small baritic Zn-Pb deposits, possibly of Sedex type, (Mineral King, Paradise, Leg) which are located near the top of the preserved rift-cover sequence (Dutch Creek and Mount Nelson formations).

AGE AND PALEOGEOGRAPHIC DISTRIBUTION

Sedex deposits span the range from the Middle Proterozoic to the present. There are two frequency peaks to the distribution of deposit ages, namely in the Middle Proterozoic and in the Paleozoic (Fig. 6.1-7A). These peaks are accentuated in terms of contained metal (Fig. 6.1-7B), emphasizing that the bulk of known reserves of the Sedex type occur in the Middle Proterozoic of Australia, and in the middle Paleozoic of Western Canada, Alaska, and Western Europe (Table 6.1-1).

The oldest Sedex deposits may be those of the highly metamorphosed Bhilwara and Aravalli supergroups of northwestern India. Model Pb dating indicates an age of about 1800 Ma for the deposits themselves, and Rb-Sr dating of an intrusive granite constrains their host rocks to a minimum age of 1500 Ma (Deb et al., 1989). The Black Angel deposit of Greenland, which is hosted by Lower Proterozoic (i.e. >1800 Ma) carbonate rocks of the Marmorilik Formation (Garde, 1978; Thomassen, 1991), has been metamorphosed and structurally deformed beyond unequivocal classification. Though considered by Sangster (1990) to be of the Sedex type and by Pedersen (1981) as a syndiagenetic (i.e., Irish) type , it could also be of the Mississippi Valley type (Carmichael, 1988). If the last, it could belong to the same metallogenetic province as the MVT deposits of the Lower Proterozoic Ramah Group in Labrador (Wilton et al., 1993) or the Middle Proterozoic Society Cliffs Formation on Baffin Island (Clayton and Thorpe, 1982). Because of its uncertain genesis, it has been excluded from the present classification. A deposit interpreted to be of Sedex type, with a Pb-Pb model age of 1350 Ma, is reported for the Lower Proterozoic of China (Hou and Zhao, 1993), but because it occurs in a Pb-Zn skarn metallogenetic province, and is itself situated within the metamorphic aureole of a granite and contains elevated molybdenum concentrations, it is excluded from the present classification because of its dubious genesis. The Boquira deposit of Brazil, containing 5.6 Mt at 1.43% Zn

Contents

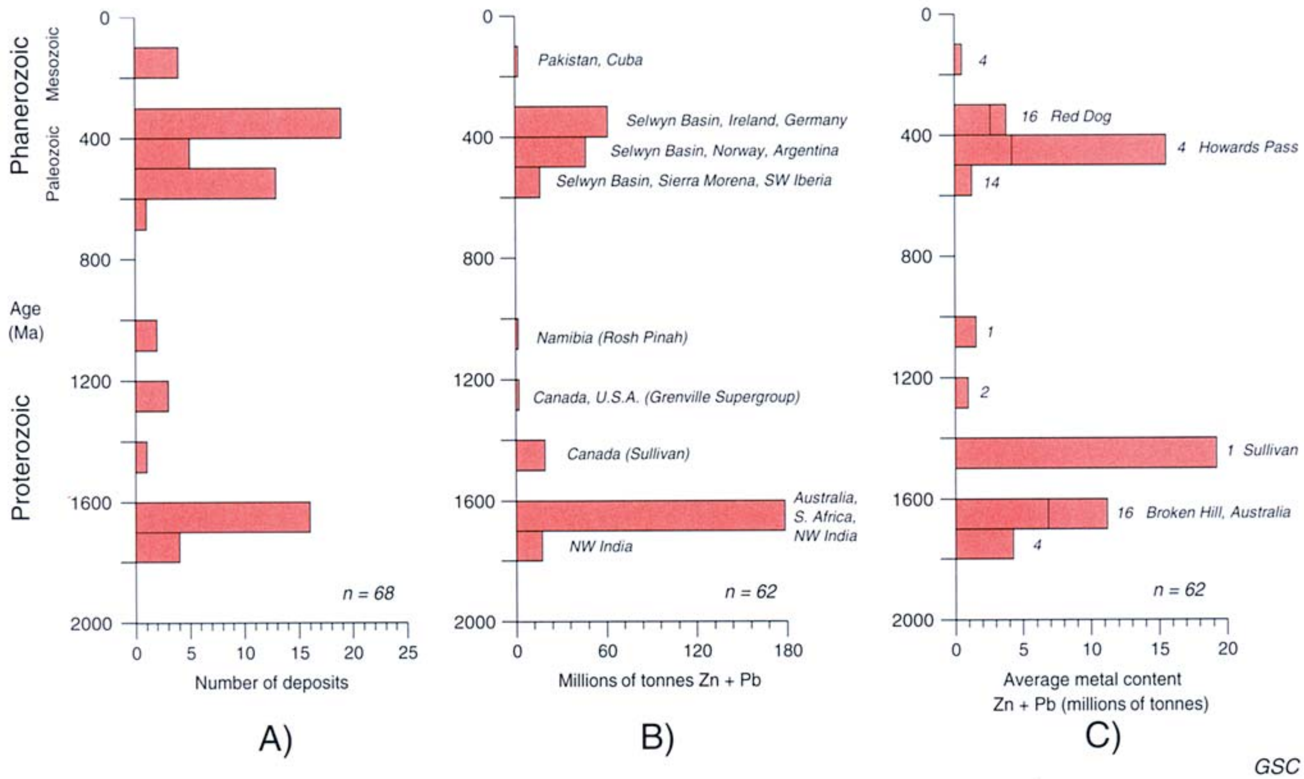

Figure 6.1-7. Age distribution of Sedex deposits.

A) Number of deposits per 100 Ma interval. Note the two frequency peaks during the Middle Proterozoic (1600-1800 Ma) and the Cambrian-Mississippian span of the Phanerozoic (300-600 Ma).

B) Tonnes of Zn+Pb per 100 Ma interval. Note that the great majority of Sedex resources are about equally divided between the Middle Proterozoic deposits of Australia and South Africa on the one hand and the Paleozoic deposits of Canada and Western Europe on the other.

C) Average metal content of deposits per 100 Ma interval. The number of deposits in each group is indicated. The vertical bar indicates the average metal content of deposits exclusive of the "giant" in each group, the name of which is indicated.

and 8.85% Pb in an amphibolite-magnetite iron-formation of attributed late Archean age (Espourteille and Fleischer, 1988), and suggested to be of sedimentary exhalative origin (Carvalho et al., 1982), is also excluded from the classification because of its suspect genesis.

There does not appear to be any compelling reason, based on current understanding, why Sedex deposits should not occur in rocks older than Middle Proterozoic. The onset of the Middle Proterozoic does not seem to coincide with any major permanent change in global climate, ocean water composition, atmosphere composition, or geotectonic processes. For example, the >3.2 Ga (Kroner et al., 1991) sedimentary baritite of the Fig Tree Group, South Africa (Heinrichs and Reimer, 1977) indicates that a deposit type most closely related to Sedex deposits (see below) was being formed very much earlier in the Earth's history than Middle Proterozoic.

The majority of Proterozoic Sedex ore deposits were formed in the time range 1650-1700 Ma and, together with the Sullivan deposit (1467 Ma – H.E. Anderson, D. Davis, and R.R. Parrish, unpub. data, Geological Survey of Canada, Minerals Colloquium, January, 1994, Ottawa, Ontario), seem to be spatially associated with the suture systems that separate the Australian, Antarctican, and South African cratons from the North American craton on a reconstruction of the Upper Proterozoic Supercontinent (see Fig. 6.1-8A). This remarkable correlation might be fortuitous, because the mineralization and the rifting with which it is associated predate the orogenic belts of Grenville age, along which assembly of the Upper Proterozoic supercontinent is inferred to have taken place. If, as suggested by Hoffman (1991), the Laurentian, Australian, and Antarctican cratons were fellow travellers from 1900 Ma to 600 Ma, then the rift systems along which the Sedex deposits are located did not lead to oceanic spreading at that time but remained intracratonic. They did, however, provide the cratonic perforations along which the cratons ultimately separated during the latest Proterozoic.

The bulk of Paleozoic Sedex resources are located in the Cambro-Silurian Road River Group of Selwyn Basin and the Devono-Carboniferous Earn Group of northwestern Canada and their continuation into Alaska. The deposits are clustered at Cambrian, Silurian, and Devonian ages. Selwyn Basin is filled by a condensed sequence of shales and carbonaceous cherts representing a semistarved basin, is bounded by a carbonate shelf, and is interpreted to cover the site of an Upper Proterozoic rift zone (Abbott et al., 1986). The unconformably overlying Earn Group comprises shales to conglomerates of coarsening upward clastic wedges of a western provenance (Gordey et al., 1982). Mississippian carbonate rocks of Ireland and Devonian shales of the Rhenish Basin in Germany are the two other most important host successions for Paleozoic Sedex deposits (Fig. 6.1-8B).

The youngest fossilized Sedex deposits reported in the literature are of Jurassic age (Table 6.1-1). Those hosted by Jurassic carbonate rocks of the Lasbela-Khuzdar Belt of Pakistan (Anderson and Lydon, 1990) were formed on the flanks of the rift system that separated Madagascar from the Indian craton. Lead-zinc-barium mineralization near the top of a thick deltaic sequence that comprises the Jurassic San Cayetano Formation in Cuba, has been interpreted to be of seafloor origin (Zhidkov and Jalturin, 1976; Simon et al., 1990; Valdes-Nodarse et al. 1993).

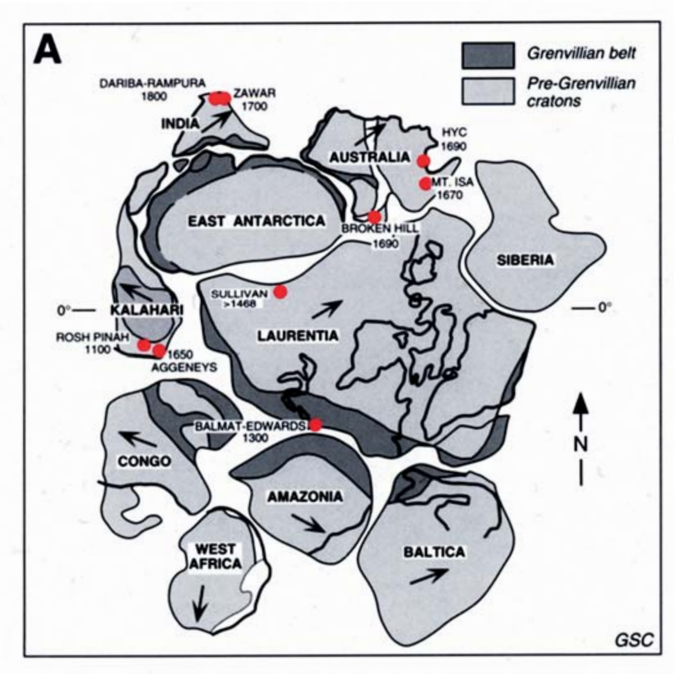

Figure 6.1-8. **A)** Geographical distribution of Proterozoic Sedex deposits shown on the continental reconstruction for the Upper Proterozoic by Hoffman (1991). Numbers refer to the most reliable radiometric age of the host rocks and bold lines indicate known outlines of modern day margins of continents. Arrows indicate present day north. **B)** Geographic distribution of Paleozoic Sedex deposits shown on the continental reconstruction for the Upper Devonian by Scotese (1984).

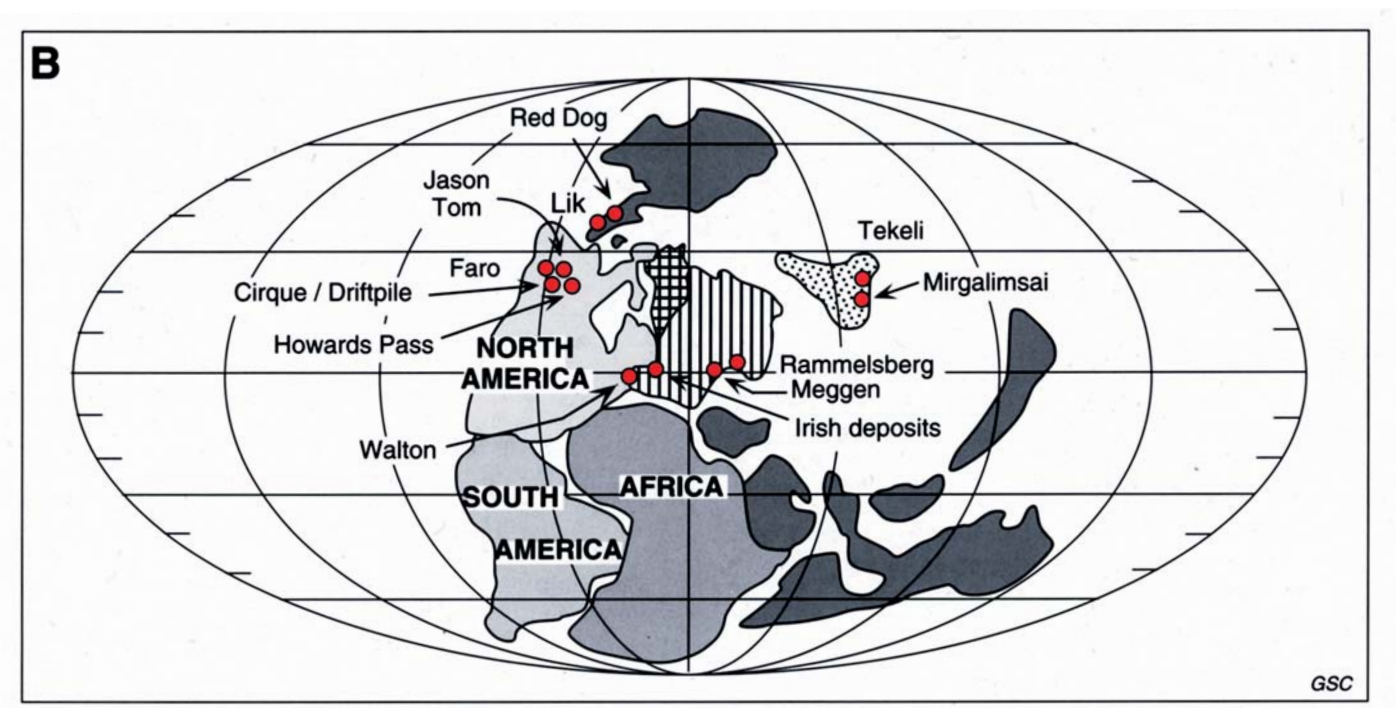

It is debatable whether there are any modern analogues of Sedex deposits. The metalliferous sediments of the Red Sea brine pools (Degens and Ross, 1969), which are often cited as the analogue for Sedex deposit genesis in connection with the brine pool model, have a Zn:Pb ratio of about 50:1 and Zn:Cu ratio of 4:1 (Bignell et al., 1976), which is not typical for Sedex deposits. The sulphide deposits of Middle Valley (Goodfellow and Franklin, 1993) and the Escanaba Trough (Zierenberg et al., 1993) are composed dominantly of pyrrhotite, and have elevated copper concentrations. The Bent Hill sulphide deposit at Middle Valley (Juan de Fuca Ridge), which is the only seafloor sulphide deposit investigated by deep drilling, has the morphology of a discordant pipe (Davis et al., 1992b), which is in contrast to typically stratiform Sedex deposits. In the geological record these modern sulphide deposits of sediment-covered oceanic ridges would be preserved in, or just above, ophiolite sequences. The brines of the Salton Sea geothermal system, which occur within deltaic sediments that infill an intracontinental rhombochasm, have both the chemical composition and geological setting typical of most Sedex deposits. If situated in a submarine, rather than a subaerial environment, brines of this hydrothermal plume would have the potential to form Sedex-type deposits.

DISTRIBUTION IN CANADA

The distribution of the major Canadian Sedex deposits is shown in Figure 6.1-1. The Sullivan deposit hosted by turbidites in the bottom part of the Middle Proterozoic Purcell Supergroup has been the major producer. Cambro-Silurian shales and carbonaceous cherts of the Selwyn Basin and the overlying Devono-Mississippian Earn Group in Yukon Territory and northern British Columbia, contain the great bulk of known Canadian Sedex resources. Only the Faro and Vangorda deposits of the Anvil district have been mined. The Howards Pass deposits (XY, Anniv, OP) are one of the world's greatest concentrations of sphalerite and galena. The Windsor Basin in Nova Scotia has similar age and geological attributes to the Irish metallogenetic province, of which it may be considered to be a pre-Atlantic opening extension. The major Zn-Pb deposit in this area, Gays River, is classified as a MVT deposit. The Walton deposit, which has Irish-type Sedex characteristics, was mined only for barite. The Grenville Supergroup contains many minor sphalerite-rich deposits in carbonates and shales that accumulated on the flanks of a rift, and is very similar in geological attributes to the Middle Cambrian Sedex metallogenetic province of the Iberian Peninsula. Intense deformation of the major deposit at Balmat-Edwards, New York, precludes an unequivocal classification as a Sedex deposit, (for example it may be a salt-dome related sulphide deposit).

Terranes considered favourable for the occurrence of Sedex deposits, but in which no examples of Sedex deposits are known, are also shown on Figure 6.1-1. The Richardson Trough has similar geological characteristics to the Selwyn Basin. The Hazen Basin, of similar age to the Selwyn Basin, is considered favourable because its extension in northern Greenland contains Sedex-type mineralization. Lower Proterozoic sediments of the Labrador Trough have all the positive regional and local indicators for the occurrence of Sedex deposits (H.S. Swinden and F. Santaguida, Geological Survey of Canada, Minerals Colloquium, January, 1994, Ottawa, Ontario), including initiation of sedimentation as redbed intracontinental rift-fill, with subsequent marine sedimentation in a volcanically active spreading environment (see "Exploration guidelines"). The Proterozoic Borden Basin and Foxe Fold Belt are considered as having Sedex potential because of their thick shale accumulations, abundant evidence for synsedimentary faulting, and scattered centres of contemporaneous magmatic activity (Sangster, 1981).

HOST ROCKS AND RELATED LITHOLOGIES

Sedex deposits occur in sedimentary rock types considered typical of most epicontinental marine environments or playa lakes of inland drainage systems. Their depositional settings range from deep water distal turbidite fans (e.g. Sullivan) through relatively deep water, off-shelf to slope shales (e.g. Rammelsberg), and shelf carbonates (e.g. Irish and Pakistani deposits) to back-reef or playa lake calcareous siltstones and shales (e.g. H.Y.C. and Mt. Isa, Australia). The siliceous carbonaceous shales of the Selwyn basin deposits reflect a euxinic, starved, semirestricted marine basin, and their depositional setting may have been comparable to the Black Sea.

Whatever the dominant lithology of the host rocks, locally derived fragmental sedimentary rocks are a typical feature of most Sedex deposits. These fragmental rocks comprise slide sheets, debris flows, stratiform and discordant breccias, conglomerates, and mud flows, and are usually composed of rock types which occur at the same or deeper stratigraphic levels as the Sedex deposit itself. The fragmental rocks may occur in the near footwall, within, or in the near hanging wall to the deposit, or as local lithological facies some distance from the locus of mineralization. The fragmental rocks may be divided into two categories:

1. Those associated with tectonic activity, and include fault scarp talus, slide sheets, slumps, and debris flows; and
2. Those associated with fluid upflow and include hydrothermal vent and eruption breccias; discordant zones of hydraulically fractured or turbated sediment; and extrusion breccias and mudflows resulting from mud volcano activity.

These sedimentary fragmental rocks are considered to be most positive indicators for favourable environmental conditions (i.e., tectonic activity and fluid upflow) for the formation of Sedex deposits.

HOST ROCK ALTERATION

Hydrothermal alteration of the host rocks to Sedex deposits has not been documented at the same level of detail as it has for VMS deposits for two main reasons:

1. Feeder zone mineralization associated with Sedex deposits usually is not, in contrast to VMS deposits, of economic grade. Hence the hydrothermal upflow zone where the most intense hydrothermal alteration takes place is not made accessible for study via underground workings or systematic drill cores.

2. The most common alteration minerals of fossilized seafloor hydrothermal systems (chlorite, muscovite, quartz, and accessory sulphides, carbonates, and oxides) is similar to the rock-forming mineralogy of terrigenous sedimentary rocks that have been metamorphosed to greenschist facies (essentially quartz, muscovite, and chlorite, and accessory carbonates, and iron sulphides). A hydrothermal alteration pipe in metamorphosed terrigenous sediments may therefore be difficult to recognize on mineralogical grounds alone, and requires significant metasomatic or textural signatures for it to be readily distinguished.

The lack of a sufficient number of case examples of host rock alteration associated with Sedex deposits precludes generalizations to the same extent as is possible for VMS deposits, and so only a range of examples is presented here.

One of the most remarkable Sedex alteration pipes is that associated with the Sullivan deposit, which is underlain by a tourmalinite pipe about 1000 m in diameter (Hamilton et al., 1982). Whether this tourmalinite is directly related to hydrothermal upflow that formed the sulphide deposit is debatable, because tourmalinite pipes without any base metal sulphide associations occur elsewhere within the Belt-Purcell Supergroup (e.g. Beaty et al., 1988). At Sullivan, the tourmalinite is cut by veins and networks of sulphides that appear to be feeder mineralization to the overlying massive ore, which suggests that the bulk of the tourmalinite predates the sulphide mineralization. Significant silicification, either by replacement or as bedded chert, has not been recognized at the Sullivan deposit. Alteration patterns at Sullivan are complicated by a postore overprinting by an albite-chlorite-pyrite alteration that is most extensively developed in the hanging wall of the deposit (Hamilton et al., 1982) and may be related to the emplacement of a thick tholeiitic sill and its offshoots (Jardine, 1966; Ethier et al., 1976) about 200 m below the ore horizon.

Silicification may have been an integral part of hydrothermal alteration at both the Tom and nearby Jason deposits, but the host siliceous carbonaceous shales make it difficult to distinguish hydrothermal silicification from normal diagenetic effects. The most obvious and extensive footwall alteration at the Tom deposit is ankerite/pyrite alteration (Goodfellow and Rhodes, 1990). Carbonatization, notably by ferroan ankerite, is strongest within the feeder zone and vent complex, where there appears to have been a concomitant removal of silica. At the Jason deposit, footwall alteration consists of variably silicified and carbonatized rocks (Bailes et al., 1986). The feeder zone and vent complex are characterized by a lower siderite zone and upper ferroan dolomite zone (Turner, 1990).

The Rammelsberg deposit is stratigraphically underlain by a zone of silica-rich lenses termed "Kniest" (Hannak, 1981). Large (1983) stated that the Kniest has a pipe-like geometry that distinctly crosscuts the bedding and contains veins of chalcopyrite. At Mount Isa, an extensive zone of quartz and dolomite with associated chalcopyrite ores occurs down dip from the Sedex-type Zn-Pb ores, but there is debate whether it is contemporaneous with the formation of the Zn-Pb ores (e.g., Stanton, 1963; Mathias and Clark, 1975) or whether it is a much later superimposed event (e.g., Perkins, 1984; Bell et al., 1988).

Dolomitization, with or without silicification, is associated with several Sedex deposits whose host rocks have a calcareous component. Generally throughout Ireland, a pervasive dolomitization is interpreted to have preceded the main sulphide-depositing event (Hitzman and Large, 1986; Hitzman, 1986). At the Silvermines deposit, pervasive iron-free dolomitization of the footwall rocks preceded seafloor sulphide and siderite mineralization, whereas iron-bearing dolomite, as fracture fillings and secondary cements, was precipitated both during and after accumulation of the stratiform ores (Andrew, 1986). Similarly at Tynagh, replacement and cementation by dolomite and ferroan calcite preceded sulphide mineralization whereas precipitation of iron-bearing dolomite took place both during and after the main sulphide event (Boast et al., 1981; Clifford et al., 1986). At the Navan deposit, replacement of micritic host rock by low-iron dolomite and minor chalcedony preceded and accompanied sulphide mineralization (Andrew and Ashton, 1985). In the H.Y.C. and Ridge II deposits of the McArthur River area, Australia, multiple generations of dolomite and the development of nodular dolomite distinguish mineralized calcareous siltstones from nonmineralized lithological equivalents (Williams, 1978a).

If the above examples are representative of the deposit type as a whole, then iron- and magnesium-bearing carbonatization is probably the most common easily recognizable hydrothermal alteration type associated with Sedex deposits. Silicification may also be significant, though more difficult to recognize. Argillic alteration, including the prominent chloritization and sericitization typical of VMS deposits, may be too cryptic to recognize, unless the host rock originally contained significant concentrations of feldspar.

ASSOCIATED STRUCTURES

As discussed above, Sedex deposits occur in structurally controlled sedimentary basins, and most of these basins are related to major rift zones. Large (1983) classified the sedimentary basins that host the deposits according to their lateral dimensions. First-order basins have lateral dimensions of the order of 100 km and correspond to the major rift structure. Second-order basins generally have lateral dimensions in excess of 10 km and third-order basins range from hundreds of metres to ten kilometres, both commonly having the form of a half-graben. Sedex deposits are spatially associated with the synsedimentary faults that control these second- and third-order basins. As noted above, Sedex deposits, and the second- and third-order basins with which they are associated, occur in the rift-cover sequence and hence postdate the main phase of rifting. It is not clear whether the localized extensional faults, which control the second- and third-order basins, form an integral part of the tectonic evolution of a sediment-covered rift, and hence are predictable, or whether they represent a separate tectonic event, and hence are unpredictable features of sediment-covered rifts. Most authors agree that a rift-cover sequence represents basinal development due to thermal relaxation after extension or the rift sag stage. For example, the Mount Isa Group of Australia is considered to represent a rift sag sequence following renewed extension of the Leichardt River Fault Trough at

1678 Ma. Large (1983) considered Sedex deposits to be associated with a tectonic extensional pulse superimposed upon postrift subsidence.

Not all Sedex deposits are directly related to a tectonic rifting process per se. In some cases at least, the second- and third-order basins are interpreted as rhombochasms or pull-apart basins associated with transcurrent faulting in a sedimentary basin. For example, the Macmillan Pass Central Block, hosting the Tom and Jason Sedex deposits, is thought to represent a Devonian pull-apart basin (Abbott et al., 1986). The clastic-filled Devonian extensional basins that control the siting of the Sedex deposits in the Mississippian carbonate rift-cover sequence in Ireland are good candidates for rhombochasms developed along transcurrent faults that are controlled by the Caledonian structural grain of the basement. It is significant to note that the Salton Sea geothermal system, the best modern analogue for a hydrothermal system capable of forming Sedex-type deposits, is located in a rhombochasm along the San Andreas transcurrent fault system (McKibben et al., 1988; McKibben and Eldridge, 1989).

DEFINITIVE CHARACTERISTICS

Sedex deposits were loosely defined in the "Introduction" as *a sulphide deposit formed in a sedimentary basin by the submarine venting of hydrothermal fluids and whose principal ore minerals are sphalerite and galena.* Irrespective of the definition used, examples of mineral deposits can invariably be cited that are intermediate in characteristics between the Sedex type on the one hand and the VMS, MVT, bedded barite, or iron-formation types on the other. The key concepts in the definition used here that distinguish Sedex deposits from these other deposit types are:

1. *Sedex deposits occur in a sedimentary basin.* The scale of sedimentary basin referred to is in the order of 10^2 to 10^3 km^2. In other words Sedex deposits occur in a geological terrane that is defined by the presence of a specified sequence of sedimentary rocks (i.e., a sedimentary basin). This criterion helps to distinguish Sedex deposits from VMS deposits, which typically occur in a geological terrane distinguished by the presence of volcanic rocks (i.e., a volcanic belt). The mere presence of sedimentary rocks in the immediate footwall of a conformable sulphide deposit is in itself not diagnostic of a Sedex deposit – the immediate host rocks of many VMS deposits are sedimentary rocks. (see subtype 6.3 "Volcanic-associated massive sulphide base metals").
2. *The principal economic minerals are sphalerite and galena.* The importance of this concept is that it not only distinguishes Sedex deposits from other nonsulphide seafloor metalliferous sediments such as baritite deposits, iron-formations, and manganese formations, but also is another criterion to distinguish them from VMS deposits, in which chalcopyrite, is almost invariably a principal ore mineral. The presence or absence of chalcopyrite as a primary hydrothermal product in a seafloor sulphide deposit directly reflects the temperature of the hydrothermal fluids. The solubility of chalcopyrite in a reduced (i.e. $H_2S >> SO_4^{2-}$) aqueous fluid in which metals are present mainly as chloride complexes is insignificant (<1 ppm) below about 300°C. Fluid inclusions and other geothermometers indicate that the temperature of the hydrothermal fluids responsible for Sedex deposits are in the range 150°C-300°C, whereas for VMS deposits the temperatures of the ore fluids are generally >300°C.
3. *Sedex deposits were formed during the submarine venting of hydrothermal fluids.* This concept emphasizes that Sedex deposits formed at or just below the seafloor and are essentially a quasi-synsedimentary phenomenon, although there is debate whether the deposits are dominantly seafloor metalliferous sediments around hydrothermal vent fields or are dominantly the products of subsurface replacement of sediments around the hydrothermal upflow conduits. This depositional environment distinguishes them from MVT deposits, which are essentially epigenetic deposits formed in lithified carbonate rocks, and for which there is a significant difference between the age of the mineralization and the age of the host rocks.

GENETIC MODELS

There are two distinct sets of problems concerning the genesis of Sedex deposits. One is with regard to the origins of the ore fluids and the reasons for their upflow to the seafloor. The other pertains to the processes of sulphide precipitation and accumulation to form the ore deposit.

Generation and upflow of hydrothermal fluids

The majority of opinion is that the ore fluids for Sedex deposits are formational waters of the sedimentary basin that for whatever reason have become unusually hot, saline, and metalliferous (e.g., Walker et al., 1981; Badham, 1981; Carne and Cathro, 1982; Lydon, 1983; Sawkins, 1984). The salient points of this model are illustrated in Figure 6.1-6. The reason the formational waters become unusually hot is thought to be unusually high geothermal gradient of an area undergoing extensional tectonism. Although this high heat flow can be ultimately linked to contemporaneous, usually deep, magmatic activity of a spreading geotectonic environment, there is little or no evidence to support direct heating by a magmatic body of the hydrothermal systems responsible for Sedex deposits. Heating by an elevated geothermal gradient, even as highly anomalous as 70°C/km, requires that the hydrothermal fluids originate from a depth of several kilometres. Lydon (1983) suggested that the most plausible geological environment which would allow the heating of large volumes of formational water to greater than 200°C was one in which a sequence of porous rocks, forming the aquifer or hydrothermal reservoir, was overlain by a sequence of argillaceous rocks. The argillaceous sequence performs the double function of an impermeable caprock, which prevents the dissipation of heat by the upward convective mass flow of heated fluids, and also a thermal insulator, which prevents the dissipation of heat by conduction, and thus allows the buildup of high temperatures in the reservoir. This is the configuration of most sediment-covered rift systems that host Sedex deposits, in which coarse clastic and volcanic rocks of the rift-fill sequence are overlain by argillaceous rocks of the rift-cover sequence, deposited during the marine transgression associated with the thermal subsidence stage of the rifting cycle.

Although the sparse fluid inclusion data (see above) suggest that the ultra high salinities of the Salton Sea, for example, are not necessary to form an ore fluid, they do suggest that the ore fluids must have salinities at least two to three times that of seawater. The origin of these high salinities in the ore fluids, like their modern analogues, is most likely to be a result of the dissolution of evaporites in the sedimentary sequence stratigraphically below the deposit. In terms of Lydon's (1983) model outlined above, these evaporites could be within or at the base of the rift-fill sequence. Candidates for such a role in the formation of Sedex deposits in the Selwyn Basin would be the evaporites of the Little Dal Group and the Coates Lake Group. These may extend completely beneath Selwyn Basin at the base of the Windermere Supergroup, which is the Upper Proterozoic rift-fill sequence to the overlying Paleozoic rift-cover sequence of the Selwyn Basin.

Processes of sulphide precipitation and accumulation

A wide spectrum of hypotheses have been suggested in attempts to explain the precipitation, accumulation, and preservation of sulphides and other hydrothermal products in Sedex deposits. The common theme in most cases is an explanation of the bedded or laminated textures typical of the bedded ores and distal hydrothermal products facies of the idealized Sedex deposit (Fig. 6.1-4). The ideas expressed can be conveniently grouped into four models.

Brine pool / bottom-hugging brine model

The brine pool model advocates that the bedded ores and distal hydrothermal products facies represent sedimentation from a stagnant brine pool, formed by the collection of hydrothermal effluent in a topographic depression adjacent to the vent area or from a migrating bottom-hugging brine. Advocates of a dense brine model for Sedex deposits include Solomon and Walshe (1979), Finlow-Bates, (1980), Russell et al. (1981), Carne and Cathro (1982), Lydon (1983), and Samson and Russell (1987). The brine pool variant of the model has a modern analogy in the brine pools and metalliferous sediments of the Red Sea (e.g., Degens and Ross, 1969; Bäcker, 1975). The merits of this model are that it explains:

i) The finely laminated nature of the bedded ores, which is consistent with the very low energy depositional environment provided by a stagnant brine pool.

ii) The sheet-like morphology of the bedded part of a Sedex deposit, suggesting uniform depositional rates of compositionally unique sediments of hydrothermal origin within the confines of a limited area.

iii) The lateral continuity of individual lamina of hydrothermal products, many of which are monomineralic, suggests synchronous precipitation and settling from an overlying water column that is distinctly different from normal seawater and whose chemical characteristics undergo repetitive cyclic changes.

iv) The lack of bioturbation of the laminated hydrothermal products, indicating a bottom environment hostile to burrowing organisms, even though, in the Phanerozoic at least, such organisms are common.

v) The preferential siting of Sedex deposits in third- or second-order basins, indicating that a topographic depression on the seafloor is required for their formation. Although a topographic depression is a requisite for the brine pool model, it is not an integral part of alternative models.

vi) The large average tonnage of metals contained in a Sedex deposit. A brine pool confines the upward dispersal of hydrothermal products to below the pycnocline which defines its upper surface, and limits lateral dispersal to the brine pool margins. As a consequence, a high proportion of the metals that are carried upward by the hydrothermal fluids are precipitated within the limits of the brine pool and not dispersed in the open ocean.

The bottom-hugging brine variant of the model was inspired by the experiments of Turner and Gustafson (1978) and Solomon and Walshe (1979). A difference between the bottom-hugging brine model and the brine pool model is that there is only a single pass of each pulse of hydrothermal fluid over the proximal site of hydrothermal precipitation (which is used to explain mineralogical zonation). Another difference is that the migrating brines may collect in a basin distal from the upflow zone and result in the hydrothermal sediments being disconnected from a hydrothermal vent zone.

Buoyant plume model

Calculations by Sato (1972) have shown that in order for hydrothermal effluent cooled to below 100°C by mixing with seawater to be denser than seawater and hence to form a bottom-hugging brine or brine pool, the vented hydrothermal solutions must have a salinity greater than four times seawater if their vent temperature is above 250°C. The basis of this model is that the only fluid inclusion data available (see above) suggests that ore fluids for Sedex deposits have salinites in the range of only two to three times seawater. Therefore, the plume formed by mixing seawater with hydrothermal fluids of these salinities and temperatures around 250°C, would remain buoyant for most of its cooling and precipitational history.

The model has only been explicitly applied to Sedex deposits (Goodfellow and Jonasson, 1986; Goodfellow and Rhodes, 1990) in conjunction with a postulated stratified oceanic water column during times of oceanic anoxia (Goodfellow, 1987). The stratified water column is required to provide sulphide for ore deposition over a long time period and to prevent the rapid oxidation of sulphides nucleated in the water column or accumulated on the normally oxic ocean floor.

Clastic apron model

Clastic sedimentary textures in Sedex deposits, such as debris flows of fragmental sulphides (e.g. Sullivan; Hamilton et al., 1983) and graded bedding (e.g. Rammelsberg; Large, 1983) have been cited as evidence for their synsedimentary seafloor origin. The origin of the clastic sulphides is by contemporaneous erosion or collapse of a topographically elevated sulphide mound formed above the hydrothermal upflow zone, with the resulting talus breccia, debris flows, and turbidites collecting as a clastic apron around the base of the mound. Modern analogies for this process have been described for Middle Valley (Goodfellow and Franklin, 1993). Although no one has advocated that the bedded ores of Sedex deposits have formed entirely by a process of clastic reworking of vent complex, the process is evidently of some significance in certain deposits.

Subsurface replacement model

This model is gaining increasing advocacy, especially by those working on the Australian Proterozoic deposits of the McArthur Basin and Mount Isa Inlier. The essence of the model is that the bedded ores of Sedex deposits represent the very early diagenetic, precompaction replacement of fine grained bedded sediments in the subsurface around seafloor hydrothermal vents. The sedimentary textures of Sedex deposits are therefore not primary but result from pseudomorphism of those of the host sediment. Prominent advocates of the model, based on studies of the McArthur River deposits (H.Y.C., Ridge II), have been Williams and Rye (1974), Williams (1978a, b), and Eldridge et al. (1993), who showed that texturally the ore sulphides postdate early diagenetic pyrite and that sulphur isotope data require interpretations involving different sulphur sources for the diagenetic and ore sulphides. It has been argued that the geochemistry of the Mount Isa ores indicates that the Cu-silica dolomite and Pb-Zn ores are cogenetic during diagenesis, and that the finely layered Pb-Zn ores inherited their textures from the original clastic sediments. Andrew and Ashton (1985) have shown that the bulk of the Zn-Pb ore of the Navan deposit postdates the earliest carbonate cements.

The merits of the subsurface replacement model are that:

i) It gives the most satisfactory explanation for the characteristic mineralogical and chemical zonation of the ores around the upflow zone. Zone boundaries form concentric shells, both in vertical and lateral sections, around the upflow zone. This suggests a zone refinement process that simultaneously affected the entire stratigraphic sequence of the ore body. Zonation patterns of the vent complex ores, which are generally agreed to be the products of subsurface replacement and infilling, continue with the same polarity and gradients into the bedded ores (e.g., Sullivan, Tom, and Jason deposits). This suggests that mineralogical and chemical distribution patterns for the bedded ores are also a product of subsurface dispersal or zone refinement.

ii) Subsurface replacement is consistent with the observations at the two modern analogues of metalliferous hydrothermal systems in unconsolidated sediments (Salton Sea and Middle Valley), that the bulk of subsurface hydrothermal fluid is contained in a plume that pervasively occupies the porosity of the host sediments and is not confined to channels.

Source of sulphide sulphur

Sedex deposits not only contain on average large quantities of metal, but also large quantities of sulphur. Experimental investigations have shown that aqueous chloride solutions with five times the salinity of seawater can carry hundreds of parts per million of zinc, lead, and hydrogen sulphide in stoichiometric proportions to form sphalerite and galena at temperatures above 200°C and pH<4 (Barrett and Anderson, 1982). However, these concentrations are reduced by orders of magnitude at the pH of hydrothermal fluids emanating from sedimentary rocks which are in the range 5.5 to 7.0 (e.g., Salton Sea pH=5.5 (McKibben et al., 1988) and Guaymas Basin pH=5.9 (Von Damm et al., 1985). For the ore fluids to carry sufficient concentrations of metal (tens or hundreds parts per million) to form a large Sedex deposit, they must be sulphur deficient (i.e., the metal:sulphide ratio in the fluid greater than stoichiometric proportions for the metal sulphide). In other words, at least some of the sulphide sulphur must be supplied at the depositional site of the Sedex deposit. The only viable source of local seafloor sulphur in the sulphide form is that produced by the bacteriogenic reduction of seawater sulphate, and stored at the depositional site either in the subsurface as hydrogen sulphide dissolved in porewater and/or as diagenetic iron sulphides (e.g., Williams, 1978a; Samson and Russell, 1987), or in the lower part of a stratified anoxic water column (e.g., Goodfellow, 1987; Turner, 1992).

In Sedex deposits that contain barite, the sulphur isotope ratios of the barite are usually close to those of coeval seawater sulphate, indicating that much of the barite was precipitated by hydrothermal barium fixing ambient marine sulphate. The sulphur isotope ratios of sulphides in the same deposit usually range from the barite values to values with an increasing proportion of ^{32}S, consistent with the explanation that most of the sulphide in Sedex deposits is derived by the bacterial reduction of coeval marine sulphate. Goodfellow and Jonasson (1986) have shown that the average sulphur isotope ratios of Sedex deposits in the Selwyn Basin closely track the stratigraphic variation in sulphur isotope ratios of diagenetic pyrite and thus supports this conclusion. Studies by Shanks et al. (1987) of the Anvil Range deposits suggested a mixed source involving reduced seawater sulphate and hydrothermal hydrogen sulphide. Interpretations of sulphur isotope analysis of bulk mineral separates from the H.Y.C. deposit led Smith and Croxford (1973) to interpret a hydrothermal source of sulphide for sphalerite and galena but a biogenic reduction of ambient sulphate for pyrite. Williams and Rye (1974) and Williams (1978a, b) interpreted the same data to indicate that all sulphur was supplied as sulphate in the ore fluid. The reduction of the sulphate supplied sulphide to form early diagenetic pyrite, which in turn was partially redissolved to form a hybrid sulphide supply, from which the texturally later ore metal sulphides were formed. Interpretation of more recent SHRIMP analyses concluded that both diagenetically early and diagenetically late pyrite were formed from the same bacterially reduced sulphate batch but that the ore sulphides were formed from an unknown independent supply of sulphide (Eldridge et al., 1993). A similar two-stage model has been advocated for the Rammelsberg deposit (Eldridge et al., 1988), although the interpretation has been disputed and a single marine sulphate source suggested (Goodfellow and Turner, 1989).

RELATED DEPOSIT TYPES

Although all seafloor metalliferous deposits that formed directly or indirectly by the submarine venting of hydrothermal fluids, such as VMS deposits, Besshi-type deposits, iron-formations and manganese formations, can be considered to be genetically related to Sedex deposits, only stratiform barite deposits appear to be consistently related to the same geological environments in which Sedex deposits occur. Barite is an important accessory mineral in the bedded ores facies and the most important constituent of the distal hydrothermal products facies of many Phanerozoic Sedex deposits. In some cases, as at Silvermines, Ireland and Walton, Nova Scotia, baritite has been mined as an ore in its own right. The Selwyn Basin is the prime example where barite deposits are directly related to Sedex deposits. Here, especially in Middle Devonian to Lower Mississippian strata, there are numerous "barren barite" deposits. In the Macmillan Pass area alone, site of the Tom and Jason Sedex deposits, there are thirteen known baritite occurrences at approximately the same stratigraphic level. The barren baritites consist of various proportions of bedded barite, limestone, and chert, and form lens-shaped bodies that usually contain less than a million tonnes of hydrothermal products.

It has been proposed by Lydon et al. (1979, 1985) that the barren baritite deposits of the Selwyn Basin were formed from hydrothermal systems that were contemporaneous with, but derived from different reservoirs than those that formed the Sedex deposits. The hydrothermal fluids that formed the baritite deposits were cooler, less saline, and derived from shallower reservoirs within the carbonaceous sediments of the Paleozoic rift-cover sequence, whereas the hydrothermal fluids for the Sedex deposits were derived from deeper reservoirs within the feldspar-rich clastic rocks of the Upper Proterozoic rift-fill sequence.

EXPLORATION GUIDELINES

Geological attributes and interpretations listed below that serve as guides for exploration for Sedex deposits are grouped according to scale, in the sequence: regional, local, and deposit scale.

Regional scale

1. A sedimentary basin that accumulated in a tectonically active environment. Extensional tectonic regimes, in which magmatic activity is contemporaneous with sedimentation, are the most favourable.
2. The deeper parts of the sedimentary basin, or precursor basin, contain, or did contain, evaporites. Low latitude intracontinental rift-fill sequences are the most favourable.
3. The most productive stratigraphic intervals for Sedex deposits are those in the rift-cover sequence, that accumulated during the thermal subsidence stage of the rifting cycle.

Local scale

1. Evidence of synsedimentary faulting. The presence of synsedimentary fragmental rocks representing fault scarp talus and debris flows are the most easily recognized criteria during reconnaissance mapping.
2. Evidence for synsedimentary hydrothermal sulphide mineralization. The presence of sulphides or barite, either as epigenetic veins along the synsedimentary fault or as clasts in synsedimentary fragmental rocks, are strong indicators that the synsedimentary fault was a conduit for mineralizing fluids.
3. Evidence of hydrothermal upflow. Discordant zones of disrupted sediments, especially those indicating hydrothermal metasomatism, and concordant mud flows and debris flows, indicating mud volcano activity, are among the most easily recognized criteria.
4. Evidence of hydrothermal sediments. Local lenses of chert, baritite, carbonate, and magnetite/hematite iron-formation are the most useful nonsulphide indicators.

Deposit scale

Increasing Pb:Zn ratios and Ag content are the best indicators for increasing proximity to the vent complex, which contains the highest grade ores.

ACKNOWLEDGMENTS

Ian Jonasson is especially thanked for freely sharing of his data and for his outstanding editorial job in reducing the weight of the original manuscript. Jari Paakki tracked down references and helped with compilations. Janice Nunney retrieved references and constructed CAD reproductions of diagrams. Ralph Thorpe, Ian Jonasson, and Charlie Jefferson made many suggestions that improved the quality and content of the manuscript.

SELECTED BIBLIOGRAPHY

References marked with asterisks (*) are considered to be the best sources of general information on this deposit subtype.

***Abbott, J.G., Gordey, S.P., and Tempelman-Kluit, D.J.**
1986: Setting of sediment-hosted stratiform lead-zinc deposits in Yukon and northeastern British Columbia; in Mineral Deposits of Northern Cordillera (ed.) J.A. Morin; The Canadian Institute of Mining and Metallurgy, Special Volume 37, p. 1-18.

Anderson, W.L. and Lydon, J.W.
1990: SEDEX and MVT deposits in Jurassic carbonates of Pakistan; in Program with Abstracts, International Association on the Genesis of Ore Deposits, Eighth Symposium, Ottawa, p. A257.

***Andrew, C.J.**
1986: The tectono-stratigraphic controls to mineralization in the Silvermines area, County Tipperary, Ireland; in The Geology and Genesis of Mineral Deposits in Ireland (ed.) C.J. Andrew, R.W.A. Crowe, S. Finlay, W.M. Pennell, and J.F. Pyne; Irish Association of Economic Geology and Geological Survey of Ireland, p. 377-418.

Andrew, C.J. and Ashton, J.H.
1985: Regional setting, geology and metal distribution patterns of Navan orebody, Ireland; Institution of Mining and Metallurgy Transactions, v. 94, p. B66-B93.

Ansdell, K.M., Nesbitt, B.E., and Longstaffe, F.J.
1989: A fluid inclusion and stable isotope study of the Tom Ba-Pb-Zn deposit, Yukon Territory, Canada; Economic Geology, v. 84, p. 841-856.

Bäcker, H.,
1975: Exploration of the Red Sea and Gulf of Aden during the M.S. VALDIVIA cruises "Erzschlämme A" and "Erzschlämme B"; Geologisches Jarbuch, D.17, p. 3-78.

***Badham, J.P.N.**
1981: Shale-hosted Pb-Zn deposits: products of exhalation of formation waters?; Institution of Mining and Metallurgy Transactions, Section B, v. 90, p. B70-B76.

***Bailes, R.J., Smee, B.W., Blackadar, D.W., and Gardner, H.D.**
1986: Geology of the Jason lead-zinc-silver deposits, Macmillan Pass, eastern Yukon; in Mineral Deposits of Northern Cordillera (ed.) J.A. Morin; The Canadian Institute of Mining and Metallurgy, Special Volume 37, p. 87-99.

Barrett, T.J. and Anderson, G.M.
1982: The solubility of sphalerite and galena in NaCl brines; Economic Geology, v. 77, p. 1923-1933.

Beaty, D.W., Hahn, G.A., and Threlkeld, W.E.
1988: Field, isotopic and chemical studies of tourmaline-bearing rocks in the Belt-Purcell Supergroup: genetic constraints and exploration significance for Sullivan type ore deposits; Canadian Journal of Earth Sciences, v. 25, p. 392-402.

Bell, T.H., Perkins, W.G., and Swager, C.P.
1988: Structural controls on the development and localization of syntectonic copper mineralization at Mount Isa, Queensland; Economic Geology, v. 83, p. 69-85.

Bignell, R.D., Cronan, D.S., and Tooms, J.S.
1976: Red Sea metalliferous brine precipitates; in Metallogeny and Plate Tectonics (ed.) D.F. Strong; Geological Association of Canada, Special Paper 14, p. 147-179.

Boast, A.M., Coleman, M.L., and Halls, C.
1981: Textural and stable isotopic evidence for the genesis of the Tynagh base metal deposit, Ireland; Economic Geology, v. 76, p. 27-55.

Both, R.A. and Rutland, R.W.R.
1976: The problem of identifying and interpreting stratiform orebodies in highly metamorphosed terrains: the Broken Hill example; in Handbook of Stratabound and Stratiform Ore Deposits (ed.) K.H. Wolfe; Elsevier, Amsterdam, v. 4, p. 261-325.

Carmichael, A.J.
1988: The tectonics and mineralization of the Black Angel Pb-Zn deposits, central West Greenland; PhD. thesis, Goldsmith's College, University of London, 371 p.

Carne, R.C. and Cathro, R.J.
1982: Sedimentary exhalative (SEDEX) zinc-lead deposits, northern Canadian Cordillera; The Canadian Mining and Metallurgy Bulletin, v. 75, p. 66-78.

Carvalho, I.G., Zantop, H., and Torquato, J.R.F.
1982: Geologic setting and genetic interpretation of the Boquira Pb-Zn deposits, Bahia State, Brazil; Revista Brasiliera de Geociencias, v. 12, p. 414-425.

Clayton, R.H. and Thorpe, L.
1982: Geology of the Nanisivik zinc-lead deposit; in Precambrian Sulphide Deposits (ed.) R.W. Hutchinson, C.D. Spence, and J.M. Franklin; Geological Association of Canada, Special Paper 25, p. 739-760.

Clifford, J.A., Ryan, P., and Kucha, H.
1986: A review of the geological setting of the Tynagh orebody, Co. Galway; in The Geology and Genesis of Mineral Deposits in Ireland (ed.) C.J. Andrew, R.W.A. Crowe, S. Finlay, W.M. Pennell, and J.F. Pyne; Irish Association of Economic Geology and Geological Survey of Ireland, p. 419-440.

Coates, J.S., Smith, C.G., Fortney, N.J., Gallager, M.J., May, F., and McCourt, W.J.
1980: Stratabound barium-zinc mineralization in Dalradian schist near Aberfeldy, Scotland; Institution of Mining and Metallurgy, Transactions, v. B.89, p. 110-122.

Deb, M.
1990: Regional metamorphism of sediment-hosted, conformable base-metal sulfide deposits in the Aravalli-Delhi Orogenic Belt, NW India; in Regional Metamorphism of Ore Deposits and Genetic Implications, (ed.) P.G. Spry and L.T. Bryndzia; (Proceedings of the Twenty-eighth International Geology Congress), VSP Utrecht, The Netherlands, p. 117-140.
1982: Crustal evolution and Precambrian metallogenesis in western India; Revista Brasiliera de Geociencias, v. 12, p. 94-104.

Deb, M. and Bhattacharya, A.K.
1980: Geological setting and conditions of metamorphism of Rajpura-Dariba polymetallic ore deposit, Rajasthan, India; in Proceedings of the Fifth International Association on the Genesis of Ore Deposits Symposium, (ed.) J.D. Ridge; E. Schweizerbart'sche Verlagsbuchhandlung, Stuttgart, v. 1, p. 679-697.

Deb, M., Thorpe, R.I., Cumming, G.L., and Wagner, P.A.
1989: Age, source and stratigraphic implications of Pb isotope data for conformable, sediment-hosted, base metal deposits in the Proterozoic Aravalli-Delhi orogeneic belt, northwestern India; Precambrian Research, v. 43, p. 1-22.

Degens, E.T. and Ross, D.A. (ed.)
1969: Hot Brines and Recent Heavy Metal Deposits in the Red Sea; Springer-Verlag, New York, 600 p.

Eisbacher, G.H.
1981: Sedimentary tectonics and glacial record in the Windermere Supergroup, Mackenzie Mountains, northwestern Canada; Geological Survey of Canada, Paper 80-27, 40 p.

Eldridge, C.S., Compston, W., Williams, I.S., Both, R.A., Walshe, J.L., and Ohmoto, H.
1993: Sulfur isotope variability in sediment-hosted massive sulfide deposits as determined using the ion microprobe SHRIMP: II. A study of the H.Y.C. deposit at McArthur River, Northern Terrotory, Australia; Economic Geology, v. 88, p. 1-26.

Eldridge, C.S., Williams, N., and Walshe, J.L.
1988: Sulfur isotope variability in sediment-hosted massive sulfide deposits as determined using the ion microprobe SHRIMP: 1. An example from the Rammelsberg orebody - a discussion; Economic Geology, v. 83, p. 443-449.

Espourteille, F. and Fleischer, R.
1988: Mina de chumbo de Boquira, Bahia; in Principais Depositos Minerais do Brasil, Volume III, (co-ordinators) C. Schobbenhaus and C.E. Silva Coelho; Ministerio das Minas e Energia, Republica Federativa do Brasil, Brasilia, chap. X, p. 91-99.

Ethier, V.G., Campbell, F.A., Both, R.A., and Krouse, H.R.
1976: Geological setting of the Sullivan Orebody and estimates of temperatures and pressures of metamorphism; Economic Geology, v. 71, p. 1570-1588.

Finlow-Bates, T.
1980: The chemical and physical controls on the genesis of submarine exhalative orebodies and their implications for formulating exploration concepts; Geologisches Jahrbuch, D. 40, p. 131-168.

Forrest, K. and Sawkins, F.J.
1984: The Lik deposit, western Brooks: Sedex mineralization along axial vent sites in a structural basin; in Abstracts with Program, Geological Society of America, Ninty-seventh Annual Meeting, Reno, Nevada, p. 511.

Forrestal, P.J.
1990: Mount Isa and Hilton silver-lead-zinc deposits; in Geology of the Mineral Deposits of Australia and Papua New Guinea (ed.) F.E. Hughes; The Australasian Institute of Mining and Metallurgy, Melbourne, Monograph 14, v. 1, p. 927-934.

Gabrielse, H. and Campbell, R.B.
1991: Upper Proterozoic assemblages, Chapter 6 in Geology of the Cordilleran Cordilleran Orogen in Canada (ed.) H. Gabrielse and C.J. Yorath; Geological Survey of Canada, Geology of Canada, no. 4, p. 125-150 (also Geological Society of America, The Geology of North America, v. G-2).

Garde, A.A.
1978: The Lower Proterozoic Marmorilik Formation, east of Marmorilik, West Greenland; Meddelelser om Grønland, v. 200, no. 3, 71 p.

Gardner, H.D. and Hutcheon, I.
1985: Geochemistry, mineralogy and geology of the Jason Pb-Zn deposits, Macmillan Pass, Yukon, Canada; Economic Geology, v. 80, p. 1257-1276.

Gemmell, J.B., Zantop, H., and Meinert, L.D.
1992: Genesis of the Aguilar zinc-lead-silver deposit, Argentina: contact metasomatic vs. sedimentary exhalative; Economic Geology, v. 87, p. 2085-2112.

Goodfellow, W.D.
1987: Anoxic stratified oceans as a source of sulphur in sediment-hosted stratiform Zn-Pb deposits (Selwyn Basin, Yukon, Canada); Chemical Geology, v. 65, p. 359-382.

Goodfellow, W.D. and Franklin, J.M.
1993: Geology, mineralogy and chemistry of sediment-hosted clastic massive sulfides in shallow cores, Middle Valley, northern Juan de Fuca Ridge; Economic Geology, v. 88, p. 2033-2064.

***Goodfellow, W.D. and Jonasson, I.R.**
1986: Environment of formation of the Howards Pass (XY) Zn-Pb deposit, Selwyn Basin, Yukon; in Mineral Deposits of Northern Cordillera (ed.) J.A. Morin; The Canadian Institute of Mining and Metallurgy, Special Volume 37, p. 19-50.

Goodfellow, W.D., and Rhodes, D.
1990: Geological setting, geochemistry and origin of the Tom stratiform Zn-Pb-Ag-barite deposits; in Mineral Deposits of the Northern Canadian Cordillera (ed.) J.G. Abbott and R.J.W. Turner; International Association on the Genesis of Ore Deposits, Eighth Symposium, Ottawa, Field Trip 14: Guidebook, Geological Survey of Canada, Open File 2169, p. 177-244.

Goodfellow, W.D. and Turner, R.J.
1989: Sulfur isotope variability in sediment-hosted massive sulfide deposits as determined using the ion microprobe SHRIMP: 1. An example from the Rammelsberg orebody - a discussion; Economic Geology, v. 84, p. 451-452.

Goodfellow, W.D., Grapes, K., Cameron, B., and Franklin, J.M.
1994: Hydrothermal alteration associated with massive sulphide deposits, Middle Valley, Northern Juan de Fuca Ridge; Canadian Mineralogist, v. 31, p. 1025-1060.

Gordey, S.P., Abbott, J.G., and Orchard, M.J.
1982: Devono-Mississippian (Earn Group) and younger strata in east-central Yukon; in Current Research, Part B; Geological Survey of Canada, Paper 82-1B, p. 93-100.

Gwosdz, W. and Krebs, W.
1977: Manganese halo surrounding Meggen ore deposit, Germany; Institution of Mining and Metallurgy Transactions, Section B, v. 86, p. B73- B77.

***Hamilton, J.M., Bishop, D.T., Morris, H.C., and Owens, O.E.**
1982: Geology of the Sullivan orebody, Kimberley, B.C., Canada; in Precambrian Sulphide Deposits (ed.) R.W. Hutchinson, C.D. Spence, and J.M. Franklin; Geological Association of Canada, Special Paper 25, H.S. Robinson Memorial Volume, p. 597-665.

Hamilton, J.M., Delaney, G.D., Hauser, R.L., and Ransom, P.W.
1983: Geology of the Sullivan deposit, Kimberley, B.C., Canada; in Sediment-hosted Stratiform Lead-zinc Deposits (ed.) D.F. Sangster; Mineralogical Association of Canada, Short Course Handbook, v. 8, p. 31-83.

Hannak, W.W.
1981: Genesis of the Rammelsberg ore deposit near Goslar/Upper Hartz, Federal Republic of Germany; in Handbook of Stratabound and Stratiform Ore Deposits, (ed.) K.H. Wolfe; Elsevier, Amsterdam, v. 9, p. 551-642.

Heinrichs, T.K. and Reimer, T.O.
1977: A sedimentary barite deposit from the Archean Fig Tree Group of the Barberton Mountain Land (South Africa); Economic Geology, v. 72, p. 1426-1441.

Hitzman, M.W.
1986: Geology of the Abbeytown mine, Co. Sligo, Ireland; in The Geology and Genesis of Mineral Deposits in Ireland (ed.) C.J. Andrew, R.W.A. Crowe, S. Finlay, W.M. Pennell, and J.F. Pyne; Irish Association of Economic Geology and Geological Survey of Ireland, p. 341-354.

Hitzman, M.W. and Large, D.E.
1986: A review and classification of the Irish carbonate-hosted base metal deposits; in Geology and Genesis of the Mineral Deposits in Ireland (ed.) C.J. Andrew, R.W.A. Crowe, S. Finlay, W.A. Pennell, and J.F. Pyne; Irish Association for Economic Geology and Geological Survey of Ireland, p. 217-237.

Hoffman, P.F.
1991: Did the breakout of Laurentia turn Gondwanaland inside-out?; Science, v. 252, p. 1409-1412.

Hou, B. and Zhao, D.
1993: Geology and genesis of the Bajiazi polymetallic sufide deposits, Liaoning, China; International Geology Review, v. 35, p. 920-943.

Höy, T.
1982: Stratigraphic and structural setting of stratabound lead-zinc deposits in southeastern B.C.; The Canadian of Mining and Metallurgical Bulletin, v. 75, p. 114-134.

Jardine, D.E.
1966: An investigation of brecciation associated with the Sullivan mine ore body at Kimberley, B.C.; MSc. thesis, University of Manitoba, Winnipeg, Manitoba, 121 p.

Jefferson, C.W., Kilby, D.B., Pigage, L.C., and Roberts, W.J.
1983: The Cirque barite-zinc-lead deposits, northeastern British Columbia; in Sediment-hosted Stratiform Lead-zinc Deposits (ed.) D.F. Sangster; Mineralogical Association of Canada, Short Course Handbook, v. 8, p. 121-139.

***Jennings, D.S. and Jilson, G.A.**
1986: Geology and sulphide deposits of the Anvil Range, Yukon; in Mineral Deposits of Northern Cordillera (ed.) J.A. Morin; The Canadian Institute of Mining and Metallurgy, Special Volume 37, p. 339-361.

Krebs, W.
1981: The geology of the Meggen ore deposit; in Handbook of Stratabound and Stratiform Ore Deposits (ed.) K.H. Wolfe; Elsevier, Amsterdam, v. 9, p. 510-549.

Kröner, A., Byerly, G.R., and Lowe, D.R.
1991: Chronology of early Archean granite-greenstone evolution in the Barberton Mountain Land, South Africa, based on precise dating by single zircon evaporation; Earth and Planetary Science Letters, v. 103, p. 41-54.

Lambert, I.B.
1976: The McArthur zinc-lead-silver deposits: features, metallogenesis, and comparisons with some other stratiform ores; in Handbook of Stratabound and Stratiform Ore Deposits, (ed.) K.H. Wolfe; Elsevier, Amsterdam, v. 6, p. 535-585.

Lang, D.Y. and Znang Xingjun
1987: Geological setting and genesis of the Jiashengpan Pb-Zn-S ore belt, Inner Mongolia; People's Republic of China, v. 6, p. 39-54 (Geological Survey of Canada Translation no. 3124).

***Large, D.E.**
1983: Sediment-hosted massive sulphide lead-zinc deposits: an empirical model; in Sediment-hosted Stratiform Lead-zinc Deposits (ed.) D.F. Sangster; Mineralogical Association of Canada, Short Course Handbook, v. 8, p. 1-29.

Laznicka, P.
1981: Data on the worldwide distribution stratiform and stratabound ore deposits; in Handbook of Stratiform and Stratabound Ore Deposits, (ed.) K.H. Wolfe; Elsevier, Amsterdam, v. 9, p. 479-576.

Lea, E.R. and Dill, D.B.
1968: Zinc deposits of the Balmat-Edwards District; in Ore Deposits of the United States, 1933-1967: Graton-Sales Volume 1, (ed.) J.D. Ridge; American Institute of Mining, Metallurgical and Petroleum Engineers, p. 20-48.

Leitch, C.H.B.
1992: A progress report of fluid inclusion studies of veins from the vent zone, Sullivan stratiform sediment-hosted Zn-Pb deposit, B.C.; in Current Research, Part E; Geological Survey of Canada, Paper 92-1E, p. 71-82.

Logan, R.G., Murray, W.J., and Williams, N.
1990: HYC Silver-lead-zinc deposit, McArthur River; in Geology of the Mineral Deposits of Australia and Papua New Guinea (ed.) F.E. Hughes; The Australasian Institute of Mining and Metallurgy, Melbourne, Monograph 14, v. 1, p. 907-911.

Louden, A.G., Lee, M.K., Dawling, J.F., and Bourn, R.
1975: Lady Loretta silver-lead-zinc deposit, Northern Territory; in Economic Geology of Australia and Paupa New Guinea, 1. Metals, (ed.) C.L. Knight; Australasian Institute of Mining and Metallurgy, Monograph 5, p. 377-382.

***Lydon, J.W.**
1983: Chemical parameters controlling the origin and deposition of sediment-hosted stratiform lead-zinc deposits; in Sediment-hosted Stratiform Lead-zinc Deposits, (ed.) D.F. Sangster; Mineralogical Association of Canada, Short Course Handbook, v. 8, p. 175-250.

Lydon, J.W., Goodfellow, W.D., and Jonasson, I.R.
1985: A general genetic model for stratiform baritic deposits of the Selwyn Basin, Yukon Territory and District of Mackenzie; in Current Research, Part A; Geological Survey of Canada, Paper 85-1A, p. 651-660.

Lydon, J.W., Lancaster, R.D., and Karkkainen, P.
1979: Genetic controls of Selwyn Basin stratiform barite/sphalerite/galena deposits: an investigation of the dominant barium mineralogy of the TEA deposit, Yukon; in Current Research, Part B; Geological Survey of Canada, Paper 79-1B, p. 223-229.

MacIntyre, D.G.
1983: Geologic setting of recently discovered stratiform barite-sulphide deposits in northeastern British Columbia; Canadian Institute Mining and Metallurgy Bulletin, v. 75, p. 99-113.
1992: Geological setting and genesis of sedimentary exhalative barite and barite-sulfide deposits, Gataga District, northeastern British Columbia; Exploration and Mining Geology, v. 1, no. 1, p. 1-20.

Mackenzie, D.H. and Davies, R.H.
1990: Broken Hill lead-silver-zinc deposit at Z.C. mines; in Geology of the Mineral Deposits of Australia and Papua New Guinea (ed.) F.E. Hughes; The Australasian Institute of Mining and Metallurgy, Melbourne, Monograph 14, v. 2, p. 1079-1084.

Mathias, B.V. and Clark, G.J.
1975: Mount Isa copper and silver-lead-zinc orebodies - Isa and Hilton mines; in Economic Geology of Australia and Paupa New Guinea, 1. Metals (ed.) C.L. Knight; Australasian Institute of Mining and Metallurgy, Monograph 5, p. 351-372.

***McClay, K.R. and Bidwell, G.E.**
1986: Geology of the Tom deposit, Macmillan Pass, Yukon; in Mineral Deposits of Northern Cordillera, (ed.) J.A. Morin; The Canadian Institute of Mining and Metallurgy, Special Volume 37, p. 100-114.

McKibben, M.A. and Eldridge, C.S.
1989: Sulfur isotopic variations among minerals and aqueous species in the Salton Sea geothermal system: a SHRIMP ion microprobe and conventional study of active ore genesis in a sediment-hosted environment; American Journal of Science, v. 289, p. 661-707.

McKibben, M.A., Andes, J.P. Jr., and Williams, A.E.
1988: Active ore-formation at a brine interface in metamorphosed deltaic-lacustrine sediments: the Salton Sea geothermal system, California; Economic Geology, v. 83, p. 511-523.

McLarsn, D.C.
1946: The New Calumet mines; Canadian Mining Journal, v. 67, p. 233-241.

Miller, D. and Wright, J.
1983: Mel barite-zinc-lead deposit, Yukon - an exploration case history: in Mineral Deposits of Northern Cordillera (ed.) J.A. Morin; The Canadian Institute of Mining and Metallurgy, Special Volume 37, p. 129-141.

Moore, D.W., Young, L.E., Modene, J.S., and Plahuta, J.T.
1986: Geological setting and genesis of the Red Dog zinc-lead-silver deposit, Western Brooks Range, Alaska; Economic Geology, v. 81, p. 1696-1727.

Morrissey, C.J., Davis, G.R., and Steed, G.M.
1971: Mineralization in the Lower Carboniferous of central Ireland; Institution of Mining and Metallurgy Transactions, Section B, v. 80, p. 174-185.

Nandan Raghu, K.R., Dhruva Rao, B.K., and Singhal, M.L.
1981: Exploration for copper, lead and zinc ores in India (incorporating the compilation made by late S. Narayanaswamy); Bulletin of the Geological Survey of India, Series A, no. 47, 222 p.

Page, D.C. and Watson, M.D.
1976: The Pb-Zn deposit of Rosh Pinah, South West Africa; Economic Geology, v. 75, p. 1022-1041.

Page, R.W.
1981: Depositional ages of the stratiform base metal deposits at Mount Isa and McArthur River, Australia, based on U-Pb zircon dating of concordant tuff horizons; Economic Geology, v. 76, p. 648-658.

Patterson, J.M.
1988: Exploration potential for argentiferous base metals at the Walton deposit, Hand County, Nova Scotia; in Report of Activities 1987, Nova Scotia Department of Mines and Energy, Report 88-1, p. 129-134.

Pedersen, F.D.
1981: Polyphase deformation of the massive sulphide ore of the Black Angel mine, central West Greenland; Mineralium Deposita, v. 16, p. 157-176.

Perkins, W.G.
1984: Mount Isa silica-dolomite and copper orebodies: the result of a syntectonic hydrothermal alteration system; Economic Geology, v. 79, p. 601-637.

Phillips, W.E.A. and Sevastopulo, G.D.
1986: The stratigraphic and structural setting of Irish mineral deposits; in The Geology and Genesis of Mineral Deposits in Ireland (ed.) C.J. Andrew, R.W.A. Crowe, S. Finlay, W.M. Pennell, and J.F. Pyne; Irish Association of Economic Geology and Geological Survey of Ireland, p. 1-30.

***Pigage, L.C.**
1986: Geology of the Cirque barite-zinc-lead-silver deposits, northeastern British Columbia; in Mineral Deposits of Northern Cordillera, (ed.) J.A. Morin; The Canadian Institute of Mining and Metallurgy, Special Volume 37, p. 71-86.

Ranawat, P.S. and Sharma, N.K.
1990: Petrology and geochemistry of the Precambrian lead-zinc deposit, Rampura-Agucha, India; in Regional Metamorphism of Ore Deposits and Genetic Implications, (ed.) P.G. Spry and L.T. Bryndzia; (Proceedings of the Twenty-eighth International Geological Congress), VSP Utrecht the Netherlands, p. 197-227.

Reid, D.L., Welke, H.J., Erlank, A.J., and Betton, P.J.
1987: Composition, age and tectonic setting of amphibolites in the central Bushmanland Group, western Namaqua Province, southern Africa; Precambrian Research, v. 36, p. 99-126.

Russell, M.J.
1974: Manganese halo surrounding the Tynagh ore deposit, Ireland: a preliminary note; Institution of Mining and Metallurgy Transactions, Section B, v. 83, p. B65-B66.
1975: Lithogeochemical environment of the Tynagh base metal deposit, Ireland, and its bearing on ore deposition; Institution of Mining and Metallurgy Transactions, Section B, v. 84, p. B128-B133.

***Russell, M.J., Solomon, M., and Walshe, J.L.**
1981: The genesis of sediment-hosted, exhalative zinc + lead deposits; Mineralium Deposita, v. 16, p. 113-127.

Ryan, P.J., Lawrence, A.L., Lipson, A.L., Moore, J.M., Paterson, A., Stedman, D.P., and Van Zyl, D.
1986: The Aggeneys base metal sulphide deposits, Namaqualand District; in Mineral Deposits of Southern Africa (ed.) C.R. Anhaeusser and S. Maske; Geological Society of South Africa, Johannesburg, p. 1447-1474.

Sangster, D.F.
1981: Three potential sites for the occurrence of stratiform, shale-hosted lead-zinc deposits in the Canadian Arctic; in Current Research, Part A; Geological Survey of Canada, Paper 81-1A, p. 1-8.
*1990: Mississippi Valley-type and Sedex lead-zinc deposits: a comparative examination; Institution of Mining and Metallurgy Transactions, Section B, v. 99, p. B21-B42.

Samson, I.M. and Russell, M.J.
1987: Genesis of the Silvermines zinc-lead-barite deposit, Ireland: fluid inclusion and stable isotope evidence: Economic Geology, v. 82, p. 371-394.

Sarkar, S.C.
1974: Sulphide mineralization at Sargipali, Orissa, India; Economic Geology, v. 69, p. 206-217.

Sato, T.
1972: Behaviours of ore-forming solutions in sea water; Mining Geology, v. 22, p. 31-42.

***Sawkins, F.J.**
1984: Ore genesis by episodic dewatering of sedimentary basins: application to giant Proterozoic lead-zinc deposits; Geology, v. 12, p. 451-454.

Schmidt, B.L.
1990: Elura zinc-lead deposit, Cobar; in Geology of the Mineral Deposits of Australia and Papua New Guinea (ed.) F.E. Hughes; The Australasian Institute of Mining and Metallurgy, Melbourne, Monograph 14, v. 2, p. 1329-1336.

Scotese, C.R.
1984: An introduction to this volume: Paleozoic paleomagnetism and the assembly of Pangea; in Plate Reconstruction from the Paleozoic Paleomagnetism (ed.) R. Van der Voo, C.R. Scotese, and N. Bonhommet; American Geophysical Union, Geodynamic Series, v. 12, p. 1-10.

Shanks, W.C., Woodruff, L.G., Jilson, G.A., Jennings, D.S., Modene, J.S., and Ryan, B.D.
1987: Sulfur and lead isotope studies of stratiform Zn-Pb-Ag deposits, Anvil Range, Yukon: basinal brine exhalation and anoxic bottom-water mixing; Economic Geology, v. 82, p. 600-634.

Shearley, E., Hitzman, M.W., Walton, G., Redmond, P., Davis, R., King, M., Duffy, L., and Goodman, R.
1992: Structural controls of mineralization, Lisheen Zn-Pb-Ag deposit, County Tipperary, Ireland; in Abstracts with Program, Geological Society of America, Annual Meeting, Cincinnati, p. A.354.

Shipboard Scientific Party
1992a: Site 858; in Proceedings of the Ocean Drilling Program, Initial Reports, Leg 139, College Station, TX(Ocean Drilling Program), p. 431-569.
1992b: Site 856; in Proceedings of the Ocean Drilling Program, Initial Reports, Leg 139, College Station, TX(Ocean Drilling Program), p. 161-281.

Simon, A.A., Garcia, L.A., and Barzana, J.A.
1990: Jurassic metallogenesis in the greater Antilles: the Matahambre-Santa Lucia ore district, western Cuba; in Program with Abstracts, International Association on the Genesis of Ore Deposits, Eighth Symposium, Ottawa, p. A184-185.

Skauli, H., Boyce, A.J., and Fallick, A.E.
1992: A sulphur isotope study of the Bleikvassli Zn-Pb-Cu deposit, Nordland, northern Norway; Mineralium Deposita, v. 27, p. 284-294.

Slack, J.F., Palmer, M.R., Stevens, B.P., and Barnes, R.G.
1993: Origin and significance of tourmaline-rich rocks in the Broken Hill District, Australia; Economic Geology, v. 88, p. 505-541.

Smirnov, V.I. and Gorzhersky, D.I.
1977: Deposits of lead and zinc; in Ore Deposits of the USSR, (ed.) V.I. Smirnov; v. 2, Pitman, London, p. 182-256.

Smith, J.W. and Croxford, N.J.W.
1973: Sulphur isotope ratios in McArthur Pb-Zn-Ag deposit; Nature, v. 245, p. 10-12.

Solomon, M. and Walshe, J.L.
1979: The formation of massive sulphide deposits on the sea floor; Economic Geology, v. 74, p. 797-813.

Spry, P.G.
1987: The chemistry and origin of zincian spinel associated with the Aggeneys Cu-Pb-Zn-Ag deposits, Namaqualand, South Africa; Mineralium Deposita, v. 22, p. 262-268.

Stanton, R.L.
1963: Constitutional features of the Mount Isa sulphide ores and their interpretation; Proceedings of the Australasian Institute of Mining and Metallurgy, v. 205, p. 131-153.

Sureda, R.J. and Martin, J.L.
1990: El Aguilar mine: an Ordovician sediment-hosted stratiform lead-zinc deposit in the Central Andes; in Stratabound Ore Deposits in the Andes, (ed.) L. Fontbote, G.C. Amstutz, M. Cardozo, E. Cedillo, and J. Frutos; Special Publication of the Society for Geology Applied to Ore Deposits, No. 8, Springer Verlag, Berlin, p. 161-174.

Sverjensky, D.A.
1984: Oil field brines as ore-forming solutions; Economic Geology, v. 79, p. 23-37.

Taylor, S.
1984: Structural and paleotopographic controls of lead-zinc mineralization in the Silvermines orebodies, Republic of Ireland; Economic Geology, v. 79, p. 529-548.

Thomassen, B.
1991: The Black Angel lead-zinc mine 1973-90; in Current Research, Grønlands Geologiske Undersøgelse, (ed.) A.K. Higgins and M. Sonderholm; Rapport 152, p. 46-50.

Tikkanen, G.D.
1986: World resources and supply of lead and zinc; in Economics of Internationally Traded Minerals, (ed.) W.R. Bush; Society of Mining Engineers, Inc., p. 242-250.

Turner, J.S. and Gustafson, L.B.
1978: The flow of hot saline solutions from vents in the sea floor - some implications for exhalative massive sulfide and other ore deposits; Economic Geology, v. 73, p. 1082-1100.

Turner, R.J.W.
1990: Jason stratiform Zn-Pb-barite deposit, Selwyn Basin, Canada (NTS 105-O-1): Geological setting, hydrothermal facies and genesis; in Mineral Deposits of the Northern Canadian Cordillera, (ed.) J.G. Abbott and R.J.W. Turner, International Association on the Genesis of Ore Deposits, Field Trip 14: Guidebook, Geological Survey of Canada, Open File 2169, p. 137-175.
1992: Formation of Phanerozoic stratiform sediment-hosted zinc-lead deposits: evidence for the critical role of oceanic anoxic events; Chemical Geology, v. 99, p. 165-188.

Valdes-Nodarse, E.L., Diaz-Carmona, A., Davies, J.F., Whitehead, R.E., and Fonseca, L.
1993: Cogenetic sedex Zn-Pb and stockwork ores, western Cuba; Exploration and Mining Geology, v. 2, no. 4, p. 297-306.

van den Heyden, A. and Edgecombe, D.R.
1990: Silver-lead-zinc deposit at South Mine, Broken Hill; in Geology of the Mineral Deposits of Australia and Papua New Guinea, (ed.) F.E. Hughes; The Australasian Institute of Mining and Metallurgy, Melbourne, Monograph 14, v. 2, p. 1073-1077.

van Vuuren, C.J.J.
1986: Regional setting and structure of the Rosh Pinah zinc-lead deposit, South West Africa / Namibia; in Mineral Deposits of Southern Africa, (ed.) C.R. Anhaeusser and S. Maske; Geological Society of South Africa, Johannesburg, p. 1593-1607.

Von Damm, K.L., Edmond, J.M., Measures, C.I., and Grant, B.
1985: Chemistry of submarine hydrothermal solutions at Guaymas Basin, Gulf of California; Geochimica et Cosmochimica Acta, v. 49, p. 2221-2237.

Whitcher, I.G.
1975: Dugald River zinc-lead lode; in Economic Geology of Australia and Papua New Guinea, 1. Metals, (ed.) C.L. Knight; Australasian Institute of Mining and Metallurgy, Monograph 5, p. 372-376.

Willan, R.C.R. and Coleman, M.L.
1983: Sulphur isotope study of the Aberfeldy barite, zinc, lead deposit and minor sulphide mineralization in the Dalradian Metamorphic Terrain, Scotland; Economic Geology, v. 78, p. 1619-1656.

Williams, N.
*1978a: Studies of base metal sulphide deposits at McArthur River, Northern Territory, Australia: I. The Cooley and Ridge deposits; Economic Geology, v. 73, p. 1005-1035.
*1978b: Studies of base metal sulfide deposits at McArthur River, Northern Territory, Australia: II. The sulfide-S and organic-C relationships of the concordant deposits and their significance; Economic Geology, v. 73, p. 1036-1056.

Williams, N. and Rye, D.M.
1974: Alternative interpretation of sulphur isotope ratios in the McArthur lead-zinc-silver deposit; Nature, v. 247, p. 535-537.

Wilton, D., Archibald, S., Hussey, A., and Butler, R.
1993: Report on metallogenetic investigations on the north Labrador coast during 1993; Newfoundland Department of Mines and Energy, Open File 996, 17 p.

Wright, J.V., Haydon, R.C., and McConachy, G.W.
1987: Sedimentary model for the giant Broken Hill Pb-Zn deposit, Australia; Geology, v. 15, p. 598-602.

Zhidkov, A. and Jalturin, N.L.
1976: Mineralizacion estratiforme piritico-polimetallica, Zonà La Oriental-Baritina; Revista La Mineria en Cuba, no. 3, p. 28-39.

Zierenberg, R.A., Koski, R.A., Morton, J.L., and Bouse, R.M.
1993: Genesis of massive sulfide deposits on a sediment-covered spreading center, Escanaba Trough, southern Gorda Ridge; Economic Geology, v. 88, p. 2065-2094.

6.2 SEDIMENTARY NICKEL SULPHIDES

Larry J. Hulbert

INTRODUCTION

The significant nickel occurrences of this type that have been recognized to date are typically thin, sheet-like, nickel-enriched pyritic sulphide layers of great lateral extent in phosphoritic marine shale basins. In the Nick basin, Yukon Territory, the main associated metals are Zn and platinum-group elements (PGEs), whereas those in several deposits in Lower Cambrian strata of southern China are mainly Mo, but also include PGEs, Cu, and Zn. These two districts contain the only presently known, near- or subeconomic examples, and the following account is based almost entirely on findings from the Nick property (Hulbert et al., 1992).

Hulbert, L.J.
1996: Sedimentary nickel sulphides; in Geology of Canadian Mineral Deposit Types, (ed.) O.R. Eckstrand, W.D. Sinclair, and R.I. Thorpe; Geological Survey of Canada, Geology of Canada, no. 8, p. 152-158 (also Geological Society of America, The Geology of North America, v. P-1).

The Nick property is centred on 64°43′N latitude and 135°13′W longitude in the Yukon Territory, Canada (Fig. 6.2-1). At this locality a thin, sheet-like, Ni-Zn-PGE-enriched, pyritic massive sulphide layer was deposited over the entire expanse of a small Middle to Upper Devonian shale subbasin known informally as the "Nick basin" that represents an outlier of (eroded) Selwyn Basin sediments. A concretionary Limestone Ball member represents an important stratigraphic marker in the immediate footwall of the mineralized horizon.

In the discussion to follow, this new style of Ni-Zn-PGE mineralization is considered from the viewpoint of (i) regional and local geology; (ii) stratigraphic, structural, and tectonic setting; (iii) base metal, metalloids, noble metal, and stable isotope characteristics; and (iv) mineralogy. A model for the origin of this unusual style of mineralization, with its extraordinary assemblage of ore-forming and ore-associated elements will be presented.

IMPORTANCE

The Nick mineralization is believed to represent a new geological environment and potentially economic deposit type for Ni and PGEs. Globally, similar mineralization is only known from southern China (Fan, 1983; Coveney and Chen Nansheng, 1991). Now that it is fully appreciated that high grade Ni mineralization can be hosted in black shale environments, there is reason to believe that additional occurrences and exploitable deposits will be discovered. One deposit near Zunyi, Guizhou province, southern China has been mined for molybdenum and oil shale since 1985 (Coveney et al., 1992).

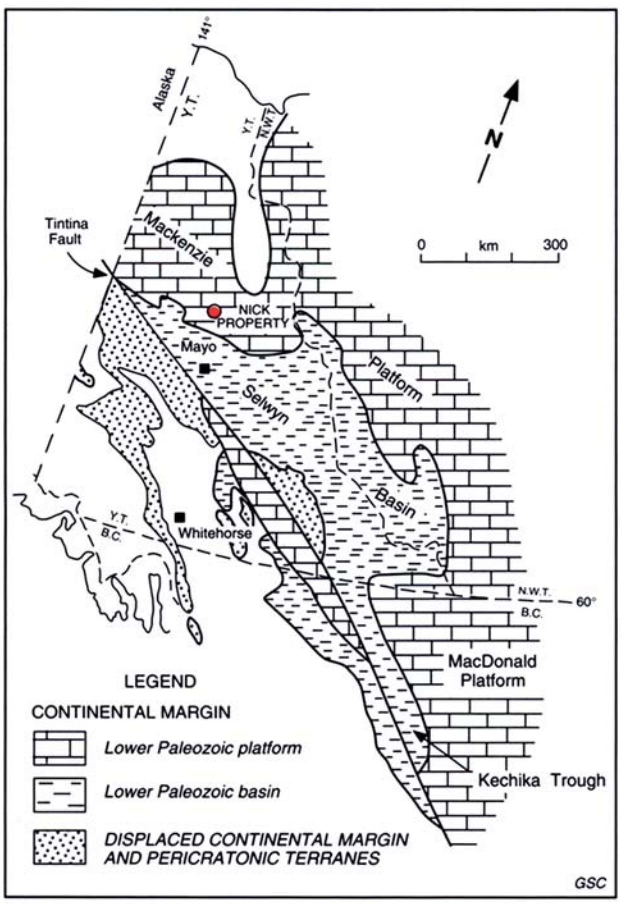

Figure 6.2-1. Map showing the location and geological setting of the Nick property and tectonic elements controlling the Lower Paleozoic facies distribution in the Northern Cordillera (modified after Tipper et al., 1978).

SIZE AND GRADE OF DEPOSIT

The mineralization in the Nick subbasin has been traced around the circumference of two major synclines, and constitutes a potentially mineralized area greater than 80 km^2 (Fig. 6.2-2). Assays of sulphide mineralization from this horizon indicate average grades of 5.3% Ni, 0.73% Zn, and 776 ppb PGEs+Au based on 9 samples (Table 6.2-1). Anomalous levels of Re, U, Mo, Ba, Se, As, V, and P are also present. Conservative estimates of the amount of Ni deposited at this mineralized horizon is about 0.90×10^6 t of Ni metal (based on an average thickness of 3 cm), clearly indicating a major North American Ni-metallogenic event. This is large by comparison with the amount of contained Ni in various major Ni camps in the world (Naldrett, 1973; Hulbert et al., 1992).

GEOLOGICAL FEATURES

Geological setting

The Nick property is located within the Mackenzie Platform tectonic province (Fig. 6.2-1). The associated stratiform Ni-Zn-PGE mineralization is hosted by two synclinal outliers of a late Paleozoic shale sequence (Fig. 6.2-2) that belong to the Road River Group and Earn Group strata typically associated with the contiguous Selwyn Basin to the south. The shale outliers overlie Cambrian to Ordovician carbonate rocks of the Mackenzie Platform and therefore the Nick basin is considered to be the erosional remnant of a local trough or embayment on the northeastern margin of the Selwyn Basin.

The main syncline is approximately 16 km by 2 km. A second syncline of about equal strike length, but of considerably narrower width, lies to the north (Fig. 6.2-2). These regional north-northwest-trending folds were generated in response to Cretaceous Laramide compression. Prominent regional-scale normal faults (Green, 1972) occur to the north, south, and east of the Paleozoic shale and are believed to represent the reactivated margins of a graben that was the site of Ordovician to Devonian deep water sedimentation within the platform (Fig. 6.2-2).

The Ni-Zn-PGE mineralization in the Nick basin occurs as a thin conformable massive sulphide horizon located near the stratigraphic contact between lower Earn Group strata, which consist of siliceous shale, mudstone, phosphatic chert, and concretionary limestone, and older calcareous rocks of the Road River Group. All strata are correlative with similar rocks of the Selwyn Basin. Preliminary age determinations based on conodonts extracted from the concretionary limestone in the immediate footwall of the mineralized horizon, suggest a Givetian-Frasnian age bracket (Middle-Upper Devonian boundary). The lower Earn Group is overlain by the Devonian-Mississippian upper Earn Group comprising noncalcareous siliceous and fine grained clastic rocks. Field relationships are illustrated in Figure 6.2-2 and stratigraphic relationships between the units and their approximate thickness are depicted in the stratigraphic column presented in Figure 6.2-3.

Contents

Stratigraphy

The oldest rocks in the vicinity of the Nick basin are part of an unnamed sequence of basinal Cambrian-Ordovician limestones (perhaps equivalent to the Rabbit Kettle Formation of the Selwyn Basin) formed during subsidence along a major east-trending, westerly deepening graben. The basin margins are now represented by regional faults. These dark calcareous rocks consist of platey dolomitic limestones that grade upward into calcareous shales. This sequence is at least 300 m thick but the base has not been observed in the map area. Following deposition of this sequence, Road River Group fetid calcareous graptolitic shale dominated sedimentation for the duration of the Ordovician to Lower Devonian. These dark grey to black shales attain a thickness of at least 100 m in the study area. The lower Earn Group rocks were deposited unconformably on Road River Group shales. Sedimentation had changed from that of a relatively quiescent and euxinic starved basinal sequence environment to an environment with increased circulation and ventilation and accompanying clastic sedimentation (Gordey et al., 1982). Locally, the

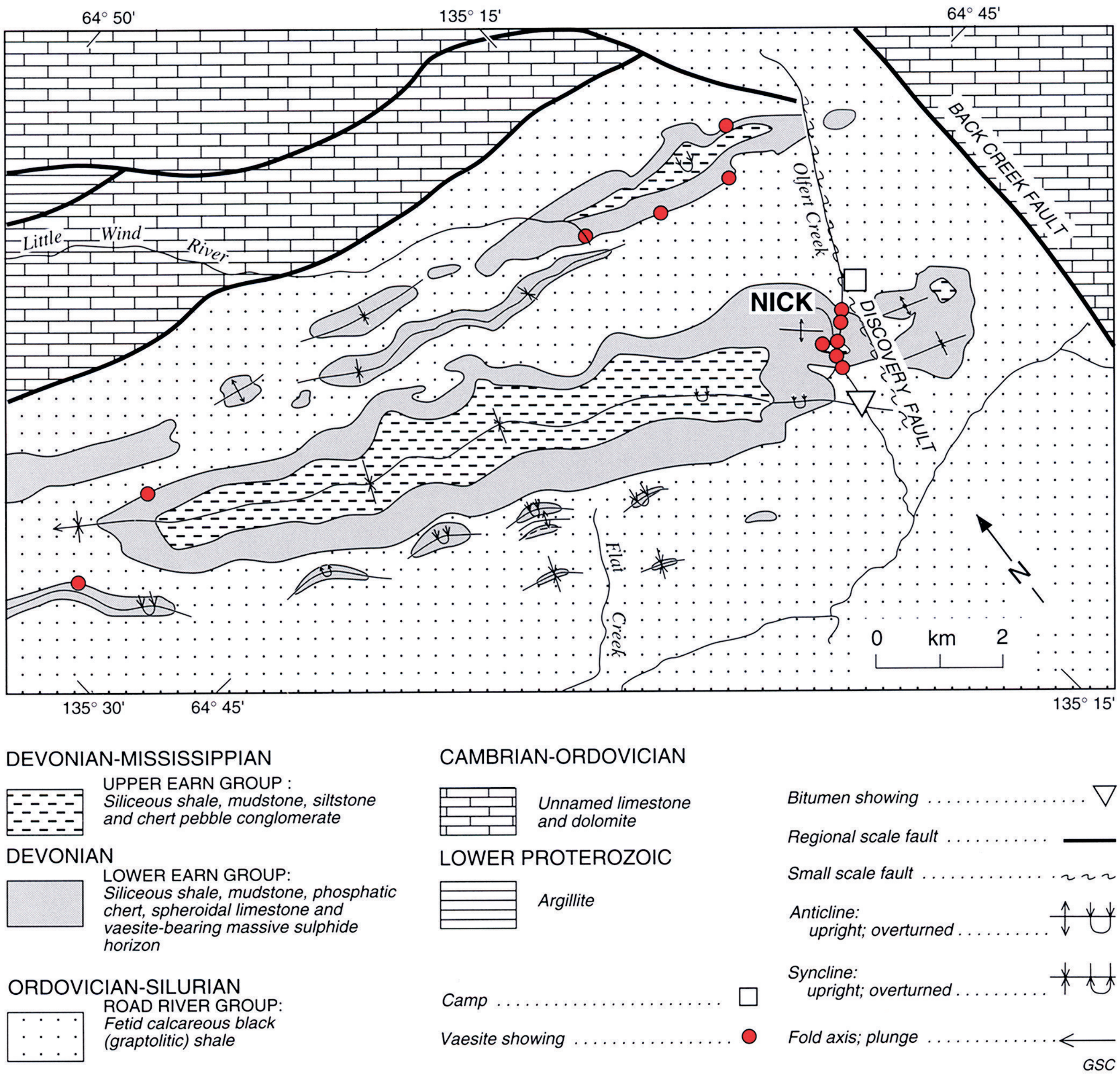

Figure 6.2-2. Geological map of the Nick basin; note reactivated basin margin faults and the Nick showing (discovery site) (after Hulbert et al., 1992).

Table 6.2-1. Metal content of 9 representative samples from the Nick horizon: C, S in wt.%; Pt, Pd, Au, Ir, Ru, Rh, Os, Re in ppb; all others in ppm (after Hulbert et al., 1992); " – " signifies no data.

Sample	1035	NICK-2	NICK-3	NICK-4	NICK-5	NICK-7A	NICK-7B	NICK-8X	DDH-1
C	2.2	2.20	2.50	1.40	1.30	1.80	2.20	1.70	1.90
S	29.10	32.40	20.70	32.70	31.70	27.80	31.70	26.10	20.20
F	349	353	360	293	336	275	533	225	229
Cl	240	<100	<100	123	<100	112	<100	<100	<100
V	880	590	740	370	720	530	570	730	560
Cr	240	160	140	160	140	160	150	180	190
Co	250	350	240	290	250	290	390	170	130
Cu	350	390	250	400	360	340	410	230	170
Ni	48000	78000	51000	62000	59000	56000	76000	38000	23000
Pb	82	90	64	100	95	84	100	57	67
Zn	10000	8700	3500	12000	2900	11000	13000	1400	6100
Se	941	2000	1400	2000	1800	1600	2400	1100	610
Sb	65	83	57	105	95	69	94	64	44
As	2434	3500	2170	3600	3500	3000	4200	3300	1900
Bi	0.42	1.7	1.3	1.5	1.5	1.3	1.5	1.3	1.1
Mo	3920	2467	2372	1907	1704	2363	2968	2472	1411
U	40	60.5	59	44.7	42.7	51.4	107.7	15.8	15.8
Y	74	170	160	110	87	87	200	44	27
Zr	29	31	53	18	24	27	33	25	31
Ba	4300	3800	4200	2300	4900	2300	2900	3900	1900
Ag	4	6	3	4	5	4	4	3	3
Pd	—	308	228	264	247	91	319	158	99
Pt	—	618	427	510	446	149	609	314	208
Au	—	103	67	138	141	29	82	69	57
Os	—	60	45	42	<15	70	60	<15	17
Ir	—	2	1.4	2.2	1.8	2.4	3	1.2	0.8
Ru	—	<30	<30	<30	<30	<30	<30	<30	<30
Rh	—	12	13	5	8	11	14	8	5
Re	—	18000	23000	10000	9600	61000	40000	34000	11400

Middle to Upper Devonian lower Earn Group is composed of four members (Fig. 6.2-3). The Transition member (20-80 m) marks the base of the Earn Group and preserves thin bedded (10 to 25 cm), black calcareous and cherty shales deposited in a restricted euxinic environment. The Limestone Ball member (3 to 20 m) is unique because of unusual texture, composition, stratigraphic confinement, and enigmatic genesis. The member consists of black- to grey-weathering, moderately phosphatic, siliceous shale containing 35 to 40% limestone spheroids. The spheroids range in size from 5 cm to 1.5 m and are interpreted to be concretions. These were probably formed under dystrophic conditions. The Phosphatic Chert member (5 to 8 m) represents a return to euxinic conditions and is dark grey, thin- to medium-bedded, and grades into the overlying siliceous shale over a distance of several metres. The base is marked by the recessive Ni-Zn-PGE sulphide horizon which characteristically occurs 20 to 120 cm above the top of the Limestone Ball member. The uppermost member of the lower Earn Group is an unnamed, 175 to 225 m sequence of rhythmically banded, thin, dark grey to black siliceous shale beds. Limy beds are common near the base of the member, whereas ochrous weathering pyritic beds are more common up-section. The pyrite occurs as thin (5 mm to 1.5 cm) interbeds and ubiquitous disseminations.

Upper Earn Group strata are composed of two lithofacies: Sequence I consists of a fine grained, black carbonaceous muddy siltstone that coarsens upwards into chert pebble conglomerate approximately 80 to 120 m from the base; Sequence II is a fine- to medium-grained, similarly coarsening upwards, siltstone sequence which ranges in thickness from 60 to 100 m. The top of the group is not exposed in the map area.

Stratiform Ni-Zn-PGE mineralization

The Nick mineralization consists of a thin nickeliferous massive sulphide layer ("vaesite horizon") that lies at the base of the Phosphatic Chert member, approximately 20 to 120 cm above the top of the Limestone Ball member (Fig. 6.2-2 and 6.2-3). The thickness of the sulphide layer ranges from 0.4 to 10 cm. The horizon is readily oxidized and highly recessive, and for this reason its recognition on the surface has been restricted to creek beds and cliff faces. However, accurate prediction of the position of the mineralized horizon can be made based on location of the underlying Limestone Ball member marker horizon. Evidence to date suggests that this mineralized horizon is a continuous sheet of sulphide that formed over the entire floor of the Nick subbasin during the Middle Devonian.

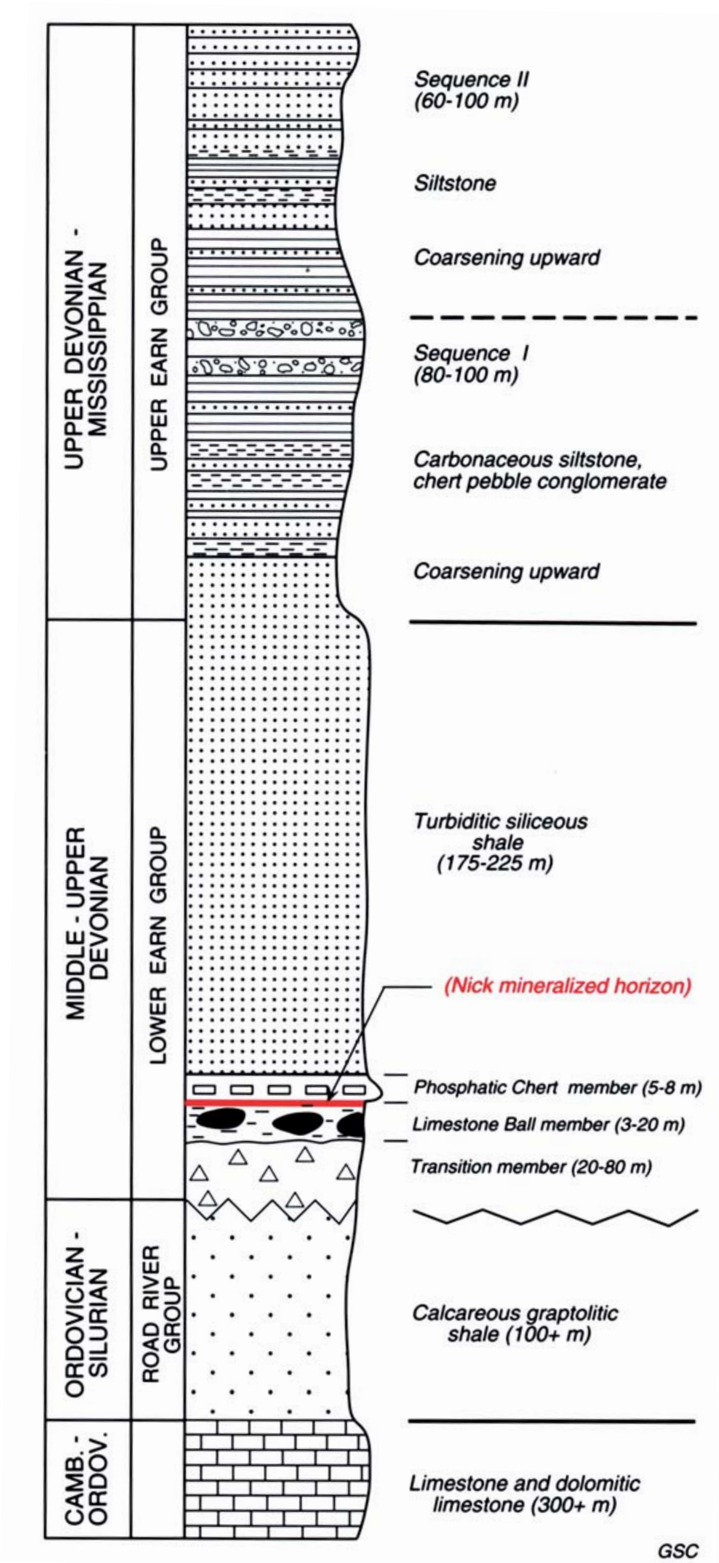

Figure 6.2-3. Stratigraphic column for the Nick basin showing the position of the stratiform Ni-Zn-PGE (Nick) mineralization and the footwall Limestone Ball member (after Hulbert et al., 1992).

Fresh mineralized specimens commonly contain 40 to 65% sulphides and display a variety of sedimentary features, the most notable being a soft sediment deformation of laminated metalliferous sediments (Fig. 6.2-4). The sulphides form thin (1 to 3 mm) convolute and discontinuous laminae ≤5 cm in length. The sulphide laminae are enclosed in a dark grey siliceous matrix that contains fine disseminations of pyrite. Some of the sulphide laminae have a vermiform structure (Fig. 6.2-4) and may have formed by replacement of organic matter or precipitation in pore space.

The stratiform Ni-Zn-PGE mineralization in the Nick basin is mineralogically unique. It consists of pyrite (46%), vaesite (NiS_2; 10%), melnikovite (2%), sphalerite and wurtzite (2%), with a gangue (39%) of phosphatic-carbonaceous chert, amorphous silica, and intergrown bitumen (1%). Although the thickness of the horizon varies, the grade and mineralogical composition are extremely consistent.

Sulphur-isotope values ($\delta^{34}S$) in sulphides of the Nick mineralization and overlying lower Earn Group pyritic intervals exhibit a compositional range of 34.6‰. The heaviest sulphur (+11.5 to +19.9‰) occurs in the pyritic bands in the overlying siliceous shale, whereas the lightest sulphur (-14.7 to -10.0‰) was found in the Nick horizon.

Bitumen veins

A number of float and outcrop occurrences of bituminous vein material have been discovered in the area and all are confined to the Road River Group. The largest is known as the Bitumen showing and is located in a fault zone on Olfert Creek (Fig. 6.2-2). It is a tabular body, 3 m wide, that is exposed in a canyon wall for a vertical extent of 9 m and for a strike length of 21 m. Internal siliceous pipe-like features are present within the bitumen infilled vein structures, and localized silicified bituminous wall rocks have also been

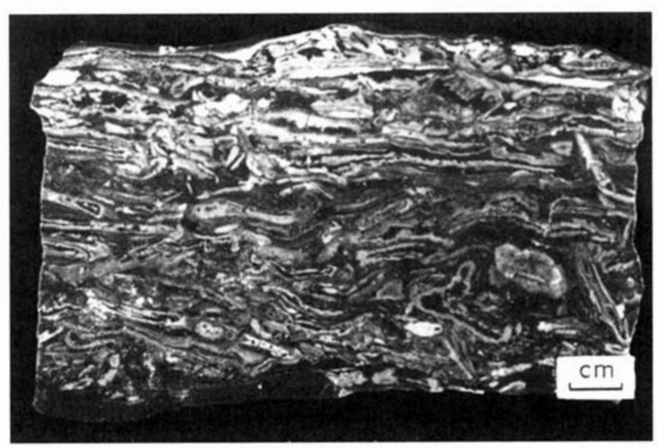

Figure 6.2-4. Typical stratiform Ni-Zn-PGE (Nick) mineralization illustrating soft sediment deformational fabrics that include load casts and slump fragmentation of sulphide-shale laminae. Note local colloform sulphides and sulphide rims surrounding some fragments. GSC 1995-026

Contents

noted. Consolidated and ashed bitumen samples contain anomalous concentrations of Ni, Zn, As, Mo, V, and Re and have a chemical signature similar to that of the Nick mineralization. These veins have been interpreted to be possible feeder structures to the stratiform Nick sulphide mineralization (Hulbert et al., 1992).

STRATIFORM Mo-Ni MINERALIZATION, SOUTHERN CHINA

The only occurrences of mineralization similar to the Nick deposit are those of the Mo-Ni sulphide mineralization of southern China (Fan Delian, 1983; Coveney and Chen Nansheng, 1991). This mineralization occurs in lowermost Cambrian black shales and is consistently associated with the widespread distribution of sapropelic organic-rich rocks that occur in a linear belt for a distance of more than 2000 km. The Mo-Ni sulphide ores consist of a mixture of sulphide clasts, phosphorite pellets and low-grade anthracitic coal referred to as "stone coal".

DEFINITIVE CHARACTERISTICS

The most definitive characteristics of the Nick mineralization are (a) the basin-wide distribution of the Ni-Zn-PGE massive sulphide layer and the ubiquitous presence of the footwall Limestone Ball member 20-120 cm below the mineralization; (b) the lateral consistency of the grade and mineralogy; (c) the laminated nature of the sulphides and associated soft sediment textural features; (d) affiliation with the most carbonaceous and phosphatic stratigraphic intervals; (e) the association of anomalous concentrations of Ba, U, V, Se, As, and Re with the Ni-Zn-PGE-rich sulphide mineralization; (f) presence of bitumen veins with chemical signatures similar to those of the stratiform Ni-Zn-PGE mineralization; and (g) the presence of sulphides isotopically enriched in ^{32}S. Most of these characteristics also apply generally to the occurrences of southern China.

GENETIC MODEL

Evidence for a sedimentary-diagenetic process of deposition for the Nick mineralization includes (a) the basin-wide stratiform distribution of the Ni-Zn-PGE massive sulphide layer and associated footwall Limestone Ball member, (b) the fine rhythmically laminated character of the mineralization, (c) the characteristic basin-wide, soft sediment deformation of the mineralization, and (d) the stratigraphic distribution of chemical sediments, i.e., phosphatic cherts and barite-rich shales within the mineralized sequence and enclosing rocks.

It is envisaged that hot basinal brines, perhaps already carrying considerable dissolved sulphate and organic matter, migrated through the organic-rich Upper Silurian and Lower Devonian sediments and extracted Ni, Zn, and other metals associated with the organic material in these sediments. The migrating hot fluids, which were localized by faults that acted as conduits, were discharged towards surface. The well-laminated nature of the mineralization suggests that periodic influxes of this fluid gave rise to the Nick mineralized horizon. The introduction of this nutrient-rich fluid into ooze-like, carbonaceous bottom sediments stimulated biogenic activity and led to sulphate reduction and sulphide precipitation. The resulting sulphides are strongly depleted in ^{34}S suggesting that they were generated by bacterial reduction of sulphate in the restricted reservoir of pore fluids in the bottom sediments, rather than from the oceanic water column. The sulphides consist mainly of a pyrite-vaesite assemblage without bravoite, which implies a minimum temperature of formation of about 137°C (Kullerud, 1962).

The presence of pyrobitumens and the organic compound-rich nature of the host rocks invites speculation on the possible role of hydrophobic hydrocarbons. Petroliferous fluid inclusions were recently discovered in hydrothermal minerals of chimneys and mounds on the seafloor in the southern trough of the Guaymas Basin, central Gulf of California (Peter et al., 1990). They contain a wide range of hydrocarbon and aqueous fluid components, indicating that the hydrothermal fluid and hydrocarbons were never a homogeneous solution, but that the hydrocarbons were transported as immiscible and, possibly, solvated forms. The presence of such hydrocarbons associated with the Nick mineralizing fluids may have facilitated generation of the ooze layer and its discharge may be likened to an oil seep. The pyrobitumen veins scattered through the Nick basin may represent degradation products of trapped petroliferous material.

EXPLORATION GUIDES

Although the presently disclosed thickness and areal extent of the Nick mineralized horizon is limited, it seems clear that this mineralizing process has been operative on an extensive scale. Future exploration should focus on identification of restricted embayments or troughs with indications of bitumen occurrences and phosphatic sediments. Known mineralization in North America and southern China appears to be associated with deep fissures developed along the margins of large epicratonic and foreland basins. Hydrothermal activity may be related to episodes of thermal subsidence following periods of extension and deep rifting

Detailed geochemical profiles through the lower Earn Group, hosting the Nick mineralization, reveal that these black shales are chemically similar to other North American black shales. However, the unusual Ni, Zn, PGE, P, U, V, and Ba element associations and their anomalous concentrations in stream sediments draining areas of "Nick"-type mineralization can be used as an exploration tool.

REFERENCES

References with asterisks (*) are considered to be the best source of general information on this deposit subtype.

Coveney, R.M., Jr. and Chen Nansheng
1991: Ni-Mo-PGE-Au-rich ores in Chinese black shales and speculations on possible analogues in the United States; Mineralium Deposita, v. 26, p. 83-88.

Coveney, R.M. Jr., Murowchick, J.B., Grauch, R.I., Chen Nansheng, and Glascock, M.D.
1992: Field relations, origins and resource implications for platiniferous molydenum-nickel ores in black shales of South China; Exploration and Mining Geology, v. 1, no. 1, p. 21-28.

*Fan Delian
1983: Polyelements in the Lower Cambrian black shale series in southern China; in The Significance of Trace Metals in Solving Petrogenetic Problems and Controversies, (ed.) S.S. Augustithis; Theophrastus Publications S.A., Athens, p. 447-474.

Gordey, S.P., Abbott, J.G., and Orchard, M.J.
1982: Devono-Mississippian Earn Group and younger strata in east central Yukon; in Current Research, Part B; Geological Survey of Canada, Paper 82-1B, p. 93-100.

Green, L.H.
1972: Geology of Nash Creek, Larsen Creek and Dawson map areas, Yukon; Geological Survey of Canada, Memoir 364, 155 p.

*Hulbert, L.J., Carne, R.C., Grégoire, D.C., and Paktunc, D.
1992: Sedimentary nickel, zinc and platinum-group element mineralization in Devonian black shales at the Nick Property, Yukon, Canada: a new deposit type; Exploration and Mining Geology, v. 1, no. 1, p. 39-62.

Kullerud, G.
1962: The Fe-Ni-S system; in Carnegie Institute of Washington Year Book, v. 61, p. 144-150.

Naldrett, A.J.
1973: Nickel sulphide deposits - their classification and genesis, with special emphasis on deposits of volcanic association; The Canadian Institute of Mining and Metallurgy, Transactions, v. 76, p. 183-201.

Peter, J.M., Simoneit, B.R.T., Kawka, O.E., and Scott, S.D.
1990: Liquid hydrocarbon-bearing inclusions in modern hydrothermal chimneys and mounds from the southern trough of Guaymas Basin, Gulf of California; Applied Geochemistry, v. 5, p. 51-63.

Tipper, H.W., Woods, G.J., and Gabrielse, H.
1978: Tectonic Assemblage Map of the Canadian Cordilleran; Geological Survey of Canada, Map 1505A, scale 1:2 000 000.

6.3 VOLCANIC-ASSOCIATED MASSIVE SULPHIDE BASE METALS

J.M. Franklin

INTRODUCTION

All volcanic-associated massive sulphide deposits occur in terranes dominated by volcanic rocks. However, the individual deposits may be hosted predominantly by volcanic or sedimentary strata, all of which form integral parts of a volcanic complex. Such deposits are also commonly referred to as volcanogenic massive sulphides, or simply as VMS.

These deposits occur in two distinct compositional groups, the **copper-zinc group** and the **zinc-lead-copper group,** according to their total contained copper, lead, and zinc (Fig. 6.3-1; Franklin et al., 1981). Using the Zn/Zn+Pb ratio, the division between these two groups is established at 0.90. All are within sequences dominated by submarine volcanic rocks, and contain about 90% iron sulphide (pyrite dominant). They consist of two parts: massive sulphide ore that formed either on or immediately below the seafloor, and generally less important vein and disseminated ore (stringer zone) that immediately underlies the massive sulphide ore. The stringer ore is usually within an intensely metasomatically altered "alteration pipe". Deposits of the volcanic-associated massive sulphide type are important sources of copper, zinc, and lead; many deposits contain economically recoverable silver and gold. Cadmium, tin, indium, bismuth, and selenium are also recovered as smelter byproducts.

Deposits of the copper-zinc group are concordant to semiconcordant massive iron sulphide bodies, commonly underlain by stringer ore, within volcanic sequences that are dominated by mafic volcanic rocks, with locally important felsic and/or sedimentary rocks. Examples in Canada (Fig. 6.3-2) are the deposits near Noranda, Quebec; Flin Flon-Snow Lake, Manitoba; and the Juan de Fuca and Explorer ridges in the northeastern Pacific. Other deposits are those of the Cyprus and Oman ophiolite sequences, and the Besshi-type deposits of the Shikoku district, Japan.

Deposits of the zinc-lead-copper group are tabular, concordant massive pyritic bodies, typically underlain by less prominent stringer ore, in felsic volcanic sequences; sedimentary rocks may form a significant portion of the footwall. Canadian examples are the Buttle Lake, British Columbia; Bathurst, New Brunswick; and Buchans, Newfoundland deposits. Other deposits are those of the Hokuroku basin, Japan; the Iberian Pyrite Belt, Spain; Neves-Corvo, Portugal; and the Tasman Geosyncline, Australia.

Volcanic-associated massive sulphide deposits have been extensively reviewed by Klau and Large (1980), Franklin et al. (1981), Lydon (1984, 1988), and Franklin (1986). These accounts provide descriptive, experimental and theoretical data that are beyond the scope of this review which will focus on Canadian examples (Table 6.3-1), and draw on other areas only where the Canadian deposits do not provide a complete perspective.

Franklin, J.M.
1996: Volcanic-associated massive sulphide base metals; in Geology of Canadian Mineral Deposit Types, (ed.) O.R. Eckstrand, W.D. Sinclair, and R.I. Thorpe; Geological Survey of Canada, Geology of Canada, no. 8, p. 158-183 (also Geological Society of America, The Geology of North America, v. P-1).

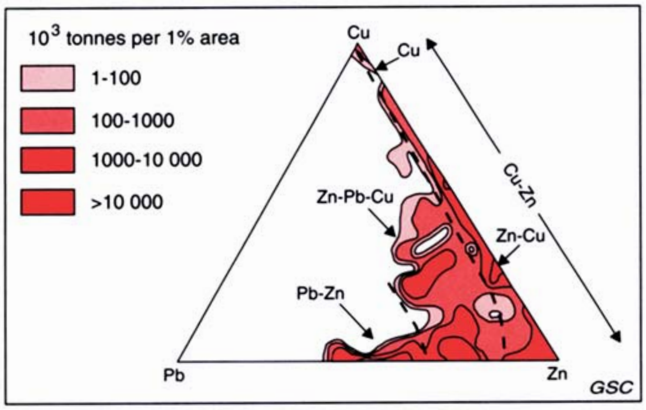

Figure 6.3-1. Contours of tonnes of contained copper, lead, and zinc, in approximately 800 massive sulphide deposits of both the volcanic-associated and sediment-associated types from Canada, U.S.A., Japan, Scandinavia, Spain, and Portugal (after Franklin et al., 1981).

IMPORTANCE

Volcanic-associated massive sulphide deposits are important sources of base metals and precious metals in Canada; in 1988 they produced 32.8% of Canada's copper, 29.4% of its lead, 56.3% of its zinc, 3.6% of its gold, and 30.4% of its silver.

SIZE AND GRADE OF DEPOSITS

Copper-zinc group

The mean and median (in brackets) grades and sizes of 142 Canadian deposits are: 5 300 000 (1 241 000) t containing 1.95% (1.60%) Cu, 4.23% (3.07%) Zn, 0.09% (0.01%) Pb, 0.8 (0.6) g/t Au, and 19.0 (8.0) g/t Ag. The lead content of most deposits in this group is rarely determined; its statistical values are approximate. The largest Canadian deposit is the Kidd Creek mine, which contains 12 000 000 t combined copper, zinc, and lead. The Horne mine at Noranda, Quebec, has a very large but sub-ore grade pyrite-sphalerite zone (No. 5 zone: 170 Mt, 0.1% Cu, 0.5% Zn, Kerr and Mason, 1990) that is not included in the calculations; with the No. 5 zone included, the Horne mine may contain more base metal than Kidd Creek. The deposit sizes of the combined Cu-Zn and Zn-Pb-Cu groups are log-normally distributed (Fig. 6.3-3).

Zinc-lead-copper group

The mean and median (in brackets) grades and sizes of 92 Canadian deposits are 5 600 000 (1 177 000) t containing 1.23% (1.01%) Cu, 3.60% (2.80%) Zn, 1.46% (0.97%) Pb, 2.0 (0.5) g/t Au, and 79.0 (57.0) g/t Ag. Brunswick #12 is the largest Canadian deposit, containing at least 10 500 000 t of combined copper, lead, and zinc.

GEOLOGICAL FEATURES

Volcanic-associated massive sulphide deposits occur in submarine volcanic rocks of all ages, from the presently-forming deposits in modern, actively-spreading ridges to deposits in the pre-3400 Ma volcanic strata of the Pilbara Block in Australia. They occur in a wide variety of tectonic regimes. Almost all deposits have a close association with at least minor amounts of sedimentary rock.

Copper-zinc group

Geological setting

These deposits occur in two principal geological settings; 1) in mafic-volcanic dominated areas, such as Archean and Proterozoic greenstone belts (Fig. 6.3-2) and modern and Phanerozoic spreading ridges and seamounts; 2) in areas containing subequal amounts of both mafic volcanic rocks and sedimentary strata, such as are in Phanerozoic arc sequences.

Volcanic rock-dominated areas

Significant variation in the composition of these deposits, and the alteration associated with them, has been related to the depth of water under which the deposits formed. Morton and Franklin (1987) defined two groups. 1) Deposits typified by the Noranda and Matagami Lake districts, Quebec (Fig. 6.3-4A), were formed at depths of considerably more than 500 m. These are associated with sequences composed primarily of massive to pillowed mafic flows. Felsic ash-flow tuff beds are usually prominent immediately below the deposits, and felsic domes may immediately underlie or enclose the ore. However, the amount of felsic rock in the footwall sequence may be only minor (Flin Flon, Manitoba), or comprise as much as 30% (e.g. Noranda). 2) A second group of deposits, typified by those near Sturgeon Lake, Ontario, Hackett River, Northwest Territories, and possibly the Kidd Creek mine near Timmins, Ontario, are associated with volcanic rocks deposited in subaerial to shallow marine environments (<500 m). These include mafic and felsic amygdaloidal and scoriaceous flows and pyroclastic rocks, volcanic breccia, and epiclastic strata (Fig. 6.3-4B). Felsic rocks typically comprise 30% of the footwall sequence.

Both groups of deposits occur in volcanic sequences that have prominent subvolcanic intrusions near their base. Trondhjemitic intrusions predominate (Noranda, Sturgeon Lake, Flin Flon, Snow Lake), but a layered mafic intrusion forms the base of the Matagami Lake sequence.

Actively forming deposits within modern mid-ocean spreading ridges occur as two types, those in sediment-free, basalt-dominated terranes (primarily axial grabens), and those in sediments. Some of the first type are associated with off-axis seamounts. The deposits in grabens within basalt-dominated active ridges may be further divided into two groups (Kappel and Franklin, 1989): small deposits forming in ridge axes which are in the active and early phases of volcanic construction, such as the Cleft segment of the southern Juan de Fuca Ridge (and the East Pacific Rise deposits at 11°N and 21°N), and larger deposits in more volcanically evolved ridge crests, such as those of the Endeavour and Explorer segments of the Juan de Fuca Ridge, and the TAG area of the Mid-Atlantic Ridge.

Deposits associated with areas of recent prolific volcanism lie along the bounding faults of the narrow central graben developed on top of a prominently elongate, but locally inactive volcano, typically 500 m high, and composed of inflated (over-filled) pillows. They are comparatively large (10^5-10^6 t), are composed of coalesced mounds, and are associated with highly fissured pillowed basalts.

The deposits in the Cyprus, Oman, U.S.A., and Canadian ophiolite sequences are the forerunners of the spreading-ridge association. In Canada, the best examples of preserved ophiolite-associated deposits are in the Ordovician sequences of Newfoundland; a few small deposits are also in Ordovician ophiolites of southeastern Quebec. These deposits occur within basaltic to andesitic pillow sequences, typically a few kilometres thick, that overlie the sheeted dyke and gabbroic portions of ophiolitic sequences.

Sediment-dominated areas

Terranes commonly ascribed to arc-related basins, composed of relatively monotonous, regular sequences of volcanic and sedimentary strata, contain many massive sulphide deposits. Deposits formed close to a tectonic boundary between ocean floor and island arcs, ocean floor and cratons, or ocean floor and continental crust are included. The volcanic component is usually dominant, and composed predominantly of mafic volcanic rocks. However, some areas also have minor quantities of felsic volcanic strata. The sedimentary rocks are dominantly pelitic. The ratio of volcanic to sedimentary strata associated with the deposits is highly variable. These terranes are typically highly deformed, making identification of primary tectonic relationships difficult. Terms such as "Besshi-type" or "Keislager-type" may be used.

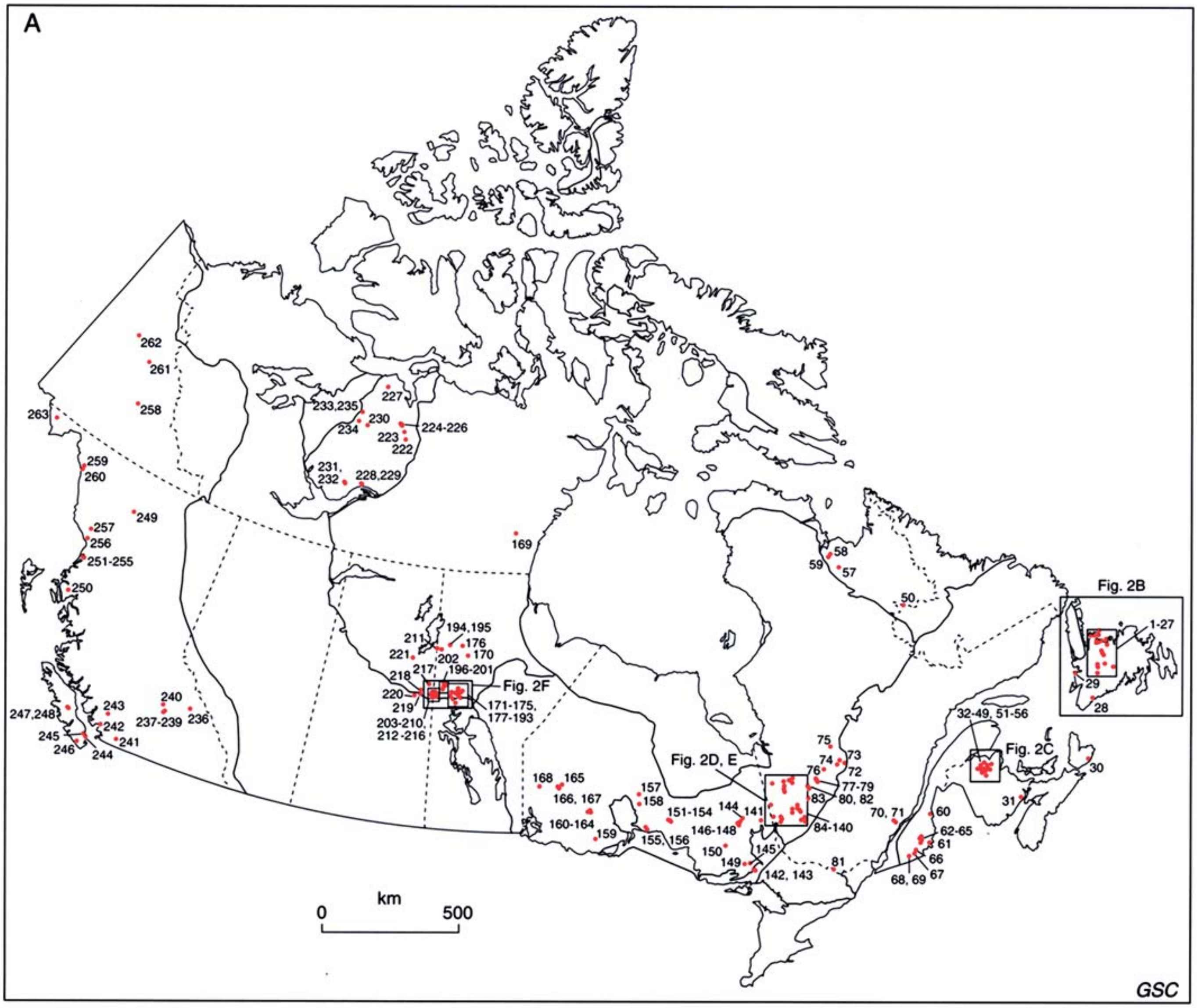

Figure 6.3-2A. Location of volcanic-associated massive sulphide deposits in Canada. The corresponding list of deposits is in Table 6.3-1. Major districts within the boxes are shown as separate maps 6.3-2B to 2E.

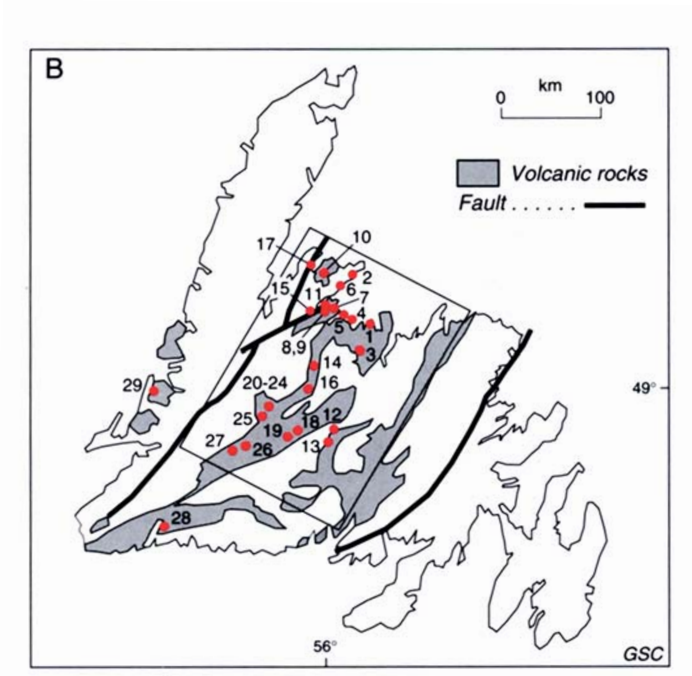

Figure 6.3-2B. Volcanogenic massive sulphide deposits in Newfoundland.

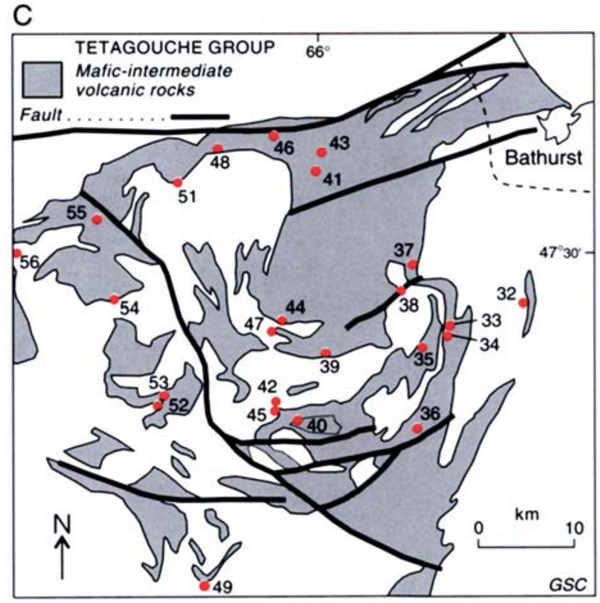

Figure 6.3-2C. Distribution of volcanogenic massive sulphide deposits in the Bathurst district, New Brunswick.

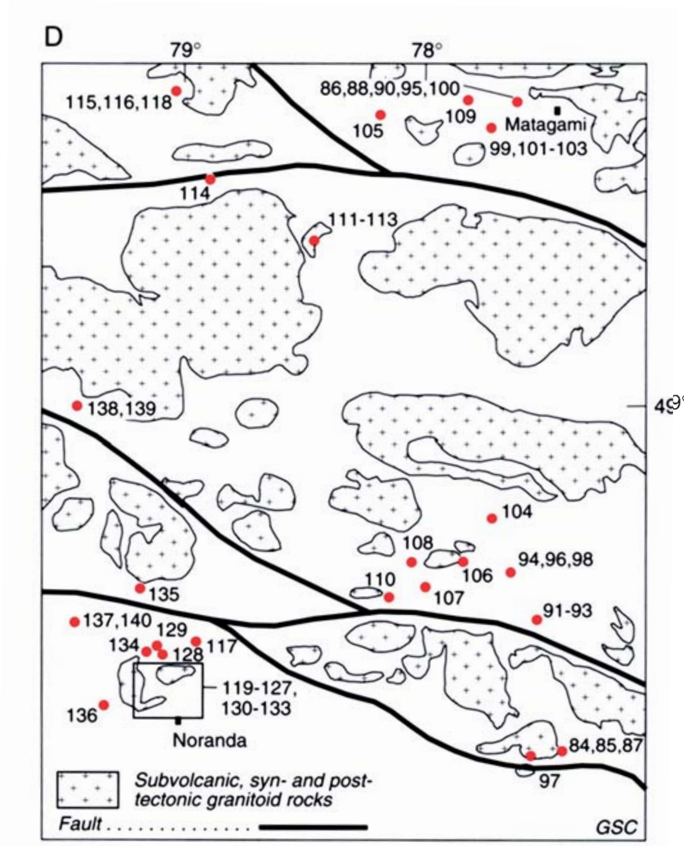

Figure 6.3-2D. Distribution of volcanogenic massive sulphide deposits in the Noranda and Val d'Or districts, Quebec. Location of deposits in box are shown in Figure 6.3-2E.

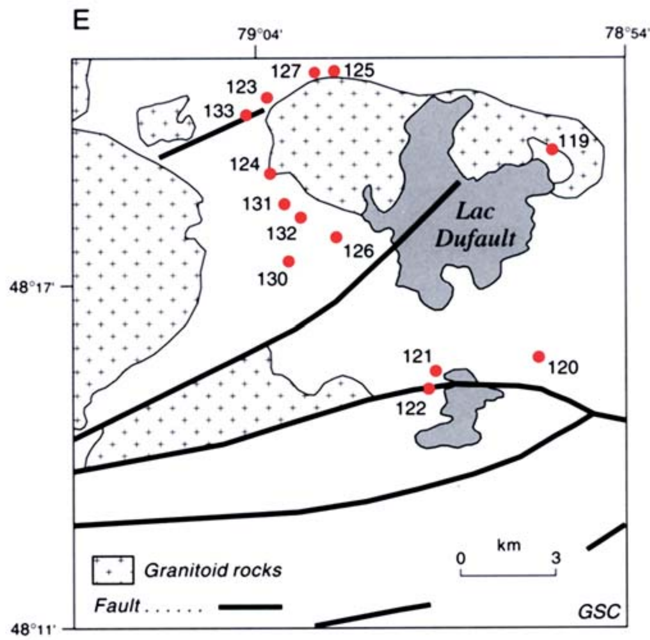

Figure 6.3-2E. Distribution of volcanogenic massive sulphide deposits in the Noranda district, Quebec.

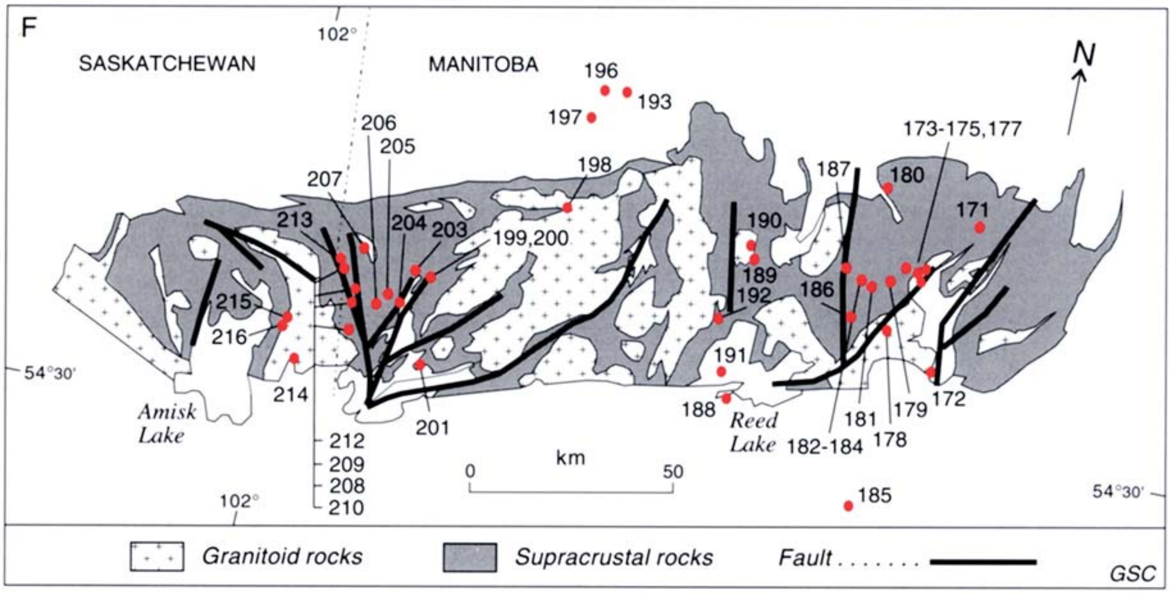

Figure 6.3-2F. Distribution of deposits in the Flin Flon-Snow Lake districts, Manitoba and Saskatchewan. Amisk volcanic rocks are shown with a light stipple.

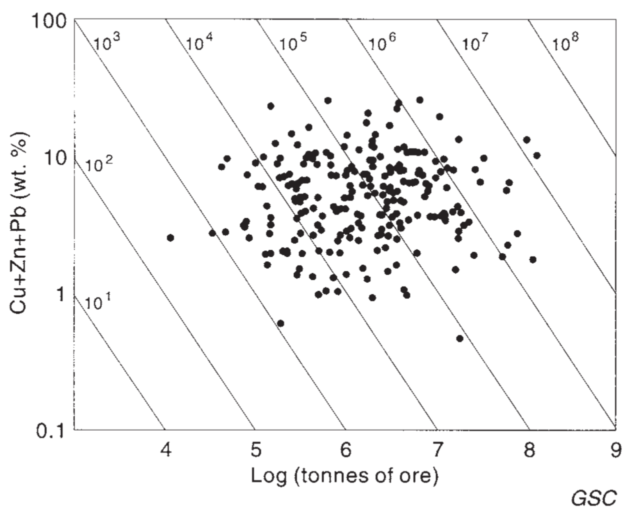

Figure 6.3-3. Tonnes of ore versus total copper, lead, and zinc (per cent) in Canadian volcanogenic massive sulphide deposits (see Table 6.3-1 for list). The size of deposits is log-normally distributed. Diagonal lines indicate tonnes of contained Cu + Zu + Pb.

Examples of copper-zinc deposits in sediment-dominated settings (Fig. 6.3-4C) are not common in Canada, but include the Granduc deposit, deposits in the Anyox and Kutcho Creek areas, and the Windy Craggy deposit, all in northern British Columbia. Possibly the Britannia mine in southwestern British Columbia (Payne et al., 1980), the Sherridon deposit in northern Manitoba, and deposits such as the Soucy #1 in the Labrador Trough, are also in this group. The Windy Craggy deposit, although low grade, is possibly the largest massive sulphide deposit in Canada; the Granduc and Hidden Creek (Anyox area) deposits are also in the upper quartile of deposit tonnages in Canada (43 and 40 million tonnes, respectively).

Deposits in the sediment-covered portions of actively spreading ridges are much larger than those in modern volcanic ridges. The Middle Valley Bent Hill deposit, one example of this type, is in the complex northern Endeavour segment of the Juan de Fuca Ridge. It has formed within the upper portion of a sequence of pelite and turbidite, about 300 m thick, that overlies a volcanic basement (Goodfellow and Franklin, 1993). The brine pools and metalliferous muds in the Red Sea are the product of a highly saline, high-temperature hydrothermal system and contribute a large sediment-hosted copper-zinc deposit in the process of formation.

Form and composition

The typical form of the Noranda-type deposits (Fig. 6.3-5) is a generally conformable bulbous or conical mound consisting of at least 60% of pyrite, sphalerite, chalcopyrite, and pyrrhotite. The length-to-thickness aspect ratio of a typical (1 million tonne) undeformed deposit is usually between 3 and 10 to 1. The largest deposits have a much greater ratio. The upper contact is sharp, but the lower is transitional into the stringer zone, composed of chalcopyrite, pyrrhotite, and pyrite. Deposits of the Mattabi type are more stratiform in shape, with contact relationships similar to those of the Noranda-type deposits. Stringer zones of deposits of the latter type commonly contain economically recoverable ore for several tens of metres below the deposit. In the Mattabi-type deposits, although alteration pipes may be extensive, the amount of ore contained in them is relatively small.

Contents

Table 6.3-1. Canadian volcanic-associated massive sulphide deposits.

NO.	NAME	LATITUDE / LONGITUDE	NTS	Cu %	Pb %	Zn %	Ag (g/t)	Au (g/t)	TONNES	REFERENCE
1	LOCKPORT	49°27′18″ 55°29′53″	2E/6	0.75		1.21			555 934	1
2	TILT COVE	49°53′24″ 55°37′12″	2E/13	6.00					8 165 000	2
3	POINT LEAMINGTON	49°16′36″ 55°37′53″	2E/5	0.50		2.00	18.00	0.90	13 800 000	3, 1
4	PILLEYS ISLAND	49°30′31″ 55°43′07″	2E/12	1.23					1 025 000	1, 3
5	MILES COVE	49°32′22″ 55°47′26″	2E/12	1.55			12.00	0.34	200 000	1, 2
6	BETT'S COVE	49°48′46″ 55°48′23″	2E/13	6.00					119 000	1, 2
7	LITTLE BAY	49°36′52″ 55°56′20″	2E/12	2.10					2 934 464	1, 2
8	WHALESBACK	49°35′45″ 56°00′22″	12H/9	0.95					3 793 561	1, 2, 3
9	LITTLE DEER	49°35′20″ 56°01′08″	12H/9	1.53					285 200	3
10	RAMBLER MAIN	49°54′02″ 56°03′32″	12H/16	1.30		2.16	23.24	2.4	572 000	1, 3
11	COLCHESTER	49°38′20″ 56°04′51″	12H/9	1.30					1 001 000	3, 2
12	SOUTH POND	48°25′36″ 56°08′23″	12A/8	1.33			12		293 000	3, 2
13	GREAT BURNT LAKE	48°20′19″ 56°09′06″	12A/8	2.40					796 500	3, 2
14	GULLBRIDGE	49°11′54″ 56°09′18″	12H/1	1.02					4 072 430	3
15	RENDELL JACK MAN	49°33′47″ 56°10′52″	12H/9	2.50				1.00	13 081	3, 2
16	LAKE BOND	49°01′39″ 56°11′11″	12H/1	0.31		2.10			1,200,000	1
17	TERRA NOVA	49°55′17″ 56°13′44″	12H/16	2.41			9.94	1.68	257 417	3, 2
18	BOUNDARY	48°39′22″ 56°26′47″	12A/9	3.50	1.00	4.00	34		500 000	3
19	DUCK(TALLY) POND	48°38′04″ 56°29′16″	12A/9	3.60	7.00		70.4		3 860 000	3, 2
20	ORIENTAL	48°49′00″ 56°53′00″	12A/15	1.48	7.90	14.18	154.63	1.95	3 326 876	4
21	MACLEAN	48°49′00″ 56°53′00″	12A/15	1.16	7.32	13.20	128.91	1.03	3 313 271	4
22	BUCHANS	48°49′00″ 56°53′00″	12A/15	1.37	7.73	14.97	127.89	1.58	567 782	4
23	ROTHERMERE	48°49′00″ 56°53′00″	12A/15	1.16	7.72	12.74	135.09	1.03	3 263 386	4
24	LUCKY STRIKE	48°49′00″ 56°53′00″	12A/15	1.51	8.20	15.20	112.46	1.6	5 899 128	1, 4
25	SKIDDER	48°42′23″ 56°56′07″	12A/10	2.00		2.00			900 000	3, 2
26	TULK'S EAST	48°32′15″ 57°07′54″	12A/11	0.24	0.12	1.50	8.5		6 230 000	3, 2
27	TULK'S HILL	48°30′53″ 57°12′07″	12A/11	1.30	2.00	5.60	41	0.40	720 000	3, 2
28	STRICKLAND	47°48′29″ 58°18′00″	11O/16		1.00	1.00	195.00		1 010 000	3
29	YORK HARBOUR	49°03′00″ 58°18′32″	12G/1	1.92		4.67			338 039	3
30	STIRLING	45°43′40″ 60°26′15″	11F/9	0.66	1.30	5.50	68.57	0.96	995 990	3
31	TEAHAN	45°42′50″ 64°59′20″	21H/10	0.46		1.46	29.83		122 445	3
32	KEY ANACON	47°26′12″ 65°42′20″	21P/5	0.22	3.47	8.41	111.43		1 519 722	3
33	BRUNSWICK #6	47°24′30″ 65°49′00″	21P/5	0.39	2.16	5.43	67.00		12 100 000	5
34	AUSTIN BROOK	47°23′48″ 65°49′21″	21P/5	0.10	1.86	2.93	34.29		907 000	3
35	FLAT LANDING	47°22′55″ 65°52′36″	21P/5		0.94	4.90	19.54		1 750 510	3
36	CAPTAIN DEPOSIT	47°17′03″ 65°52′58″	21P/5	1.99			9.60	0.58	311 101	3
37	BRUNSWICK #12	47°28′00″ 65°53′00″	21P/5	0.30	3.60	8.87	100.00		134 100 000	5
38	PABINEAU RIVER	47°26′58″ 65°55′07″	21P/5		0.87	2.65			136 050	3
39	NINE MILE BROOK	47°23′25″ 65°55′59″	21P/5	0.42	1.00	1.07	90.86	1.03	133 329	3
40	NEPISIGUIT	47°22′00″ 66°02′00″	21O/8	0.40	0.60	2.80	10.29		3 537 300	3
41	ARMSTRONG	47°36′06″ 66°02′33″	21O/9	0.29	0.42	2.29	2.40	0.68	3 100 000	3
42	HEATH STEELE	47°17′00″ 66°05′00″	21O/8	0.70	2.50	6.30	60.00	0.62	33 777 000	3, 6
43	ROCKY TURN	47°38′00″ 66°04′15″	21O/9	0.30	1.50	7.00	78.86		180 000	3
44	CANOE LANDING	47°24′39″ 66°06′24″	21O/8	0.56	0.64	1.82	29.50	1.07	20 380 000	3
45	STRATMAT WEST	47°18′30″ 66°07′31″	21O/8	0.59	2.44	6.29	31.89		4 353 600	3
46	ORVAN BROOK	47°37′37″ 66°08′07″	21O/9	0.00	3.25	6.30	34.29		181 400	3
47	WEDGE	47°23 ′50″ 66°08′30″	21O/8	2.17	0.24	0.46	0.70	0.03	1 500 000	5

Table 6.3-1. (cont.)

NO.	NAME	LATITUDE / LONGITUDE		NTS	Cu %	Pb %	Zn %	Ag (g/t)	Au (g/t)	TONNES	REFERENCE
48	MCMASTER	47°36′26″	66°13′59″	21O/9	0.60					181 400	3
49	CHESTER	47°05′54″	66°14′50″	21O/1	0.44					16 235 300	3
50	FREDRICKSON LAKE	55°03′02″	66°15′09″	23O/1	0.77		4.38	42.17	0.69	279 356	3
51	CARIBOU	47°34′50″	66°17′56″	21O/9		3.84	8.46	109.60	1.70	5 694 000	3
52	HALF MILE NORTH	47°18′00″	66°19′00″	21O/8	0.39	0.87	4.95	8.23	0.17	789 250	3
53	HALF MILE	47°17′00 ″	66°19′00″	21O/8	0.39	2.49	6.60			7 847 142	3
54	DEVILS ELBOW	47°25′51″	66°23′57″	21O/8	1.00					471 640	3
55	MURRAY BROOK	47°31′30″	66°26′00″	21O/9	0.44	0.86	1.95	31.20	0.34	20 861 000	3
56	RESTIGOUCHE	47°30′20″	66°33′50″	21O/10	0.32	5.99	7.72	124.11	1.20	997 700	7 (26/11/90)
57	BOYLEN(KOKE)	57°39′42″	69°27′00″	24F/11	0.70	1.03	6.86	54.51	1.03	1 060 433	3
58	SOUCY NO.1 ZONE	58°19′12″	69°52′12″	24K/5	1.40	0.10	1.09	19.20	2.06	4 324 032	3
59	PRUDHOMME NO.1	58°15′36″	69°54′30″	24K/5	1.50	0.20	1.90	26.06	1.37	5 729 161	3
60	PANET METALS	46°35′18″	70°13 ′00″	21L/9	0.40	0.43	2.67	19.89	2.06	272 100	3
61	CLINTON COPPER	45°27′36″	70°54′30″	21E/7	1.84		1.58	13.71		1 380 809	3
62	CUPRA DESTRIE	45°46′24″	71°18′48″	21E/14	2.75	0.47	1.48	37.71	0.51	3 007 451	3
63	SOLBEC COPPER	45°49′00″	71°18′30″	21E/14	1.60	0.70	4.60	59.66	0.79	1 860 000	8, 9
64	LINGWICK	45°39′18″	71°23′00″	21E/11	0.60		6.00	17.14		317 450	3
65	WEEDON	45°42′00″	71°23′00″	21E/11	2.50	0.08	0.40	6.86		1 700 000	8, 9
66	MOULTON HILL	45°24′30″	71°49′30″	21E/5	1.00					331 055	3
67	SUFFIELD	45°19′12″	71°57′36″	21E/5	0.83		4.25	63.09	4.94	205 889	3
68	IVES	45°17′36″	72°19′24″	31H/8	3.50					771	3
69	HUNTINGDON	45°15′48″	72°19′54″	31H/8	0.90			1.03	0.10	1 814 000	3
70	TETREAULT	46°49′30″	72°20′00″	31I/16		1.40	4.00	100.46	1.23	2 670 208	8
71	MONTAUBAN	46°50′06″	72°20′48″	31I/16		1.07	3.46	38.74	0.55	3 339 514	3
72	LEMOINE(PATINO)	49°45′44″	74°06′10″	32G/16	4.20		9.50	92	4.4	750 000	5
73	ANTOINETTE(TACHE)	49°56′30″	74°24′18″	32G/16	0.33		3.31	11.31	1.89	2 305 594	3
74	SCOTT TWP	49°51′52″	74°37′47″	32G/15	0.14		6.91	11.66	0.34	704 739	3, 7 (21/01/91)
75	DOMERGUE(LESSARD)	50°38′30″	74°38′30″	32J/10	1.82		3.30	38.40	0.72	952 350	3
76	LA-RIBOURDE	49°49′00″	75°31′24″	32G/13	1.35		2.73	42.51		408 150	3
77	EMPIRE OIL	49°25′04″	76°08′09″	32F/8	0.23		2.45	5.49		300 217	8
78	SOMA ALTA	49°26′48″	76°09′30″	32F/8			2.70	0.34		31 745	3, 8
79	CONIAGAS S	49°29′54″	76°09′48″	32F/8			10.70	182.00		700 000	3, 5, 10
80	GREVET (M ZONE)	49°14′06″	76°40′02″	32F/2	0.48	0.10	8.65	34.00		6 200 000	10
81	NEW CALUMET	45°42′12″	76°40′24″	31F/10		1.77	6.00	80.23	0.48	3 651 618	3
82	GREVET (B ZONE)	49°14′00″	76°45′00″	32F/2	0.58		9.67	24.00		477 000	7 (10/90)
83	TONNANCOURT-3	48°51′48″	76°59′24″	32C/15	2.07		3.17	25.03	0.38	54 420	3
84	LOUVEM(ZN ORE)	48°05′54″	77°31′00″	32C/4	0.21		5.59	34.29	0.69	2 358 200	3
85	LOUVICOURT	48°05′54″	77°31′00″	32C/4	3.40		2.20	31.00	0.90	15 700 000	11(22/04/94)
86	RADIORE	49°45′03″	77°33′03″	32F/13	1.57		1.34	6.86	0.34	150 000	8, 5
87	QUE MANITOU	48°05′30″	77°35′06″	32C/4	1.26			3.43		692 041	3
88	GARON LAKE	49°46′24″	77°34′06″	32F/13	1.45		2.22	4.53		512 455	3, 8
89	MANITOU-BARVUE	48°05′12″	77°36′36″	32C/4	0.07	0.07	0.36	11.66	0.34	13 750 120	3
90	BELL CHANNEL#1	49°46′12″	77°37′24″	32F/13	1.95		0.57	29.14	0.34	82 084	3, 8
91	BELFORT (ROYMONT)	48°25′24″	77°39′42″	32C/5	0.21	0.12	7.00	23.04	0.38	226 750	3
92	BARVALLEE	48°25′24″	77°39′42″	32C/5	1.23		5.71	48.69		181 400	3
93	MOGADOR	48°25′24″	77°39′42″	32C/5	0.47	0.34	7.30	55.89	1.17	1 107 447	3
94	BARVUE	48°31′03″	77°40′05″	32C/12	0.05	0.00	3.50	41.14		8 341 679	8

Contents

Table 6.3-1. (cont.)

NO.	NAME	LATITUDE / LONGITUDE		NTS	Cu %	Pb %	Zn %	Ag (g/t)	Au (g/t)	TONNES	REFERENCE
95	NORITA (RADIORE A)	49°46′00″	77°41′00″	32F/13	1.80		3.80	27.43	0.69	4 000 000	8, 5
96	CONS. PERSHCOURT	48°31′24″	77°41′06″	32C/12			2.42	91.89		4 824 333	8
97	EAST SULLIVAN	48°04′18″	77°42′30″	32C/4	1.07		4.0	7.92	0.27	15 186 638	3, 10
98	FREBERT	48°31′00″	77°43′00″	32C/12			2.50	50.40		2 721 000	8
99	MATTAGAMI LAKE	49°43′18″	77°43′00″	32F/12	0.42		5.10	21.60	0.30	25 600 000	5
100	LYNX (OBASKA)	49°38′48″	77°43′18″	32F/12	1.60		0.35			204 075	3
101	BELL ALLARD	49°41′00″	77°44′00″	32F/12	1.14		9.30	41.14		234 000	10
102	ORCHAN S	49°42′00″	77°44′00″	32F/12	1.20		8.70	37	0.5	4 500 000	10
103	ISLE DIEU	49°43′05″	77°44′06″	32F/12	1.03		17.80	82.00	0.45	2 060 000	10
104	TRINITY PROPERTY	48°42′30″	77°45′36″	32C/12	1.18		0.74			133 329	3
105	NEW HOSCO	49°47′24″	77°50′06″	32F/13	1.41		1.11	4.11	0.03	2 040 750	3
106	MONPAS (ALBAR)	48°36′54″	77°52′12″	32C/12	2.00		0.75	20.57		45 350	3
107	CONIGO	48°35′48″	78°03′30″	32D/9	1.26			17.14		2 735 512	3
108	JAY COPPER	48°36′45″	78°03′30″	32D/9	1.26			6.86		1 959 120	7 (22/04/91)
109	LA GAUCHETIERE	49°45′54″	78°10′00″	32E/16	1.10		4.90			1 541 900	3
110	NEWCONEX FIGUERY	48°28′43″	78°10′15″	32D/8			5.00	68.57		453 500	3
111	CONS. NORTH EXPL.	49°26′06″	78°19′54″	32E/8	0.73		6.95	34.29		996 893	3
112	JOUTEL COPPER	49°27′12″	78°21′12″	32E/8	2.16		3.90			1 702 439	3
113	POIRIER	49°26′36″	78°23′18″	32E/8	2.22		5.08	7.60		7 082 143	3, 5
114	ESTRADES	49°35′12″	78°51′24″	32E/10	1.02	0.90	9.90	218.40	6.72	2 000 000	3, 10, 12
115	DETOUR (A2 ZONE)	49°49′00″	78°55′55″	32E/15	2.26		1.24	16.80	0.79	8 852 320	8
116	DETOUR (A1 ZONE)	49°49′00″	78°55′58″	32E/15	0.39		2.30	35.66	0.31	32 107 800	8
117	MOBRUN	48°24′00″	78°56′00″	32D/7	.63		4.66	31.4	1.55	8 640 000	5
118	DETOUR (B ZONE)	49°49′04″	78°56′16″	32E/15	4.49		0.80	39.43	1.23	3 061 125	8
119	GALLEN	48°19′30″	78°57′12″	32D/7	0.08		3.36	2.40	0.06	8 100 000	3, 10
120	DELBRIDGE	48°15′53″	78°57′52″	32D/7	0.55		8.60	68.60	2.40	360 000	5
121	QUEMONT	48°15′00″	78°58′00″	32D/6	1.32	0.02	2.44	30.90	5.50	13 800 000	10
122	HORNE	48°15′18″	79°00′42″	32D/6	2.20			13.00	6.10	54 000 000	10
123	EAST WAITE	48°21′00″	79°02′00″	32D/6	4.10		3.25	31.00	1.80	1 500 000	5
124	AMULET (F ZONE)	48°20′00″	79°03′00″	32D/6	3.40		8.60	46.30	0.30	270 000	5
125	NORBEC	48°21′12″	79°03′05″	32D/6	2.77		4.50	48.00	0.70	3 950 000	5
126	MILLENBACH	48°18′04″	79°03′15″	32D/6	3.46		4.33	56.20	1.00	3 560 000	5
127	LD-75	48°18′14″	79°03′39″	32D/6	2.8		4.2	60.00	1.71	90 000	8
128	LAC DUFAULT 2	48°18′27″	79°03′45″	32D/6	0.50		8.30	113.49	1.51	90 700	8
129	VAUZE	48°21′35″	79°04′50″	32D/6	2.90		0.94	24.00	0.70	354 000	5
130	CORBET	48°18′00″	79°04′55″	32D/6	3.0		1.96	21.00	1.00	2 780 000	5
131	AMULET (C ZONE)	48°19′00″	79°05′00″	32D/6	2.20		8.50	86.70	0.60	570 000	5
132	AMULET (LOWER A)	48°19′00″	79°05′00″	32D/6	5.14		5.30	44.20	1.40	4 690 000	5
133	OLD WAITE	48°20′24″	79°05′20″	32D/6	4.70	0.04	2.98	22.00	1.10	1 120 000	5
134	ANSIL	48°21′15″	79°07′00″	32D/6	7.22		0.94	26.50	1.60	1 580 000	5, 10
135	HUNTER	48°33′06″	79°08′24″	32D/11	1.06					438 988	3
136	ALDERMAC	48°13′12″	79°14′00″	32D/3	1.40		4.12	7.0	0.3	1 880 000	5
137	NEW INSCO	48°26′27″	79°21′06″	32D/6	2.59			20.57	0.9	886 139	3, 10
138	NORMETAL	49°00′18″	79°22′18″	32D/14	0.79	0.18	5.30	65.0	0.8	10 100 000	10
139	NORMETMAR	49°00′18″	79°22′18″	32E/3			11.72	7.06		571 410	3
140	MAGUSI RIVER	48°26′30″	79°22′24″	32D/6	1.20		3.55	31.20	1.10	3 727 770	3
141	POTTER	48°29′27″	80°11′50″	42A/9	15.20		4.15	92.5	1.54	1 758	13

Table 6.3-1. (cont.)

NO.	NAME	LATITUDE / LONGITUDE		NTS	Cu %	Pb %	Zn %	Ag (g/t)	Au (g/t)	TONNES	REFERENCE
142	ERRINGTON	46°32′15″	81°15′30″	41I/11	1.20	0.99	3.82	54.51	0.82	12 391 541	3
143	VERMILION LAKE	46°31′11″	81°21′20″	41I/11	1.26	0.90	3.92	48.00	0.86	5 410 003	3
144	KIDD CREEK	48°41′30″	81°22′00″	42A/11	2.20	0.28	7.25	147.43		117 547 200	13
145	LAKE GENEVA	46°47′35″	81°30′57″	41I/13		3.34	9.21	754.29	2.74	227 102	3
146	JAMELAND	48°34′00″	81°34′00″	42A/12	.99		.88	3.12	0.03	461 805	13, 8
147	CAN JAMIESON	48°30′55″	81°34′07″	42A/12	2.39		4.05	30.17	0.31	800 600	13, 8
148	KAM KOTIA	48°36′09″	81°36′45″	42A/5	1.09		1.03	3.39	0.03	6 007 194	13, 8
149	STRALAK	46°48′09″	81°41′50″	41I/13	0.50	0.50	3.18	68.57		680 250	3
150	SHUNSBY	47°42′48″	82°39′30″	41O/10	0.40		2.40			2 176 800	3
151	GECO	49°09′15″	85°47′40″	42F/4	1.86	0.15	3.45	50.06		58 400 000	8, 13
152	WILLROY	49°09′26″	85°48′30″	42F/4	1.64		2.84	27.77		3 949 985	8, 13
153	BIG NAMA CREEK	49°09′51″	85°50′46″	42F/4	0.83	0.02	4.16	35.66		180 493	8, 13
154	WILLECHO	49°10′30″	85°53′00″	42F/4	0.50	0.18	4.43	67.89		1 961 841	8, 13
155	ZENITH	48°58′40″	87°21′48″	42D/14	0.95		17.81	25.37	0.86	2 840 724	8, 13
156	WINSTON LAKE	49°00′10″	87°24′30″	42E/3	1.00		15.60	30.87	1.02	3 077 000	13
157	KENDON COPPER	50°25′20″	87°35′13″	42L/5	1.22		4.20	84.00	0.79	2 237 569	3
158	HEADVUE	50°01′14″	87°39′38″	42L/4		0	4.60	49.71		272 100	3
159	NORTH COLDSTREAM	48°36′05″	90°35′05″	52B/10	2.51					1 814 000	8
160	CREEK ZONE	49°52′54″	90°52′00″	52G/15	1.66	0.76	8.80	141.50		908 000	5,13
161	STURGEON LAKE	49°52′30″	90°52′00″	52G/15	2.55	1.21	9.17	164.20		2 070 000	5, 13
162	LYON LAKE	49°53′00″	90°52′00″	52G/15	1.24	0.63	6.53	141.50		3 945 000	5,13
163	F GROUP	49°52′30″	90°58′30″	52G/15	0.64	0.64	9.51	60.40		340 000	5,13
164	MATTABI S	49°52′30″	90°58′30″	52G/15	0.74	0.85	8.28	104.00		11 400 000	5,13
165	SOUTH BAY	51°06′30″	92°40′45″	52N/2	2.30		14.50	82.29		1 534 644	8
166	COPPER LODE (E ZONE)	50°57′54″	92°52′48″	52K/15	0.60		4.36	13.71		306 799	3
167	COPPER LODE (MAIN ZONE)	50°58′48″	92°57′18″	52K/15	1.01			19.54		774 584	3
168	TROUT BAY CU	51°00′10″	94°12′20″	52M/1	1.50	0.24	7.80	58.29	0.24	125 643	3
169	HENINGA GEMEX	61°46′25″	96°12′10″	65H/16	1.30		9.00	68.57	1.03	5 442 000	3
170	RUTTAN LAKE	56°28′00″	99°28′00″	65B/5	1.28		1.40	7.54	0.38	69 839 000	14 (90)
171	OSBORNE LAKE	54°57′48″	99°43′42″	63J/13	3.14		1.50			3 380 000	3, 13
172	COPPER MAN	54°39′00″	99°52′24″	63J/12	2.63		4.46			221 308	3, 13
173	ROD 2	54°51′38″	99°55′12″	63J/13	7.23		3.08			688 000	13
174	LINDA	54°50′00″	99°56′00″	63J/13	0.30		0.80	10.29	1.71	11 791 000	3
175	STALL LAKE	54°51′34″	99°56′50″	63J/13	4.42		0.50	11.66	1.47	6 513 000	8, 13
176	KNOBBY(MCBRIDE)	56°53′06″	99°55′00″	64B/13	0.35		8.77	11.66	1.47	1 819 666	3
177	ANDERSON LAKE	54°51′00″	100°00′30″	63K/16	3.46		0.10	11.66	1.47	3 354 000	15, 13
178	MORGAN LAKE	54°45′42″	100°13′06″	63K/16			16.00		3.43	362 800	3
179	JOANNIE	54°49′42″	100°02′00″	63K/16	1.28					394 545	8, 3
180	WIM	55°01′30″	100°02′36″	63N/1	2.91			8.23	1.71	989 000	3
181	GHOST LAKE	54°49′10″	100°04′00″	63K/16	1.38	0.75	8.50	44.91	1.65	646 000	15, 13
182	CHISEL LAKE NORTH	54°50′05″	100°06′05″	63K/16	0.30	0.40	9.00			2 457 000	13
183	LOST LAKE	54°49′47″	100°06′36″	63K/16	1.45	1.00	4.90	89.14	3.22	76 188	8
184	CHISEL LAKE	54°49′43″	100°07′00″	63K/16	0.50	1.40	10.90	56.23	2.40	7 490 000	15, 13
185	DYCE SIDING	54°24′24″	100°09′00″	63K/8	2.08		1.60			1 197 240	3
186	POT LAKE	54°46′48″	100°10′54″	63K/16	1.43		4.50	18.86	3.77	101 584	3
187	BOMBER(COOK L)	54°51′18″	100°11′00″	63K/16	0.04		1.00	8.57	0.10	620 388	3
188	SPRUCE POINT	54°34′30″	100°24′00″	63K/9	2.70		4.30	32.57	1.92	1 763 000	13

Table 6.3-1. (cont.)

NO.	NAME	LATITUDE / LONGITUDE		NTS	Cu %	Pb %	Zn %	Ag (g/t)	Au (g/t)	TONNES	REFERENCE
189	DICKSTONE	54°51′18″	100°29′24″	63K/16	2.42		3.17	12.69	0.69	1 083 000	3, 13
190	NORRIS LAKE	54°53′00″	100°30′18″	63K/15	2.51		4.82	20.9	0.55	226 750	3
191	REED LAKE	54°38′12″	100°32′54″	63K/10	1.30					1 361 000	3, 13
192	RAIL LAKE	54°44′54″	100°35′30″	63K/10	3.00		0.70			295 000	3, 13
193	JUNGLE LAKE	55°09′48″	100°58′18″	63N/2	1.42		1.10			3 355 900	3
194	DH FL GROUPS	56°49′00″	101°01′30″	64C/14	0.91		1.86			513 362	3
195	Z DEPOSIT	56°49′42″	101°01′30″	64C/14	1.11		2.49		0.55	138 771	3
196	BOB LAKE	55°09′30″	101°02′30″	63N/3	1.33		1.18	9.26	0.34	2 158 660	3
197	SHERRIDON	55°06′39″	101°05′00″	63N/3	2.75		3.39	30.86	0.69	7 018 366	8
198	VAMP LAKE	54°56′18″	101°10′05″	63K/14	1.34		1.90	13.03	3.98	739 205	3
199	NORTH STAR	54°46′00″	101°35′00″	63K/13	6.10			8.57	0.34	242 000	15
200	DON JON	54°46′00″	101°35′00″	63K/13	3.09			15.09	0.93	79 000	15
201	COPPER REEF	54°36′45″	101°36′24″	63K/12	1.50		0.50			453 500	16
202	FOX LAKE	56°38′00″	101°37′00″	64C/12	1.81		1.77	4.46	0.17	10 799 649	8
203	PINEBAY CU	54°45′48″	101°37′18″	63K/13	1.3					1 361 000	13, 15
204	CENTENNIAL	54°42′03″	101°39′59″	63K/12	1.56		2.20	26.40	1.51	2 366 000	13, 15
205	CUPRUS	54°43′45″	101°42′13″	63K/12	3.24		6.40	31.89	1.51	462 000	13, 15
206	WHITE LAKE	54°42′40″	101°43′30″	63K/12	1.97	0.50	4.63	36.00	0.69	850 000	13, 15
207	TROUT(EMBURY)	54°49′45″	101°49′18″	63K/13	1.80		5.80	11.20	1.45	6 600 000	7 (19/11/90)
208	SCHIST LAKE	54°43′00″	101°49′50″	63K/12	4.30	0.03	7.25	39.43	1.41	1 871 000	13, 15
209	MANDY	54°43′45″	101°50′00″	63K/12	8.03		15.05	61.71	3.09	150 000	13
210	WESTARM	54°38′36″	101°50′12″	63K/12	3.70		1.50			1 702 000	13, 15
211	LAR(LAURIE)	56°38′06″	101°52′48″	64C/12	0.80		2.15			1 360 500	3
212	FLIN FLON	54°45′28″	101°53′00″	63K/13	2.20		4.10	43.20	2.85	62 927 000	13, 15
213	CALLINAN	54°47′03″	101°53′08″	63K/13	1.5		4.1	11.20	1.45	2 619 000	13, 15
214	CORONATION	54°35′00″	102°00′00″	63K/12	4.25		0.24	5.66	2.26	1 282 498	8
215	FLEXAR	54°40′37″	102°01′43″	63L/9	4.08		0.44	5.49	1.17	305 659	8
216	BIRCH LAKE	54°39′41″	102°01′58″	63L/9	6.17			4.53		278 449	8
217	SCHOTTS LAKE	55°05′45″	102°13′35″	63M/1	0.61		1.35			1 982 702	3
218	RAMSAY SHOWING	54°44′17″	102°45′05″	63L/10	2.16		1.77	6.96		738 884	3
219	HANSON(MCILVENNA)	54°37′30″	102°51′00″	63L/10	0.95		5.76	30.17	0.69	8 888 600	12
220	BIGSTONE	54°34′58″	103°11′40″	63L/11	1.87		1.11	9.94	0.45	3 628 000	3
221	MCKENZIE(PEG)	56°07′20″	103°42′04″	64D/4	0.55		4.84	0.18	18.63	3 695 000	3
222	MUSK	65°19′20″	107°36′00″	76G/5	1.20	1.40	10.00	343.00		340 000	3
223	YAVA	65°36′10″	107°56′00″	76G/12	0.50	0.50	3.00	102.80	2.09	1 500 000	3
224	HACKETT (A ZONE)	65°55′00″	108°22′00″	76F/16	0.25	1.40	8.50	240.00	1.89	4 535 000	3
225	BOOT LAKE	65°54′55″	108°25′50″	76F/16	0.29	4.97	0.99	200.91	0.48	4 535 000	3
226	EAST CLEAVER	65°55′55″	108°27′30″	76F/16	0.47	0.94	4.08	108.34	0.48	7 256 000	3
227	HIGH LAKE	67°22′45″	110°51′19″	76M/7	3.53	0.20	2.46	37.71	0.79	4 722 749	3
228	KENNEDY LAKE	63°01′57″	110°56′57″	75M/2		1.10	7.30	137.49		39 001	3
229	INDIAN MTN(BB)	63°01′57″	110°56′57″	75M/2	0.20	0.70	9.54	116.57		879 790	3
230	GONDOR	65°33′43″	111°48′00″	76E/12	0.50	0.50	6.00	50.00		7 500 000	3
231	SUNRISE LAKE	62°54′06″	112°22′30″	85I/16	0.02	4.20	8.90	404.57	0.96	1 865 699	3, 13
232	BEAR	62°53′36″	112°23′30″	85I/16		2.32	6.11	219.77	0.89	809 700	3, 13
233	HOOD RIVER #10	66°03′35″	112°45′15″	86I/2	5.00		3.50	34.29		453 500	3
234	IZOK LAKE	65°37′50″	112°47′50″	86H/10	2.85	1.46	14.40	75.09		9 795 600	3
235	HOOD RIVER #41	66°02′30″	112°48′00″	86I/2	1.57	0.20	4.12	17.83		272 100	3
236	GOLDSTREAM RIVER	51°37′00″	118°13′00″	82M/9	4.81		3.08	20.60		2 287 886	17
237	REA GOLD	51°09′00″	119°49′00″	82M/4	0.57	2.14	2.25	73.37	6.51	242 822	3

Table 6.3-1. (cont.)

NO.	NAME	LATITUDE / LONGITUDE		NTS	Cu %	Pb %	Zn %	Ag (g/t)	Au (g/t)	TONNES	REFERENCE
238	SAMATOSUM	51°09′40″	119°49′00″	82M/4	1.10	1.50	2.50	685.00	1.40	483 000	7 (01/04/91)
239	HOMESTAKE	51°06′27″	119°49′45″	82M/4	0.55	2.50	4.00	240.00		919 296	17
240	CHU CHUA	51°22′10″	120°03′30″	92P/8	2.00		0.50	8.00	0.50	3 000 000	3
241	SENECA	49°19′00″	121°56′37″	92H/5	0.63	0.15	3.60	41.14	0.82	1 506 334	3
242	BRITANNIA	49°36′40″	123°08′30″	92G/11	1.90		0.65	6.86	0.69	48 815 534	3, 17
243	TEDI (BRANDY)	50°05′00″	123°08′30″	92J/3	0.22	2.07	2.04	126.17	0.34	132 255	3
244	TWIN J	48°52′00″	123°47′00″	92B/13	1.60	0.65	6.60	140.57	4.11	594 992	3
245	LARA (HOPE)	48°52′50″	123°54′20″	92B/13	1.01	1.22	5.87	100.11	4.73	529 000	17
246	SUNRO	48°27′00″	124°01′00″	92C/8	1.47			1.37	0.14	2 032 587	3
247	WESTMIN (HW)	49°34′20″	125°35′10″	92F/12	2.20	0.30	5.30	37.71	2.40	13 815 424	18
248	WESTMIN(L,M,P)	49°34′32″	125°36′07″	92F/12	1.50	1.10	7.60	109.71	2.06	5 646 075	18
249	KUTCHO CREEK	58°12′10″	128°21′40″	104I/7	1.76	0.06	2.54	35.00	0.37	14 300 000	3, 7 (25/03/91)
250	ECSTALL RIVER	53°52′25″	129°30′40″	103H/13	0.86	0.20	2.30	24.34	0.69	4 535 000	3, 17
251	HIDDEN CREEK(ANYOX)	55°26′33″	129°49′35″	103P/5	0.90			8.23		23 721 524	3, 17
252	BONANZA(ANYOX)	55°23′45″	129°51′15″	103P/5	1.88					882 456	3, 17
253	DOUBLE ED(ANYOX)	55°24′45″	129°52′35″	103P/5	1.00		0.60			3 628 800	3
254	RED WING	55°22′50″	129°53′00″	103P/5	1.84			29.49		181 400	3
255	EDEN	55°25′40″	129°53′30″	103P/5	2.00					226 800	3
256	GRANDUC	56°12′45″	130°20′30″	104B/1	1.79	0.02	0.10	10.63	0.17	25 063 140	8, 17
257	ESKAY CREEK	56°37′01″	30°27′55″	104B/9		2.20	5.40	998.40	26.40	3 954 520	7 (31/12/90)
258	SWIM LAKE	62°12′50″	133°01′50″	105K/3		3.80	4.70	50.4		4 308 250	7 (25/03/91)
259	TULSEQUAH CHIEF	58°44′20″	133°34′30″	104K/12	1.60	1.31	7.02	100.50	2.74	6 193 609	3, 8, 17
260	BIG BULL	58°38′24″	133°35′24″	104K/12	1.32	1.31	6.06	113.14	3.15	4 107 803	8
261	MARG	64°00′40″	134°28′20″	106D/1	1.90	2.60	4.99	64.11	0.89	2 857 050	3, 7 (3/12/90)
262	HART RIVER	64°38′00″	136°51′00″	116A/10	1.45	0.87	3.65	49.71	1.41	1 067 539	3
263	WINDY CRAGGY	59°44′00″	137°45′00″	114P/12	1.59			3.60	0.20	113 000 000	3, 17

[1]**Evans, D.T.W., Swinden, H.S., Kean, B.S., and Hogan, A.**
1992: Metallogeny of the vestiges of Iapetus, Island of Newfoundland; Newfoundland Department of Mines and Energy, Map 92-19, scale 1:500 000.

[2]**Swinden, H.S. and Kean, B.F. (ed.)**
1988: The Volcanogenic Sulphide Districts of Central Newfoundland; Geological Association of Canada Guidebook, 250 p.

[3]**Energy, Mines and Resources Canada**
1989: Canadian Mineral Deposits Not Being Mined in 1989; Mineral Policy Sector, Energy Mines and Resources Mineral Bulletin, MR223.

[4]**Swanson, E.A., Strong, D.F., and Thurlow, J.G. (ed.)**
1981: The Buchans Orebodies: Fifty Years of Geology and Mining; Geological Association of Canada, Special Paper 22, 350 p.

[5]**Gibson, H.L. and Kerr, D.J.**
1993: Giant volcanic-associated massive sulphide deposits: with emphasis on Archean examples; in Giant Ore Deposits (ed.) B.H. Whiting, R. Mason, and C.J. Hodgson; Society of Economic Geologists Special Publication No. 2, p. 319-348.

[6]**Anon**
1993: Canadian Mines Handbook 1992-93; (ed.) D. Giancola; Northern Miner Press, Toronto, Ontario.

[7]**Northern Miner newspaper** (issue in brackets)

[8]**National Mineral Index,** Geological Survey of Canada, Room 652, 601 Booth Street, Ottawa, Ontario.

[9]**Fyffe, L.R., van Staal, C.R., and Winchester, J.A.**
1990: Late Precambrian-early Paleozoic volcanic regimes and associated massive sulfide deposits in northeast mainland Appalacians; The Canadian Mining and Metallurgical Bulletin, v. 83, no. 938, p. 70-78.

[10]**Rive, M., Verpaelst, P., Gaganon, Y., Lulin, J.M., Riverin, G. and Simard, A. (ed.)**
1990: The Northwestern Quebec Polymetallic Belt; The Canadian Institute of Mining and Metallurgy, Special Volume 43, 423 p.

[11]**Mining Journal magazine** (London) (issue in brackets).

[12]**Mining Annual Review,** 1990: Mining Journal Press, London

[13]**International Association for the Genesis of Ore Deposits, Eighth Symposium, Ottawa,**
1990: **Guidebooks:**
2158 - Lithotectonic and associated mineralization of the eastern extremity of the Abitibi Greenstone belt
2159 - Mineral deposits of Noranda, Quebec, and Cobalt, Ontario
2161 - Geology and ore deposits of the Timmins district, Ontario
2164 - Mineral deposits in the western Superior Province, Ontario
2165 - Geology and mineral deposits of the the early Proterozoic Flin Flon Belt and Thompson Belt, Manitoba
2168 - Mineral deposits of the Slave Province, N.W.T.

[14]**Manitoba Energy and Mines Report of Activities** (issue in brackets)

[15]**Bailes, A.H., Syme, E.C., Galley, A., Price, D.P., Skirrow, R., Ziehlke, D.J. (ed.)**
1987: Early Proterzoic Volcanism, Hydrothermal Activity, and Associated Ore Deposits at Flin Flon and Snow Lake, Manitoba; Geological Association of Canada/Mineralogical Association of Canada guidebook, 95 p.

[16]**Gale, G.H., Baldwin, D.A., and Koo, J.**
1980: Geological evaluation of Precambrian massive sulphide deposit potential in Manitoba; Manitoba Energy and Mines, Economic Geology Report 79-1, 137 p., 23 maps.

[17]**McMillan, W.J., Howy, T., MacIntyre, D.G., Nelson, J.L., Nixon-Graham, T., Hammack, J.L., Panteleyev, A., Ray, G.E., and Webster, I.C.L.**
1991: Ore deposits, teconics and metallogeny in the Canadian Cordillera; British Columbia, Ministry of Energy, Mines and Petroleum Resources, Paper 1991-4, 276 p.

[18]**Fleming, J., Walker, R., and Wilton, P. (ed.)**
1983: Mineral Deposits of Vancouver Island: Westmin Resources (Au-Ag-Cu-Pb-Zn), Island Copper (Cu-Au-Mo), Argonaut (Fe); Geological Association of Canada/Mineralogical Association of Canada guidebook.

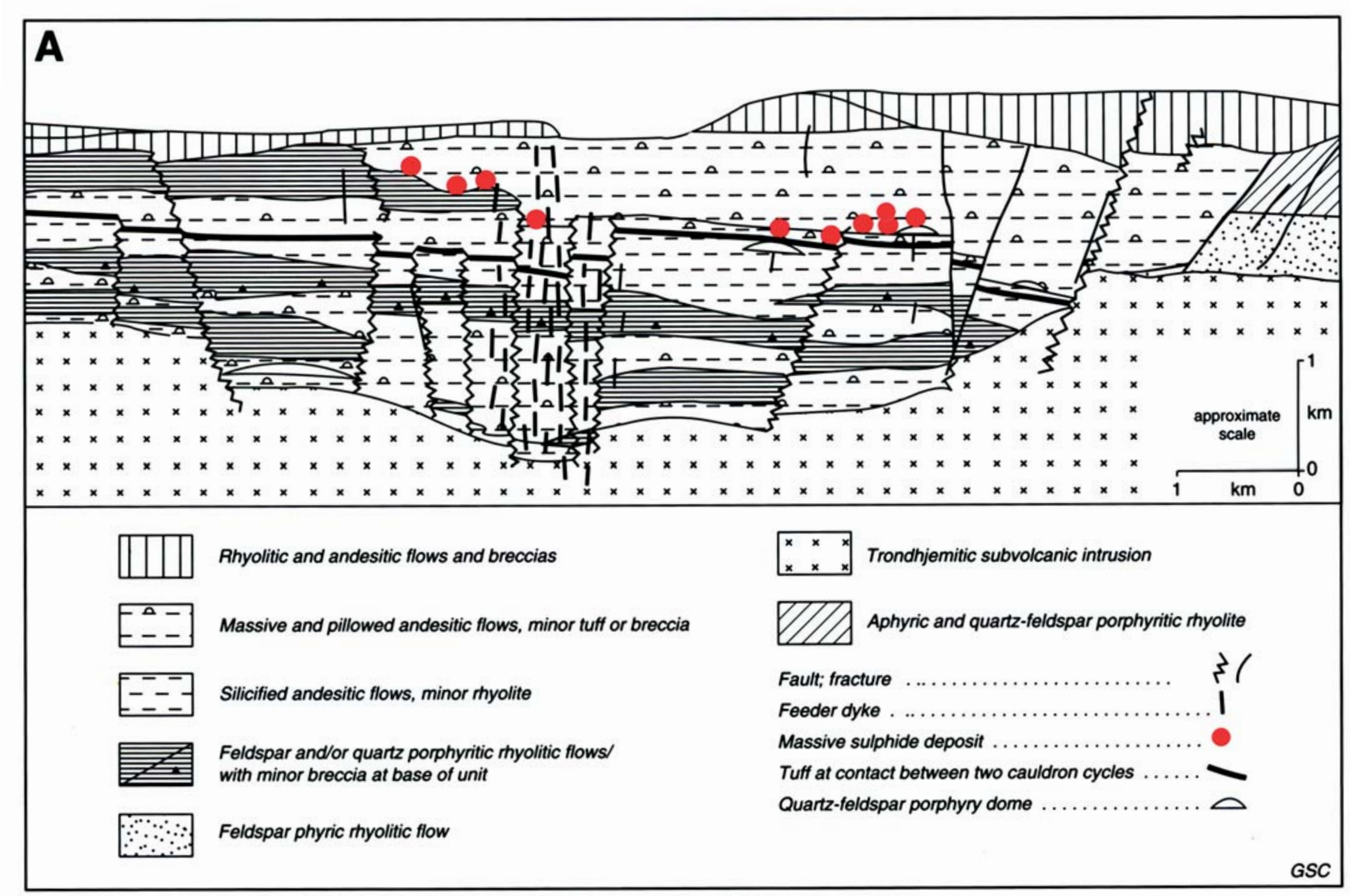

Figure 6.3-4A. Cross-section of the main caldera, Noranda massive sulphide district (after Gibson and Watkinson, 1990). This section is oriented approximately north-south, and is based on information from mines and drill holes.

In contrast, deposits in sediment-covered areas are tabular, circular to elliptical in plan, and commonly display distinctive layering or bedding within the sulphide zones. The sulphides are locally interbanded with silicate layers. Some parts of the Besshi-type deposits are composed of massive ore. Lateral dimensions of more than a kilometre are common. Ore thickness is typically a few tens of metres. Iron-formations (both oxide and silicate facies) are common at the ore horizon (e.g., the Vasskis of Norway). Alteration zones are not as pronounced as for the deposits in more volcanic-dominated areas, but iron- and magnesium-enriched zones, containing disseminated sulphides, underlie many of the Caledonide deposits, such as those near Bathurst, New Brunswick.

Volcanic rock-dominated deposits are commonly overlain by sedimentary strata, composed of both clastic and chemical components. These strata may have considerable lateral continuity; the Key Tuffite horizon, coincident with or immediately overlying all of the deposits on both limbs of the Mattagami Lake "anticline", is a laminated chert-pyrite unit containing some volcaniclastic fragments (Piche et al., 1990). Graphitic shale overlies the Kidd Creek orebody. This shale may represent the residues of vent-specific bacterial colonies, but does not extend far beyond the limits of the deposit. Tuff horizons are associated with some of the deposits in the Noranda district (e.g. Ansil, Corbet, and the Amulet bodies). Iron-formation is not common, but is prominently associated with the hanging wall of the Manitouwadge, Ontario deposits, and the footwall to the Lyon Lake and Creek Zone deposits near Sturgeon Lake, Ontario. Iron oxide zones (ochre) occur at the top of some of the ophiolite-associated deposits, and in some cases may be the product of seafloor oxidation of sulphides, as observed on the Mir mound (TAG), Mid-Atlantic Ridge (Hannington and Jonasson, 1992).

Mineralogical composition, textures, and structures within orebodies

Virtually all massive sulphide deposits are mineralogically simple. They contain at least 50%, and commonly more than 80% sulphides by volume (Sangster and Scott, 1976).

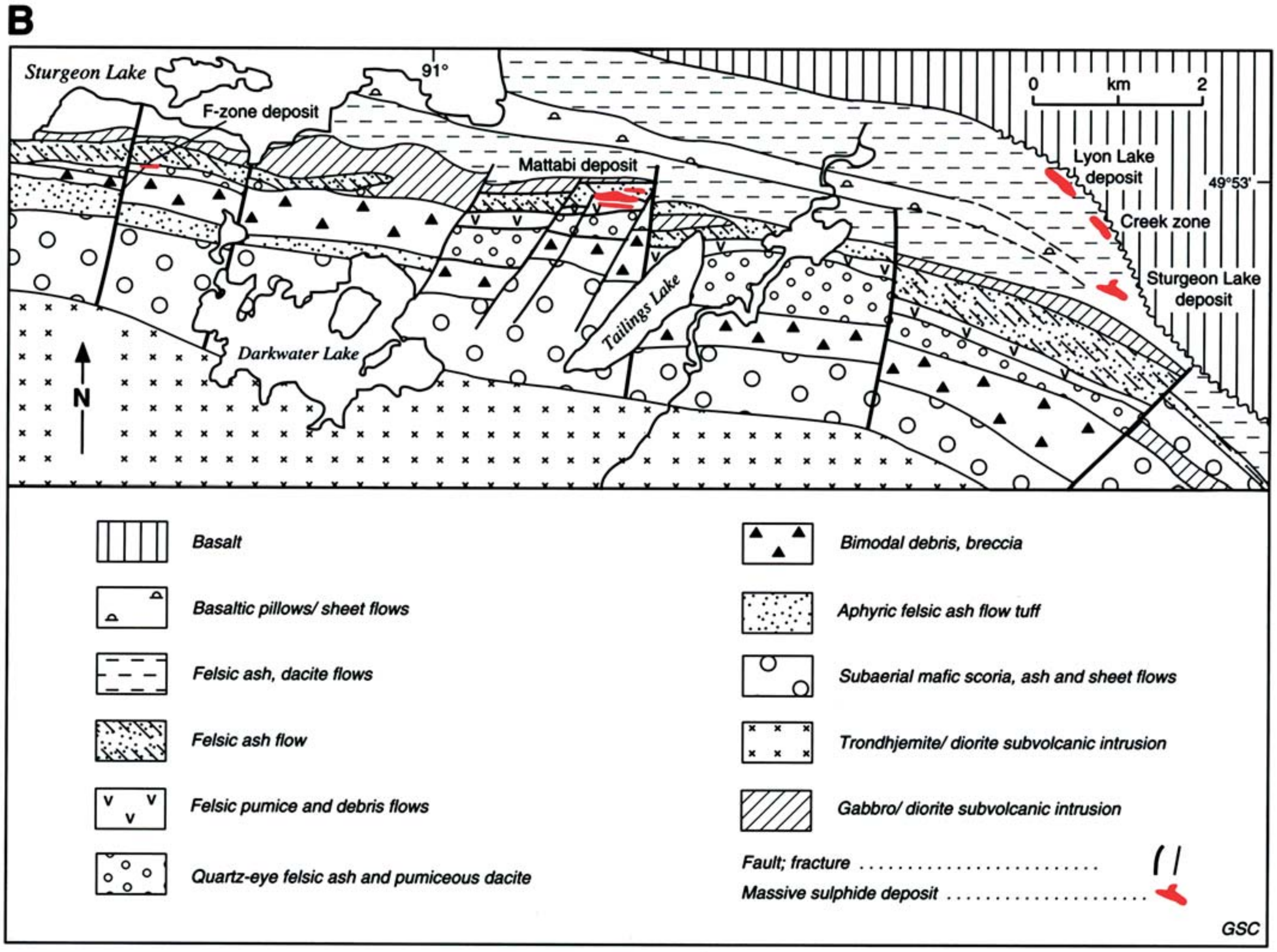

Figure 6.3-4B. Map of the Sturgeon Lake massive sulphide camp, northwestern Ontario (after Morton et al. 1990). This map represents closely a cross-section through the Sturgeon Lake caldera, and is at about the same scale as Figure 6.3-4A. Both diagrams closely reflect a right-section through their respective districts. Note that both districts have subvolcanic intrusions at their base, and subequal amounts of felsic and mafic volcanic rock. However, the Noranda district is dominated by felsic flows, whereas Sturgeon Lake is dominated by subaerial mafic scoria deposits, and subaqueous pyroclastic flows and breccia.

Pyrite typically constitutes 50-90% of the massive ore, with sphalerite, chalcopyrite, and galena forming about 10%. Some metamorphosed deposits, such as those at Manitouwadge, Ontario, contain abundant pyrrhotite (Kissin, 1974). Deposits formed in deep water (Noranda type) contain only sphalerite and chalcopyrite as their principal ore minerals, but those that formed in shallow water typically also contain recoverable galena. Curiously, barite occurs in the oldest deposits in Australia and South Africa (pre-3.0 Ga) and in some Phanerozoic deposits, but is much less common in late Archean and Proterozoic deposits. Massive magnetite constitutes about one-third of the Ansil deposit, Quebec (Riverin et al., 1990).

Gangue minerals are poorly documented, and consist primarily of quartz, with chlorite, sericite, and aluminosilicate minerals (or their metamorphic equivalents) predominant. Gahnite is an accessory mineral at virtually all deposits that have attained amphibolite grade of metamorphism.

The mineral assemblage of the stringer ores is usually also very simple, with chalcopyrite, pyrite, pyrrhotite, sphalerite, and magnetite present. One orebody and the stringer zone at the Kidd Creek mine have a local bornite zone with an unusual proliferation of selenium minerals (Thorpe et al., 1976). Tellurides occur beneath the Mattagami Lake deposit (Thorpe and Harris, 1973).

Within the deposits in volcanic-dominated areas, the well-known pattern of high Cu/(Cu+Zn) ratios in the lower zones and lower ratios in the upper zones is so common that Sangster (1972) suggested that it can be used reliably as an indicator of stratigraphic facing. The massive zones are

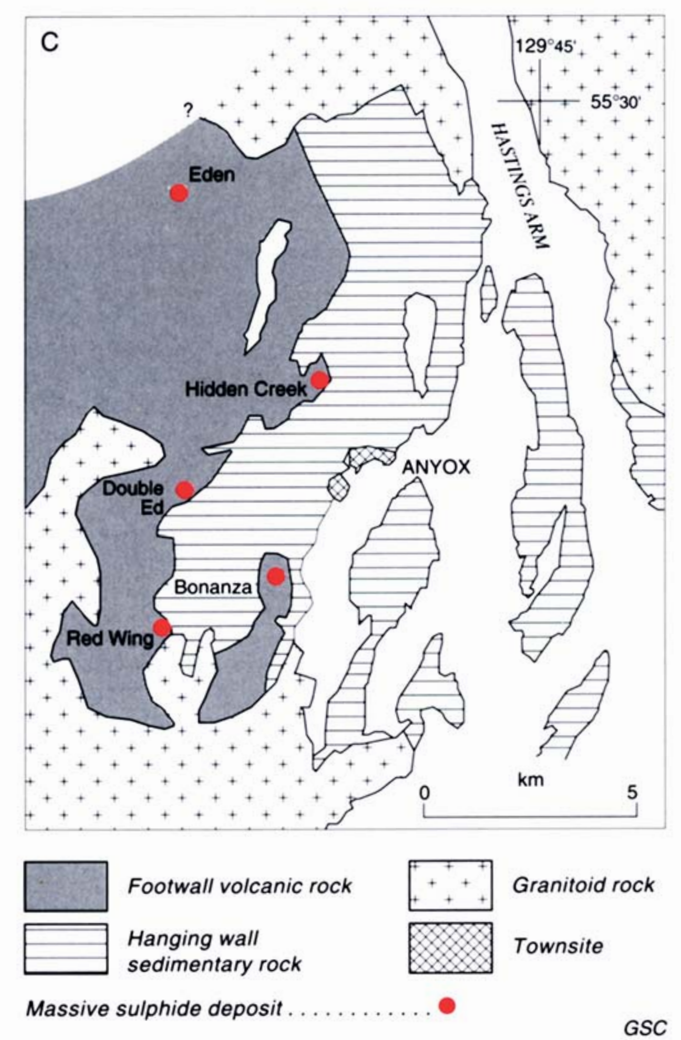

Figure 6.3-4C. Geology of the Anyox massive sulphide area, northern British Columbia. Note that most of the deposits are at or near the contact between hanging wall sedimentary and footwall volcanic rocks (after Alldrick, 1986).

iron-rich (pyritic) at the tops and flanks of the deposit. Some stringer zones exhibit a narrow zinc-rich fringe zone (Purdie, 1967; Simmons, 1973) and a copper-rich core. Copper-zinc ratios within some of the less deformed orebodies (e.g., Millenbach deposit) indicate the presence of a distinct copper-rich spine (Knuckey, 1975) that is transgressive to bedding. This "spine" is present even where the pyrite-sphalerite zone is brecciated and locally transported, indicating that it "grew" after emplacement of the zinc ore. The spine is composed of massive chalcopyrite and pyrite; pyrrhotite is more abundant in the laterally adjacent pyrite-sphalerite ore. The ophiolite deposits, and some of the deposits in which sedimentary rocks are important, are usually copper-rich (Cu/Zn = 3/1 to 4/1). Some of the latter group of deposits have high (~1000 ppm) cobalt contents.

Layered (and possibly bedded) sulphide is present at the tops and peripheral parts of many of the massive sulphide mounds. The central parts of the orebodies are paragenetically complex, with zoned "veins" or pseudo-beds of sulphide following fractures and joints within massive sulphides, as at Mine Gallen (Watkinson et al., 1990). The margins of the massive bodies may consist of sulphide breccia, possibly formed from fallen chimney structures.

Alteration beneath Cu-Zn massive sulphide deposits

Alteration has been studied more extensively than most attributes of these deposits. Alteration mineral assemblages and associated chemical changes have been very useful exploration guides. Alteration occurs in two distinct zones beneath these deposits (Fig. 6.3-6 and 6.3-4A). **Alteration pipes** occur immediately below the massive sulphide zones; here a complex interaction has occurred between the immediate substrata to the deposits and both ore-forming (hydrothermal) fluids and locally-advecting seawater. **Lower, semiconformable alteration zones** (Franklin et al., 1981) occur several hundreds of metres or more below the massive sulphide deposits, and may represent in part the "reservoir zone" (Hodgson and Lydon, 1977) where the metals and sulphur were leached (Spooner and Fyfe, 1973) prior to their ascent to and expulsion onto the seafloor.

Beneath Precambrian deposits formed in deep water (Noranda type), alteration pipes typically have a chloritic core, surrounded by a sericitic rim. Some, such as at Mattagami Lake, contain talc, magnetite, and phlogopite (Costa et al., 1983). The pipes usually taper downwards within a few tens of metres to hundreds of metres below the deposits, to a fault-controlled zone less than a metre in diameter. Beneath deposits formed in shallow water (Mattabi type; Fig. 6.3-7), the pipes are silicified and sericitized; chlorite is subordinate and is most abundant on the periphery of the pipes. Aluminosilicate minerals are prominent.

Alteration pipes under Phanerozoic Cu-Zn deposits are similar to, but more variable than those under their Precambrian counterparts. For example, Aggarwal and Nesbitt (1984) described a talc-enriched alteration core, surrounded by a silica-pyrite alteration halo, beneath the Chu Chua, British Columbia deposit. The Newfoundland, Cyprus, Oman, and East Galapagos Ridge deposits have Mg-chlorite in the peripheral parts of their pipes, together with illite. The presence of abundant Fe-chlorite, quartz, and pyrite typify the central parts of the pipes.

The lower semiconformable alteration zones have been recognized under deposits in several massive sulphide districts (Galley and Jonasson, 1992). These include laterally extensive (several kilometres of strike length) quartz-epidote zones that are several hundred metres thick, and extend downwards from a few hundred metres stratigraphically below the Noranda, Matagami, and Snow Lake deposits of the Canadian Shield. Zones containing epidote, actinolite, and quartz in the lower pillow lavas and sheeted dykes of the ophiolite sequences at Cyprus (Gass and Smewing, 1973) and in East Liguria, Italy, were explained by Spooner and Fyfe (1973) as being due to increased heat flow as a result of convective heat transfer away from the cooling intrusions at the base of these sequences. All of the

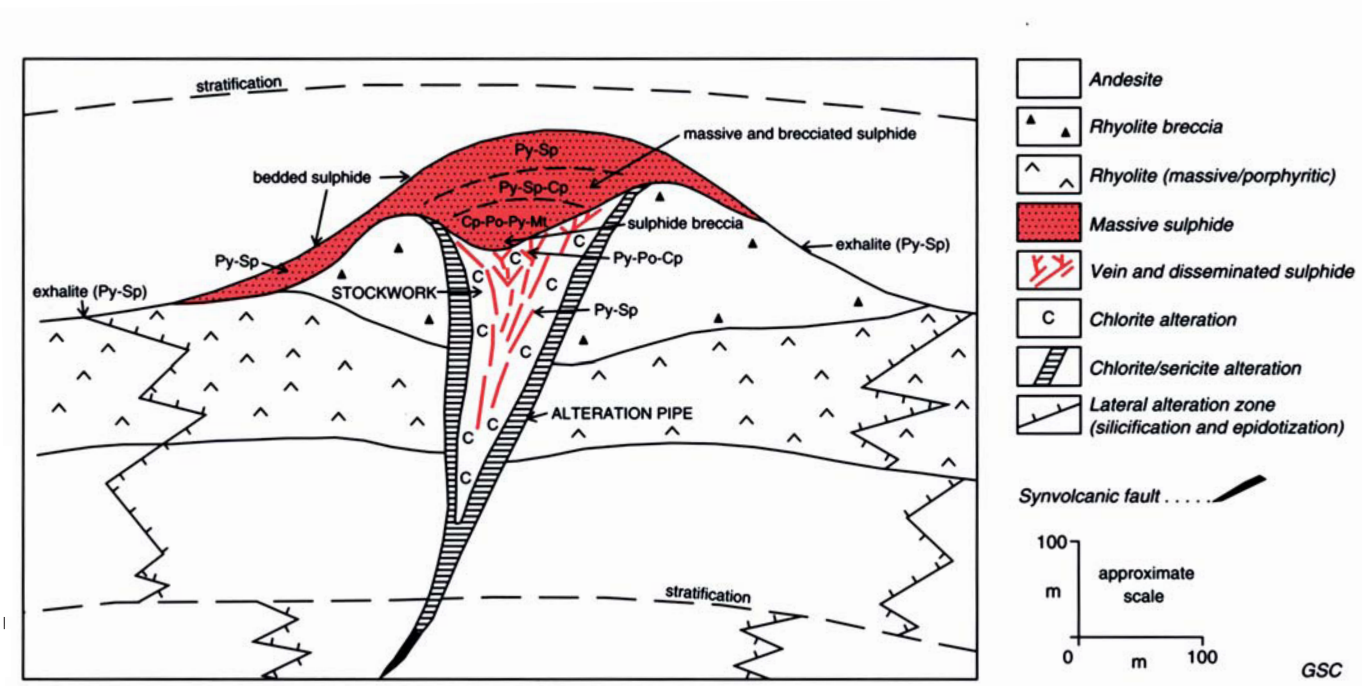

Figure 6.3-5. Summary cross-section of a typical Noranda type deposit. Py: pyrite; Sp: sphalerite; Cp: chalcopyrite; Po: pyrrhotite; Mt: magnetite.

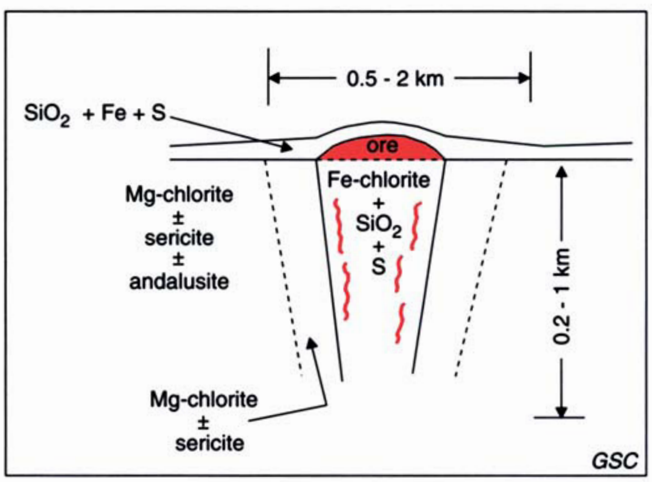

Figure 6.3-6. Synthesis of alteration zones immediately beneath Cu-Zn deposits, such as at Noranda, Cyprus, and the Proterozoic deposits of the Canadian Shield. Note that the "Mg-chlorite±sericite" zone is gradational into both the central Fe-chlorite+SiO_2+S and the outermost andalusite zones.

epidote-quartz zones are metal depleted. They represent the zone of high temperature hydrothermal reaction (ca. 400°C), under low water-rock ratio conditions, where the metals and sulphur entered into the ore-forming solution (Spooner, 1977; Spooner et al., 1977a, b; Richards et al., 1989).

Zones of alkali-depleted, variably carbonatized strata occur immediately beneath some deposits in sedimentary rocks, and also in volcanic rocks under the Mattabi-type deposits. These may extend for as much as tens of kilometres along strike, and occur in the upper few hundred metres of the footwall. These zones probably represent a sealed cap to the hydrothermal reservoir, and formed through progressive heating of downward percolating seawater, with some possible input of CO_2 from an underlying magma chamber, or by thermal breakdown of organic compounds in the footwall.

Zinc-lead-copper group

These deposits, most commonly Phanerozoic in age, occur primarily in arc-related terranes where felsic volcanic rocks, with or without associated sedimentary strata, are dominant (Fig. 6.3-8). The deposits range from those in felsic volcanic-dominated terranes, such as those in the Buttle Lake area of Vancouver Island and the Buchans area of Newfoundland, to those with thick sedimentary sequences in their footwall section, such as the deposits of the Bathurst district, New Brunswick. Deposits of the latter group are similar in many of the characteristics of their geological settings to the sediment-associated deposits in the Cu-Zn group. Notably, however, the deposits in the Zn-Pb-Cu group have little or no mafic volcanic rock in their footwall sequences. Modern examples of this group have been discovered in the Lau Basin (Von Stackelberg and Brett, 1990) and the Okinawa Trough (Urabe et al., 1990).

Geological setting

Volcanic rock-dominated areas

The best known major district of this type is the Hokuroku district of Japan. This area of the Green Tuff Belt is a 13 Ma old basin containing a bimodal suite of island arc-related volcanic rocks and mudstone. Extensive reviews of the

"Kuroko deposits" of this district (Tatsumi, 1970; Tatsumi and Watanabe, 1971; Ishihara and Terashima, 1974; Ohmoto and Skinner, 1983) serve as a comparative model for similar deposits in Canada, at Buchans, Newfoundland and Buttle Lake, British Columbia (Juras and Pearson, 1990), as well as for deposits in the Tasman Geosyncline (Lambert, 1979). The Canadian and Australian deposits of this group are in much more deformed terranes, however, and some characteristics of the orebodies are best exemplified in the Hokuroku district.

The footwall sequences to these deposits are composed primarily of calc-alkaline felsic porphyritic ash-flow tuff, rhyolite domes and flows, and some felsic epiclastic rocks. Basalt may occur near the base of the sequence (Buchans and Buttle Lake). Most of the host strata probably were deposited in submarine calderas. The deposits formed during periods of extension following island arc construction, and may be temporally related to caldera resurgence.

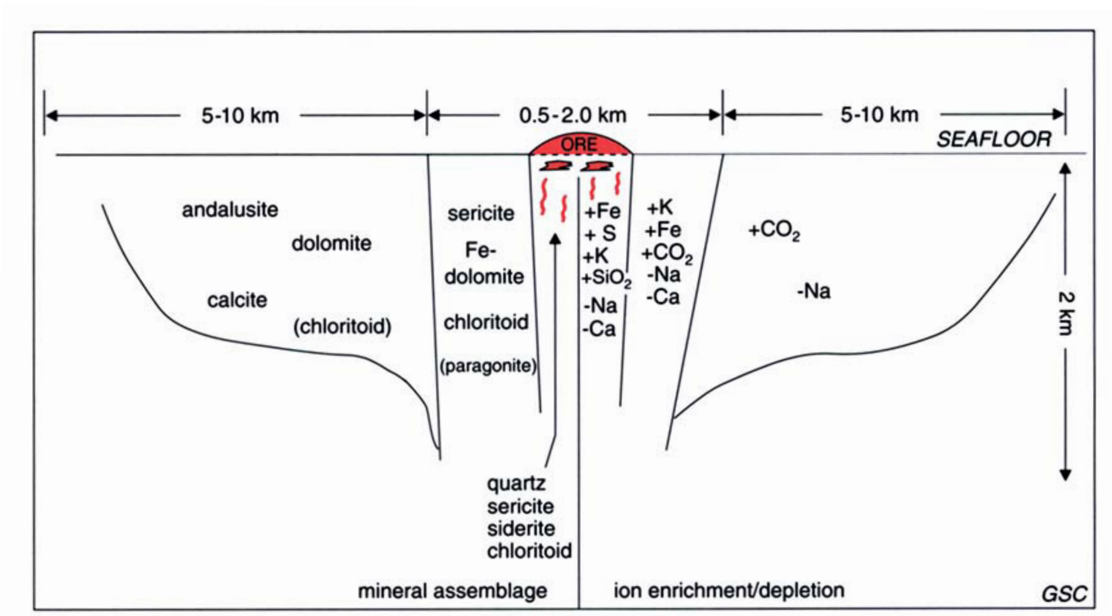

Figure 6.3-7. Synthesis of alteration zones adjacent to Zn-Cu-Pb deposits such as the Mattabi deposit, Ontario and others that formed in sequences dominated by felsic tuff, breccia, and mafic scoria and sheet flows. Adjacent to the main alteration pipe, the alteration zones are not well defined. Sodium depletion is laterally extensive but confined to a few hundred metres vertically. Metasomatic carbonate alteration is pervasive in the footwall. Minerals in brackets are present in minor amounts.

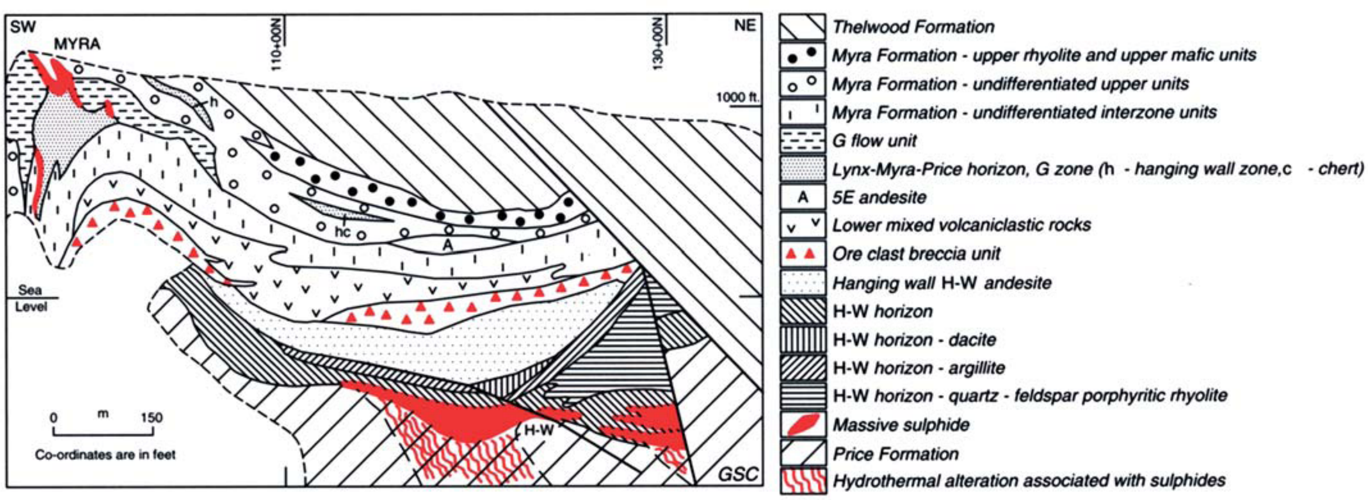

Figure 6.3-8. Cross-section of the H-W ore deposit in the Buttle Lake area, British Columbia (from Juras and Pearson 1990). This is a typical Kuroko-like deposit.

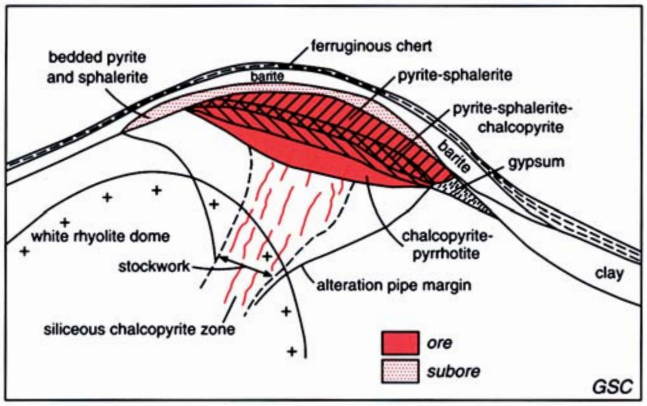

Figure 6.3-9. Typical cross-section of Pb-Zn-Cu ore zone illustrating the principal ore zones. Compiled from Eldridge et al. (1983), Lambert and Sato (1974), and others.

Volcano-sedimentary areas

The largest deposits of this group are in lower Carboniferous rocks of the Iberian pyrite belt in southern Portugal and southwestern Spain. The best Canadian examples are in the Bathurst district, New Brunswick; the Sudbury Basin, Ontario; the Omineca crystalline belt, British Columbia; and in several enclaves in the Coast Batholith in British Columbia. The great lateral continuity of ore, lack of extensive alteration, and association with sedimentary rocks make deposits of this group similar to arc-related deposits of the Cu-Zn group. However, the Zn-Pb-Cu deposits are usually in sequences in which felsic volcanic rocks predominate near the ore horizon. Deposits in the Bathurst camp, for example, have a few hundred metres of felsic ash flow tuff as their most common immediate footwall rock, underlain by thousands of metres of greywacke and pelite. Iron-formation is the immediate hanging wall to 7 of the 30 deposits in this camp. Basalt is restricted to the hanging wall sequence of most of the deposits. Van Staal (1987) has established that the Tetagouche rocks are part of a series of thrust slices, which include ophiolite-associated slices near the base, and arc-like volcanic rocks in the uppermost slice. Van Staal interpreted the strata containing the massive sulphide deposits to have formed as part of a back-arc basin sequence, immediately southeast of a magmatic arc. The Iapetus ocean floor separated this arc from the North America craton, further to the northwest.

Form and composition

Deposits in volcanic-dominated areas are typically well zoned bulbous massive bodies, underlain by variably developed stringer ore (Fig. 6.3-9). Lambert and Sato (1974) described the following zones for the Kuroko deposits: 1) Siliceous ore (keiko): pyrite-chalcopyrite-quartz stockwork ore; 2) "Gypsum ore (sekkoko): gypsum-anhydrite-(pyrite-chalcopyrite-sphalerite-galena-quartz-clays) stratabound ore; 3) "Pyrite ore (ryukako): pyrite-(chalcopyrite-quartz) ore"; 4) "Yellow ore (oko): pyrite-chalcopyrite-(sphalerite-barite-quartz) stratiform ore"; 5) "Black ore (kuroko): sphalerite-galena-chalcopyrite-pyrite-barite stratiform ore." Towards the top of the zone, tetrahedrite-tennantite is common. Bornite occurs in a few deposits. 6) "Barite ore: thin well-stratified bedded ore consisting almost entirely of barite, but sometimes containing minor amounts of calcite, dolomite, and siderite"; 7) "Ferruginous chert (tetsusekiei bed): a thin bed of cryptocrystalline quartz and hematite." Similar zoning is present at many Canadian examples, including the Buttle Lake deposits (Juras and Pearson, 1990).

Mechanically-transported breccias are commonly associated with this type of deposit, and are particularly prominent in the Buchans, Newfoundland deposits (Binney, 1987), where they constitute about 50% of the ore. In most deposits, the breccia formed as a sulphide talus at the base of the endogenous mounds that were presumably primary vent sites. Lateral transport of the Buchans sulphide breccias for hundreds of metres or more indicates that these deposits formed on steep slopes, or were rapidly uplifted immediately after deposition.

Orebodies in sediment-dominated terranes, such as those in the Bathurst district, New Brunswick, are tabular and laterally extensive. These deposits exhibit primary metal zoning, although less prominent than their volcanic-hosted counterparts. Luff (1977) described three zones at Brunswick # 12. Unit 1, at the bottom and south of the ore, consists of massive pyrite with minor sphalerite and galena, and variable but locally significant amounts of chalcopyrite and pyrrhotite. Unit 2, the main zone, is distinctly layered sphalerite-galena-pyrite ore with minor chalcopyrite and pyrrhotite. Unit 3, the upper pyrite unit, consists of massive, fine grained pyrite with minor sphalerite, galena, and chalcopyrite.

Iron-rich rocks are common in the immediate hanging wall sequence of deposits in both the volcanic- and sediment-associated deposits of this compositional group. These are of two distinctly different genetic types. Some ferruginous strata have formed through seafloor weathering of sulphides, forming poorly bedded, massive oxide zones. Others are ferruginous (and usually cherty) precipitates which formed from low-temperature hydrothermal fluids. The tetsusekiei zone that caps many of the Kuroko deposits, and the manganiferous iron-formation that overlies the Bathurst deposits is "Algoma type" (Gross, 1965). These are probably not a product of oxidation of sulphides, but may have precipitated from low-temperature fluids that were associated with the terminal stage of their respective hydrothermal events.

Mineralogical composition, textures, and structures within orebodies

Deposits of this group are more mineralogically complex than those of the copper-zinc group. In addition to pyrite, sphalerite, galena, and chalcopyrite, barite is common, particularly in the volcanic-associated deposits such as Buchans and Buttle Lake. In the Bathurst district, barite is absent; sulphosalts, arsenopyrite, and stannite occur in minor amounts (Chen and Petruk, 1980). Nonsulphide minerals in the deposits in the Bathurst district include quartz (major mineral); chlorite, siderite, calcite, and dolomite are all present (Jambor, 1979). In the Bousquet district, Quebec, Au-rich sulphide deposits have similar mineralogical characteristics to this group, and may be highly deformed volcanic-associated massive sulphide

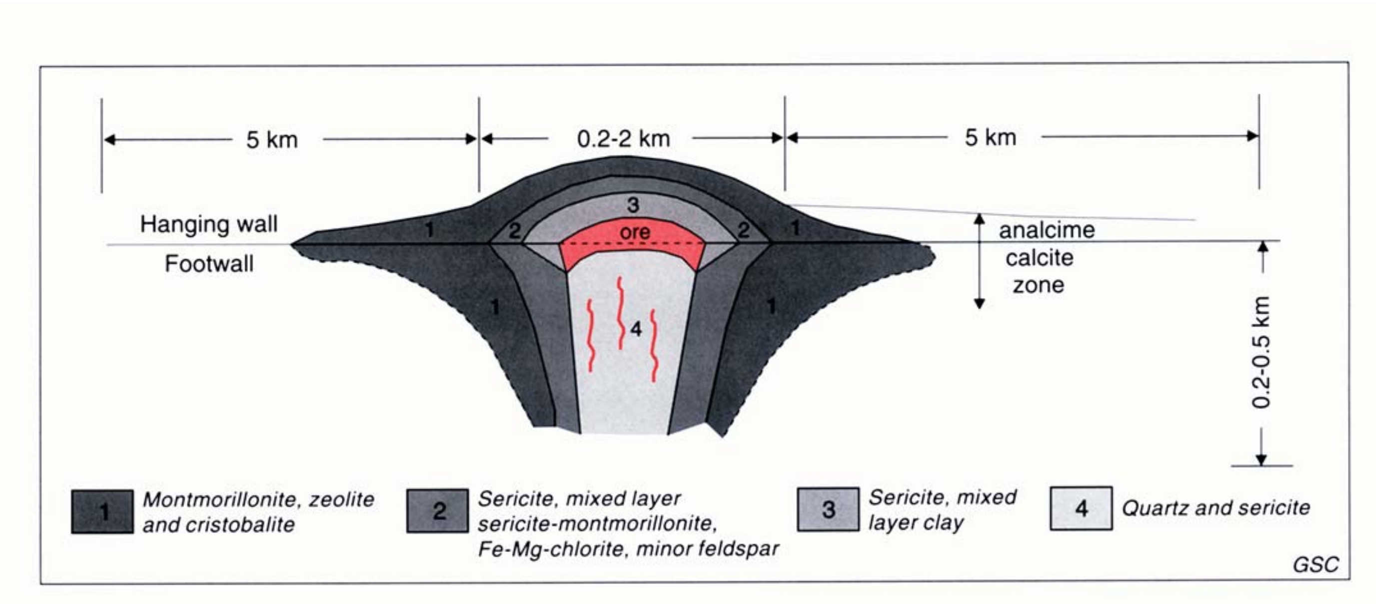

Figure 6.3-10. Alteration immediately associated with Zn-Pb-Cu deposits (after Shirozu, 1974).

deposits (Marquis et al., 1990). Most of the zinc-lead-copper deposits are fine grained, which causes recovery problems during processing. Most copper-zinc deposits, in contrast, are coarse grained and easily milled.

Alteration beneath zinc-lead-copper massive sulphide deposits

Alteration associated with Zn-Pb-Cu deposits, including Canadian deposits, is typified by that in the Hokuroku district of Japan (Fig. 6.3-10). The "lower semiconformable" alteration zones, such as those which underlie the Cu-Zn deposits, are unknown under these deposits. However, the lower strata are difficult to access in Japan, and structural complexities at Buchans and Buttle Lake, and in the Tasman geosyncline, may have removed these parts of their sequences.

Four alteration zones (Fig. 6.3-10) in the Hokuroko district have been described by Shirozu (1974), Iijima (1974), and Date et al. (1983). The most intense zone of alteration, zone 4, is immediately below the deposits, and consists of silicified, sericitized rock, with a small amount of chlorite. Zone 3 contains sericite, Mg-chlorite, and montmorillonite, and is not silicified. Feldspar is absent from zones 3 and 4. Zone 2 consists of sericite, mixed-layer smectite minerals, and feldspar. Zone 1 contains zeolite (typically analcime) as an essential mineral, as well as montmorillonite. Outside these four zones, the volcanic rocks have been affected by deuteric alteration, which formed clinoptilolite and mordenite. Under many older deposits, metamorphism and deformation obscure the alteration minerals associated with zones 1 to 3. At Buttle Lake, for example, zone 4 alteration is most prominent; carbonate is also present, in contrast to the Hokuroko deposits. Although chlorite is much less abundant under Zn-Pb-Cu deposits than under Cu-Zn deposits, the alteration pipe under the Woodlawn deposit (New South Wales, Australia) is highly chloritic (Petersen and Lambert, 1979). Alteration under the sediment-associated deposits of this group consists of locally distributed sericite-quartz; many deposits do not have obvious alteration zones.

GENETIC MODEL

The basic process of formation of massive sulphide deposits, as syngenetic accumulations on or near the seafloor, of sulphide and sulphate minerals from hydrothermal fluids has been well established since the late 1950s (Oftedahl, 1958). Their stratiform nature, sharp upper contact, close association with immediately overlying, well-bedded chemical sedimentary rocks that contain abundant transported products from the hydrothermal vents, beds of locally transported sulphide breccia, and extensive alteration and stringer zones confined almost exclusively to the stratigraphic footwall of the massive sulphides, all gave credibility to this model. Discovery of active seafloor vent systems from which massive sulphide deposits are forming has since ended any doubt about the applicability of the general model. Many of the genetic aspects have been considered in depth by Lydon (1988), and are summarized here. The basic tenets of the genetic model apply to both the Cu-Zn and Zn-Pb-Cu groups of deposits (Fig. 6.3-11).

Source of fluid

Two possible sources of fluid are a) circulating seawater and b) magmatic water. The hydrothermal fluids emanating from modern seafloor vents are considered to be seawater, that has been modified by progressive heating and water-rock interactions during its descent into heated crust, leading to loss of Mg, Sr, and some Ca (due to formation of magnesium hydroxysulphate, anhydrite, zeolites, and clay minerals), and eventual reaction with deeper parts of the crust under high temperature conditions. Excluding the hypersaline brines of the Red Sea (7x sea-water), where the fluid has interacted with Miocene evaporites, salinities of mid-ocean ridge hydrothermal fluids vary from 20% to 150% of seawater for the cooled vapour-phase and brine fluids respectively, at Axial Seamount, to close to seawater values for fluids at the majority of the East Pacific Rise and central and northern Juan de Fuca vent areas, and to almost twice seawater at the southern Juan de Fuca site (Von Damm and Bischoff, 1987). Experimental data (e.g. Bischoff and Seyfried, 1978; Seyfried and Janecky, 1985) together with investigations of the silicified and epidotized lower semiconformable alteration zones (e.g. Spooner and Fyfe, 1973; Gibson et al., 1983), indicate that the reaction between modified seawater and basalt at about 385°C causes sufficient depression of pH to mobilize metals and sulphur from the rocks into the fluid. Virtually any volcanic rock or immature sediment contains sufficient metals to produce a viable ore-forming hydrothermal fluid. Lower semiconformable silicified alteration zones are greatly depleted in metals (MacGeehan and MacLean, 1980; Skirrow, 1987), and a few hundred cubic kilometres of this type of alteration, commensurate with observations at Noranda, Mattagami Lake, and Snow Lake, could provide the metals for a major mining district. The metal contents between districts are highly variable, and some of this variation, particularly between the two principal groups of massive sulphide deposits, could be explained by the difference in metal contents of the source of the rocks (Lydon, 1988). Differences between camps that have closely similar geological attributes, such as Noranda and Sturgeon Lake, are more probably related to thermal and mixing conditions affecting the fluids in the ascent and precipitation regimes. Metals and sulphur could be derived directly from sediments or felsic rocks at lower temperature, as they buffer the fluid to a low pH at lower temperatures than does basalt.

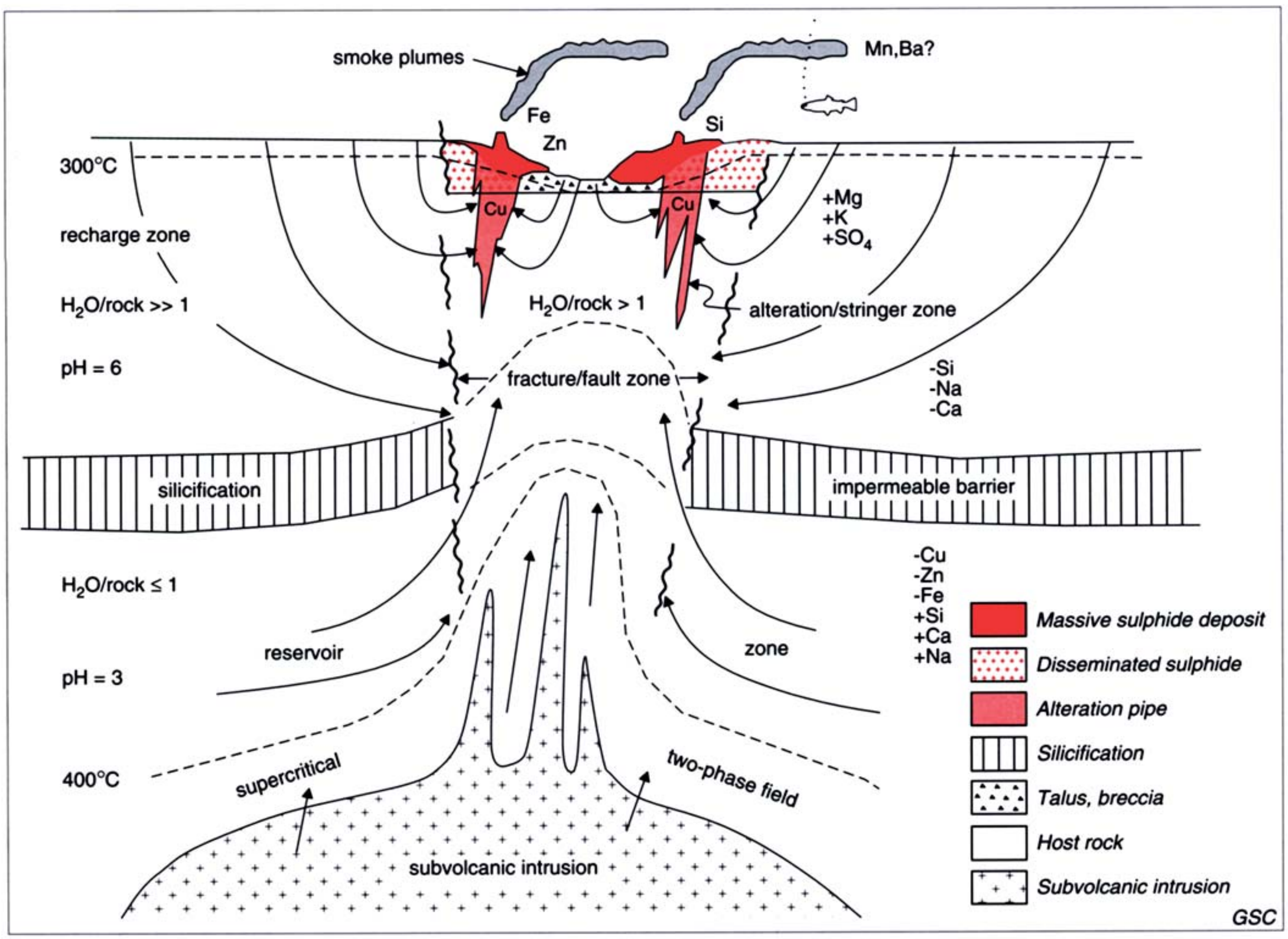

Figure 6.3-11. Model of VMS-producing hydrothermal system, incorporating elements of all subtypes of VMS deposits. The subvolcanic intrusion may be contributing some metals and gases to the hydrothermal fluid. Copper precipitates within the alteration pipes, as well as in the core of the massive sulphide mounds. This diagram is drawn perpendicular to the fracture system which controls hydrothermal discharge.

Hydrothermal fluids of seawater salinity are very buoyant at 385°C, and would rise quickly to the seafloor (Franklin, 1986). Thus identification of high-temperature reaction zones within footwall strata may be an important guide to areas with massive sulphide potential.

Some contribution from magmatic sources is possible. This is indicated by anomalous salinities, the carbon and oxygen isotope compositions (Taylor, 1990) and high CO_2 and ^3He contents of some hydrothermal fluids, together with the loss of sulphur in highly fractionated magmas associated with the Galapagos deposits (Perfit et al., 1983). This contribution, although a small percentage of the total fluid, might be responsible for a significant proportion of its metals.

The source of the heat for a hydrothermal system has been examined by Cathles (1981, 1983) and Cann et al. (1985). Sufficient heat is required to produce fluid temperatures in the reaction zone that were high enough for these fluids to dissolve sufficient metals (at least several parts per million) to ultimately form deposits. Obviously, the ability of this zone (called the "reservoir" by Hodgson and Lydon, 1977) to attain these temperatures also requires sufficient hydrological "insulation" to prevent excessive cooling through mixing with downward advecting cold seawater. Cathles (1983) has calculated that sufficient heat to form all the deposits in the Hokuroko basin could only be attained from a magma chamber containing at least 169 km^3 of felsic melt. The Noranda deposits would require a magma chamber larger than 78 km^3. Using the parameters suggested by Cann et al. (1985), a district of moderate size containing 30 million tonnes of sulphide would require a chamber of 300 km^3. Intrusions of an appropriate size are associated with most of the Archean and Proterozoic Cu-Zn districts in Canada. The provision of heat for the deposits in the back-arc, inter-arc, and off-ridge areas where sedimentary rocks form a significant footwall component is more problematic. The sediments at Middle Valley, which are 300 to 600 m thick, provide natural hydrological and thermal insulation, greatly reducing heat loss from the underlying cooling oceanic crust (Davis et al., 1987). The necessity of contemporaneous intrusions as a heat source is unresolved. In the Guaymas Basin and Escanaba Trough, small sills, themselves insufficient in size to provide all the heat needed for a major hydrothermal system, may be indicative of larger intrusions near the base of the sedimentary sequence. At Middle Valley, carbon and oxygen isotopic data (Taylor, 1990) indicate that no actively degassing magma chamber presently underlies the area, but at Escanaba Trough such a chamber probably is present.

An impermeable "cap" to the hydrothermal reaction zone is most important, as suggested by Hodgson and Lydon (1977) and demonstrated in mid-ocean ridge areas by Kappel and Franklin (1989). This cap can take many forms. The aforementioned sediments in the back-arc and off-ridge areas for both Cu-Zn and Pb-Zn-Cu deposits probably provide this. Massive pyroclastic ash flows which overlie more permeable mafic sequences, as at Mattagami Lake, Sturgeon Lake, and Snow Lake, are similar impermeable caps. The hydrothermal system itself may have formed an impermeable zone within the footwall strata. For example, the lower semiconformable alteration zones that are composed of silica, epidote, albite, and tremolite, and which are excellent candidates as the sources of constituents for the hydrothermal fluids, contain uppermost zones of pervasive silicification (Gibson et al., 1983; Skirrow, 1987) that probably sealed the rocks very effectively, thus preventing the escape of buoyant hydrothermal fluid through unfocused discharge. The broad-scale carbonate alteration associated with copper-zinc deposits in shallow water regimes such as Sturgeon Lake, Ontario and the Hackett River district in Slave Province would similarly reduce cross-stratal permeability.

Fluid composition

Analyses of fluids from seafloor vents in volcanic-dominated ridge crests are available for most of the East Pacific Rise and Juan de Fuca hydrothermal areas, as well as for some vents along the Mid-Atlantic Ridge. Fluids in sediment-covered ridges are less well studied, although data are available for the Escanaba Trough and Guaymas Basin vents. All of the end-member compositions are calculated for zero Mg content, on the assumption the Mg is totally removed from the descending, progressively heated seawater, through retrograde solubility of Mg-hydroxysulphates such as caminite, and loss through metasomatic alteration of basalt (Humphris and Thompson, 1978). The maximum temperature is near 400°C for fluids from Endeavour Ridge (Delaney et al., 1984); maxima for many other sites are about 350°C, but are lower at southern Juan de Fuca, Axial, Explorer, and the sediment-covered ridge sites.

Summary

Combined information from modern and ancient hydrothermal systems, lead to the following important points.

Chemical composition of the fluids: a) the salinities of the fluids range widely, from less than 20% of seawater for one of the fluids of Axial Seamount, to slightly less than seawater for some East Pacific Rise and Axial Seamount fluids, and to almost twice seawater for the southern Juan de Fuca fluids; b) the zinc contents range to as much as 59 mg/kg, and Fe to more than 1000 mg/kg (both at Southern Juan de Fuca); c) SiO_2 contents are about 1000 mg/kg; d) pH is about 3.5; e) both the vapour-dominated and residual fluids at Axial Seamount contain subequal amounts of gold, H_2S, and arsenic, but the vapour-dominated phase has no base metals; f) virtually all measured fluids have been partially cooled prior to venting and many of their constituents may have precipitated from them during cooling.

Mechanisms of focusing fluid discharge: the faults or fracture zones that form the conduits for discharging hydrothermal fluids are all tectonically generated. Specific patterns of fractures have been established in some districts; Knuckey and Watkins (1982) have identified specific faults in the Noranda district, and Scott (1978) has identified two linear elements in the Hokuroku district which may have provided the fluid channelways. Identification of subvolcanic faults requires careful mapping in each district. Discovery of such faults usually occurs after initial discovery of deposits, and may best be applied in well explored districts.

Alteration and stringer zone formation: stringer zones beneath all types of massive sulphide deposits are copper-rich. Experimental and thermodynamic data indicate that copper solubility in most highly reduced hydrothermal fluids decreases relatively quickly with decreasing temperature, compared with zinc and lead (Franklin et al., 1981). Thus conductive cooling of a hydrothermal fluid near the seafloor would promote precipitation of chalcopyrite, provided that no mixing with ambient oxidizing seawater took place, and a copper-stringer zone would form. Mixing with oxidizing seawater seems unlikely (Solomon et al., 1988) in the stringer zone, although it is more possible in the massive ore zone (Ohmoto and Skinner, 1983).

The alteration assemblages associated with these stringer zones are variable. That each alteration assemblage is closely related to a specific group of deposits, with silicification associated primarily with the Zn-Pb-Cu group (Franklin et al., 1981), is clearly an over-simplification. Silicification occurs beneath copper-zinc deposits of the "Mattabi type", as well as beneath many ophiolite-associated deposits in Cyprus and Oman, and 5000 year old lavas of the Galapagos Rift (Embley et al., 1988). Chloritization occurs beneath both the Noranda type deposits, and those representing the Zn-Pb-Cu group (Solomon et al., 1988).

Seafloor hydrothermal fluids generally contain abundant silica, which is highly over-saturated with respect to cold seawater; its precipitation as amorphous silica and cristobalite (as observed in the Galapagos alteration zone; Embley et al., 1988) through cooling may be slow, as the kinetic effect on silica precipitation seems to be important. Thus in areas of the pipe where the fluid flow was restricted, silica precipitation through cooling was likely more effective. Boiling may also promote silica precipitation (Lydon and Galley, 1986), explaining the abundant silicification beneath deposits formed in relatively shallow water, such as the Mattabi type. The abundance of Mg-chlorite may be related either to the rate of advection of cold seawater into the area of the sub-seafloor hydrothermal fluid conduit, or to the Mg content of the hydrothermal fluid. All data on the composition of modern seafloor hydrothermal fluids is calculated to zero magnesium content, assuming that magnesium was completely stripped from progressively heated seawater during its descent into the reaction zone; such an assumption is consistent with experimental data (Seyfried and Janecky, 1985). These data are inconsistent with the Mg loss observed in the major silicified areas in most lower semiconformable alteration zones. In the advection model, cold seawater was probably drawn down rapidly, particularly in highly permeable areas, and Mg lost through reaction with wall rocks. This mechanism would have been particularly effective beneath Archean deposits, as seawater at that time probably contained much less sulphate than did Proterozoic and younger seawater, due to the lack of an early oxidizing atmosphere. Thus during the Archean (or at any time or place where bottom water was reducing), Mg might not have been lost to Mg-hydroxysulphate, but would have been available to form Mg-smectites and chlorite. As noted by Lydon (1988), the amount of magnesium in a pipe zone may increase as the pipe collapses upwards; thus the composition of alteration pipes may be largely established during the waning stages of formation of the deposits. Even in a modern example at Galapagos (Embley et al., 1988), Mg-silicates formed later, or peripheral to, the core Fe-S-SiO_2 alteration zone.

Sulphides are precipitated on or near the seafloor primarily by rapid cooling of the hydrothermal fluid. Reduction of seawater sulphate is unimportant as a principal source of sulphur (Janecky and Shanks, 1988). Precipitation processes for seafloor sulphides in individual chimneys in ridge crests have been examined by Haymon (1983) and Goldfarb et al. (1983), and have been summarized by Franklin (1986) and Lydon (1988). The initial precipitate at a vent orifice is anhydrite, derived entirely from ambient seawater. As the chimney grows, the porous accumulation of coarse anhydrite crystals is infiltrated by hydrothermal fluid, which mixes with seawater; a combination of overgrowth and replacement of anhydrite results in formation of a well zoned chimney, typically with an isocubanite- or chalcopyrite-rich lining of the orifice, a sphalerite (and/or wurtzite)-pyrite-chalcopyrite-anhydrite inner ring, and an outer wall of marcasite-pyrite-sphalerite-anhydrite-silica with surficial organic material. Individual vents have very short lives (Johnson and Tunnicliffe, 1986), and fluid flow is tortuous through most chimneys. Individual chimneys with multiple orifices commonly vent grey to black smoke (from high-temperature fluids) and much more rarely, clear water (from depleted fluids) from separate orifices within a few centimetres of each other, attesting to a very complex "plumbing system" within their uppermost parts.

Less is known about the internal composition of the mounds beneath the chimneys. On their outer edges, pyrite is abundant. In the inner parts of the oldest seafloor deposits that have been studied, the inactive deposits at Galapagos (Embley et al., 1988) and on a seamount at 12°N (Hekinian and Fouquet, 1985), chalcopyrite has replaced much of the pre-existing sulphide. Initial growth of a mound probably occurred as chimneys collapsed, and formed sulphide talus through which hydrothermal fluid continued to pass. The talus became infilled, the sulphide blocks coalesced, and a mound probably began to grow by "inflation" or overgrowth, through a very complex and irregular sequence of precipitation and dissolution mechanisms (Watkinson et al., 1990). Metal zonation formed through incremental precipitation of metals from high temperature fluids across a large thermal gradient within the chimneys or mounds. Silicification throughout the outer portions of mounds and chimneys partially sealed them from massive ingress of cold seawater, and also provided some strength (Tivey and Delaney, 1986).

Ancient deposits have undoubtedly experienced the same complex precipitation history. The "copper-spine" observed at Millenbach (Knuckey et al., 1982) is, in modified form, present in many massive sulphide deposits. Progressive heating of a sulphide mound could induce replacement of earlier-formed pyrite by sphalerite and then chalcopyrite. Thus, sulphide mounds that have been subject to heating by the passage of high temperature fluid for an extensive period of time may become progressively enriched in copper. This process could have formed the "Yellow-ore" in the Kuroko deposits (Eldridge et al., 1983).

Barite is forming in modern seafloor hydrothermal discharge areas regardless of source rock or depositional environment. Its presence is more dependent on the temperature of discharge, with low temperature (about 250°C or less) vent fluids, which are depleted in most base metals and sulphur, forming barite-rich chimneys. Most of the barite-rich chimneys are isolated from the metalliferous (higher temperature) vent sites by at least a few tens of metres. Thus near ancient deposits, barite formed where the hydrothermal system continued to vent after (or away from) its peak (or geographic centre) of high temperature activity, and where the seawater contained abundant sulphate. Hydrothermal systems which essentially were terminated while venting high temperature fluids would not have formed significant barite accumulations, most barium being lost to smoke plumes.

Coincidentally, gold-rich massive sulphides are commonly associated with barite-rich assemblages. Hannington and Scott (1989) showed that gold is effectively preserved in hydrothermal fluids by bisulphide transport, and efficiently precipitated from such fluids by ligand oxidation. Bisulphide complexing in a typical seafloor hydrothermal fluid is enhanced by cooling, raising of pH, and increasing P_{O_2}. Some of these conditions are promoted by boiling. Boiling also causes precipitation of copper, iron, and zinc as sulphides (through cooling) in the subsurface, leaving the remaining fluid relatively enriched in gold, barium, and lead. Thus gold-enriched massive sulphide deposits might form preferentially in depositional environments that are relatively shallow (<1900 m), and in which ambient seawater is oxidizing. The high gold content of the Axial Seamount and Explorer Ridge sulphides is evidence that shallow water depth (i.e. boiling can occur) may be a contributing factor to gold enrichment (Kappel and Franklin, 1989).

Significantly, however, gold-rich samples from the TAG hydrothermal field on the Mid-Atlantic Ridge (Hannington et al., 1990), which formed at about 3700 m depth, are attributed, in part, to a "diagenetic" redeposition process that involves dissolution of gold from paragenetically early (about 0.5 ppm) sulphides by later fluids that are drawn through the sulphide mound, and deposition of this gold in the cooler, well oxidized outer edges of the mound. In addition, zones of seafloor-oxidized sulphides (i.e. "supergene" altered zones) are prospective areas for gold enrichment, through a scavenging and redeposition mechanism.

Finally, the strata of presumed hydrothermal origin that cap many of the deposits appear to have highly diverse origins. Particulate sulphides are abundant in black smoke, but in the modern oceans these become widely dispersed (Converse et al., 1984; McConachy, 1988); oxidation destroys the primary minerals, and sulphide "fallout" is minimal, even immediately adjacent to the deposits. If the near-bottom waters were reducing, however, sulphide fallout could have accumulated. The abundant sulphides in the tuff horizons associated with many of the Noranda deposits and in the Key Tuffite horizon at Mattagami Lake may have been plume particulates. Clay minerals have been noted in hydrothermal plumes and probably contribute to the thin layers of pelagic sediment commonly associated with modern vent sites. Such layers, once they reach a metre or more in thickness, could be important in maintaining well-focused discharge at vent sites, as well as preventing cooling of the rising fluid by inhibiting local advection of cold seawater.

The ferruginous chert zone overlying many deposits may be the product of low temperature discharge. Considerable dissolved silica is discharged through the high temperature vents, but does not appear to form an important particulate constituent of the "smoke". Slow precipitation rates for silica from vent fluids mixing with seawater may cause it to be diluted prior to precipitation. Silica is precipitated in and around low temperature vents, particularly where the discharging fluid has no H_2S. Jonasson and Walker (1987) and Juniper and Fouquet (1988) have shown that opal-A is precipitated on filamentous bacteria, and in open spaces in chimneys, as a silica gel. These bacteria require an H_2S supply, but if this supply is stopped, they die and are replaced by iron oxide, on which opal-A precipitates. Some ferruginous caps probably are the products of syndepositional oxidation of seafloor sulphide mounds. Such oxidation in the modern ocean can destroy a small deposit in about 100 000 years, unless it is protected by sediments or volcanic strata, or by an oxidized cap, especially if it is silicified (i.e., iron-formation).

EXPLORATION GUIDES

1. Presence of submarine volcanic strata. Paleo-water depth probably controlled some variations in volcanic morphology, as well as alteration assemblages and ore composition. Volcanological studies will provide useful information to help determine which assemblages and compositions to expect.
2. Presence of a subvolcanic magma chamber at shallow crustal levels (about 2 km). These can be any composition represented in the overlying volcanic rocks, and are sill-like, but locally transect stratigraphy; are texturally variable, multiple intrusions; are highly fractionated, with "reverse zonation" common in felsic intrusions; have little or no metamorphic halo relative to intrusions emplaced at deeper, drier crustal levels; and are potential hosts to very low grade porphyry copper zones that are superimposed on all rock types. In some districts, synvolcanic dyke swarms occupy faults and fractures, and may be spatially and temporally coincident with hydrothermal conduits.
3. Presence of high-temperature reaction zones (one form of semiconformable alteration) within about 1.5 km of the subvolcanic intrusions. Quartz-epidote-albite alteration, commonly mistakenly mapped as intermediate to felsic rocks, are prevalent under many copper-zinc deposits.
4. Near deposits that formed in relatively shallow water (accompanied by explosion breccia, debris flows, some subaerial volcanic products), laterally extensive carbonatized (and more locally silicified) volcanic strata which are depleted in sodium, are prevalent. These possibly represent the zone in which ambient seawater reacted with the upper part of the hydrothermal reservoir. Some massive sulphide deposits that formed under relatively shallow water may have the alteration and compositional characteristics of epithermal deposits.
5. Synvolcanic faults are recognizable because: they do not extend far into the hanging wall of most deposits; they are commonly altered, with pipe-like assemblages, in their stratigraphically highest portions; they may have asymmetric zones of growth-fault-induced talus; and

they may be locally occupied by synvolcanic dykes. Virtually all of these formed in tensional tectonic regimes, and may be listric. Some may be related to caldera margins, and thus curvilinear; others may be margins of elongate axial summit depressions (grabens), and subparallel to the axis of spreading.

6. Alteration pipes may have sufficient vertical stratigraphic extent to be mappable. Virtually all are sodium depleted, but mineralogical characteristics vary. Most commonly, these are silicified near the deposits, sericitized less locally, and have variable amounts of both Mg- and Fe-rich chlorite or smectite. Less commonly, but important in many Cu-Zn districts, these may have intensely chloritized cores, with sericitized rims. Peripheral to the distinctive pipes, commonly there is a broad zone of more subtly altered rock; smectite and zeolite minerals may be important. Chemical changes in these latter alteration zones may be very subtle, requiring mineralogical or isotopic studies to detect them.

   Metamorphosed pipe assemblages are usually relatively easy to recognize. Magnesium-enriched pipes will be recrystallized to anthophyllite and cordierite. Adjacent, less intensely altered rocks may contain staurolite. Gahnite and Mn-rich garnets may be important accessories. The relatively high ductility of altered volcanic rocks compared with their hosts has resulted in them being exceptionally deformed in some districts. They may have become detached completely from their attendant orebodies. Structural mapping and synthesis are essential to finding additional resources in established massive sulphide districts.

7. The immediately overlying strata may contain indications of mineralization. Hanging wall volcanic rocks may contain alteration pipe assemblages, or at least zeolite-smectite assemblages similar to the peripheral alteration associated with the pipes.

   More importantly, hydrothermally-related precipitates, such as ferruginous chert, sulphidic tuff, and products of oxidation of sulphide mounds may be sufficiently laterally extensive to be detected. Base metal contents within these may increase towards the deposits, whereas Ni, V, Mn, and Ba may increase away from deposits.

RELATED DEPOSIT TYPES

Although some Algoma-type iron-formations are spatially related to massive sulphide deposits (Gross, 1965), this is rather rare. Both Algoma-type and Superior-type oxide-facies iron deposits originated as precipitated products on the seafloor, but almost no evidence indicates that they are the product of focused discharge. At Axial Seamount on the Juan de Fuca Ridge, a laterally-extensive bed of ferruginous silica surrounds the area of high temperature venting. Silica is being fixed by bacterial remains, presumably from low temperature, silica-enriched, but metal- and sulphur-depleted hydrothermal fluid that is discharging throughout the area of the caldera floor at Axial Seamount. Some iron-formation may thus be indirectly related to the high temperature massive sulphide-forming process. As Shegelski (1978) has shown, however, much other Algoma-type iron-formation is not related to this process.

A few epithermal vein deposits may be the product of high temperature hydrothermal systems, similar to those which formed massive sulphide deposits, that discharged into subaerial environments. The Headway-Coulee prospect in northwestern Ontario (Osterberg et al., 1987; Anglin et al., 1988) is an example of a syndepositional epithermal occurrence of zinc-lead-copper-silver mineralization.

Synvolcanic intrusions underlying many of the copper-zinc districts contain extensive low grade porphyry copper occurrences (Franklin et al., 1977). These may be the product of collapsed hydrothermal systems, that penetrated the predominantly crystallized magma chambers following termination of volcanism.

DEFINITIVE CHARACTERISTICS

Volcanic-associated massive sulphide deposits have these distinctive geological characteristics:

1. Spatial association with submarine volcanic rocks and commonly with associated sedimentary sequences.
2. Bulbous to tabular stratiform accumulations of massive pyrite and subordinate pyrrhotite, and contain about 8 to 10% total combined zinc, lead, and copper.
3. Underlain by discordant alteration zones, which may occupy synvolcanic faults.
4. Regionally characterized by manifestations of high heat flow; subvolcanic intrusions, laterally extensive semi-conformable alteration zones, and anomalous petrogenetic trends in the volcanic sequence, all of which indicate proximity to massive sulphide deposits.

SELECTED BIBLIOGRAPHY

References noted with an asterisk (*) are summary papers, providing a thorough review of volcanic-associated massive sulphide deposits.

Aggarwal, P.K. and Nesbitt, B.T.
1984: Geology and geochemistry of the Chu Chua massive sulphide deposit, British Columbia; Economic Geology, v. 79, p. 815-825.

Alldrick, D.J.
1986: Stratigraphy and structure in the Anyox area (103 P/5); British Columbia Ministry of Energy, Mines and Petroleum Resources, Geological Fieldwork, 1985, British Columbia Department of Energy and Mines, Paper 1986-1, p. 211-216.

Anglin, C.D.A., Franklin, J.M., Loveridge, W.D., Hunt, P.A., and Osterberg, S.A.
1988: Use of zircon U-Pb ages of felsic intrusive and extrusive rocks in eastern Wabigoon Subprovince, Ontario, to place constraints on base metal and gold mineralization; in Radiogenic Age and Isotopic Studies: Report 2, Geological Survey of Canada, Paper 88-2, p. 109-115.

Binney, W.P.
1987: A sedimentological investigation of MacLean channel transported sulphide ores; in Buchans Geology, Newfoundland, (ed.) R.V. Kirkham; Geological Survey of Canada, Paper 86-24, p. 107-147.

Bischoff, J.L. and Seyfried, W.E.
1978: Hydrothermal chemistry of seawater from 25° to 350°C; American Journal of Earth Science, v. 278, p. 838-860.

Cann, J.R., Strens, M.R., and Rice, A.
1985: A simple magma-driven thermal balance model for the formation of volcanogenic massive sulfides; Earth and Planetary Science Letters, v. 76, p. 123-134.

Cathles, L.M.
*1981: Fluid flow and genesis of hydrothermal ore deposits; in Economic Geology, Seventy-Fifth Anniversary Volume 1905-1980, (ed.) B.J. Skinner; p. 424-457.

Cathles, L.M., (cont.)
1983: An analysis of the hydrothermal system responsible for massive sulphide deposition in the Hokuroku basin of Japan; in Kuroko and Related Volcanogenic Massive Sulphide Deposits, (ed.) H. Ohmoto and B.J. Skinner; Economic Geology Monograph 5, p. 439-487.

Chen, T.T. and Petruk, W.
1980: Mineralogy and characteristics that affect recoveries of metals and trace elements from the ore at Heath Steele mines, New Brunswick; The Canadian Mining and Metallurgical Bulletin, v. 73, no. 823, p. 167-179.

Converse, D.R., Holland, H.D., and Edmond, J.M.
1984: Flow rates in the axial hot springs of East Pacific Rise (21°N): implications for the heat budget and the formation of massive sulphide deposits; Earth and Planetary Science Letters, v. 69, p. 159-175.

Costa, U.R., Barnett, R.L., and Kerrich, R.
1983: The Mattagami Lake mine Archean Zn-Cu sulphide deposit, Quebec: hydrothermal coprecipitation of talc and sulphides in a seafloor brine pool - evidence from geochemistry, $^{18}O/^{16}O$, and mineral chemistry; Economic Geology, v. 78, no. 6, p. 1144-1203.

Date, J., Watanabe, Y., and Saeki, Y.
1983: Zonal alteration around the Fukazawa Kuroko deposits, Akita prefecture, northern Japan; in Kuroko and Related Volcanogenic Massive Sulphide Deposits, (ed.) H. Ohmoto and B.J. Skinner; Economic Geology, Monograph 5, p. 365-386.

Davidson, A.J.
1977: Petrography and chemistry of the Key Tuffite at Bell Allard, Matagami, Quebec; MSc. thesis, McGill University, Montreal, Quebec, 131 p.

Davis, E.E., Goodfellow, W.D., Bornhold, B.D., Adshead, J., Blaise, B., Villinger, H., and Lecheminant, G.M.
1987: Massive sulphides in a sedimented rift valley, northern Juan de Fuca Ridge; Earth and Planetary Science Letters, v. 82, p. 49-61.

Delaney, J.R., McDuff, R.E., and Lupton, J.E.
1984: Hydrothermal fluid temperatures of 400°C on the Endeavour segment, northern Juan de Fuca Ridge; EOS transactions, American Geophysical Union, v. 65, p. 973.

Eldridge, C.S., Barton, P.B., Jr., and Ohmoto, H.
1983: Mineral textures and their bearing on formation of the Kuroko orebodies; in Kuroko and Related Volcanogenic Massive Sulphide Deposits, (ed.) H. Ohmoto and B.J. Skinner; Economic Geology, Monograph 5, p. 241-281.

Embley, R.W., Jonasson, I.R., Perfit, M.R., Tivey, M., Malahoff, A., Franklin, J.M., Smith, M.F., and Francis, T.J.G.
1988: Submersible investigation of an extinct hydrothermal system on the eastern Galapagos Ridge: sulfide mounds, stockwork zone, and differentiated lavas; Canadian Mineralogist, v. 26, p. 517-540.

***Franklin, J.M.**
1986: Volcanic-associated massive sulphide deposits - an update; in Geology and Genesis of Mineral Deposits in Ireland (ed.) C.J. Andrew, R.W.A. Crowe, S. Finlay, W.M. Pennell, and J.F. Pyne; Irish Association for Economic Geology, Dublin, p. 49-69.

Franklin, J.M., Gibb, W., Poulsen, K.H., and Severin, P.
1977: Archean metallogeny and stratigraphy of the south Sturgeon Lake area; Institute on Lake Superior Geology, 23rd Annual Meeting, Thunder Bay, Ontario, Guidebook, 73 p.

***Franklin, J.M., Lydon, J.W., and Sangster, D.F.**
1981: Volcanic-associated massive sulfide deposits; in Economic Geology Seventy-fifth Anniversary Volume 1905-1980, (ed.) B.J. Skinner; p. 485-627.

Galley, A.G. and Jonasson, I.R.
1992: Semi-conformable alteration and volcanogenic massive sulphide deposits; Proceedings, 14th New Zealand Geothermal Workshop, (ed.) S.F. Simmons, J. Newson, and K.C. Lee; p. 279-284.

Gass, I.G. and Smewing, J.D.
1973: Intrusion, extrusion and metamorphism at constructive plate margins: evidence from the Troodos massif, Cyprus; Nature, v. 242, p. 26-29.

Gibson, H.L. and Watkinson, D.H.
1990: Volcanogenic massive sulphide deposits of the Noranda Cauldron and Shield volcano, Quebec; in The Northwestern Quebec Polymetallic Belt, (ed.) M. Rive, P. Verpaelst, Y. Gagnon, J.M. Lulin, G. Riverin, and A. Simard; The Canadian Institute of Mining and Metallurgy, Special Volume 43, p. 119-133.

Gibson, H.L., Watkinson, D.H., and Comba, C.D.A.
1983: Silicification: hydrothermal alteration in an Archean geothermal system within the Amulet Rhyolite Formation, Noranda, Quebec; Economic Geology, v. 78, p. 954-971.

Goldfarb, M.S., Converse, D.R., Holland, H.D., and Edmond, J.M.
1983: The genesis of hot spring deposits on the East Pacific Rise, 21°N. in Kuroko and Related Volcanogenic Massive Sulphide Deposits, (ed.) H. Ohmoto and B.J. Skinner; Economic Geology, Monograph 5, p. 507-522.

Goodfellow, W.D. and Franklin, J.M.
1993: Geology, mineralogy and chemistry of sediment-hosted clastic massive sulphides in shallow cores, Middle Valley, northern Juan de Fuca Ridge; Economic Geology, v. 88, no. 8, p. 2037-2068.

Gross, G.A.
1965: General geology and evaluation of ore deposits; Volume 1 in Geology of Iron Deposits in Canada; Geological Survey of Canada, Economic Geology Report 22, 181 p.

Hannington, M.D and Jonasson, I.R.
1992: Fe and Mn oxides at seafloor hydrothermal vents; Catena Supplement 21, p. 351-370.

Hannington, M.D. and Scott, S.D.
1989: Gold mineralization in volcanogenic massive sulphide deposits: implications of data from active hydrothermal vents on the modern sea floor; in The Geology of Gold Deposits, (ed.) R.R. Keays, W.R.H. Ramsay, and D.I. Groves; Economic Geology, Monograph 6, p. 491-507.

Hannington, M.D., Herzig, P.M., and Scott, S.D.
1990: Auriferous hydrothermal precipitates on the seafloor; in Gold Metallogeny and Exploration, (ed.) R.P. Foster; Blackie and Son, Glasgow, p. 250-282.

Haymon, R.
1983: The growth history of hydrothermal "black smoker" chimneys; Nature, v. 301, p. 695-698.

Hekinian, R. and Fouquet, Y.
1985: Volcanism and metallogenesis of axial and off-axial structures on the East Pacific Rise near 13°N. Economic Geology, v. 80, p. 221-249.

***Hodgson, C.J. and Lydon, J.W.**
1977: The geological setting of volcanogenic massive sulfide deposits and active hydrothermal systems: some implications for exploration; The Canadian Institute of Mining and Metallurgy, Bulletin, v. 70, p. 95-106.

Humphris, S.E. and Thompson, G.
1978: Hydrothermal alteration of oceanic basalts by seawater; Geochimica et Cosmochimica Acta, v. 42, p. 107-125.

Iijima, A.
1974: Clay and zeolitic alteration zones surrounding Kuroko deposits in the Hokuroko district, Northern Akita, as submarine hydrothermal-diagenetic alteration products; Society of Mining Geologists of Japan, Special Issue 6, p. 267-290.

Ishihara, S. and Terashima, S.
1974: Base metal contents of the basement rocks of Kuroko deposits - an overall view to examine their effect on the Kuroko mineralization; Society of Mining Geologists of Japan, Special Issue 6, p. 421-431.

Jambor, J.L.
1979: Mineralogical evaluation of proximal-distal features in New Brunswick massive sulfide deposits; Canadian Mineralogist, v. 17, p. 649-664.

Janecky, D.R. and Shanks, W.C., III
1988: Computational modelling of chemical and sulphur isotopic reaction processes in seafloor hydrothermal systems: chimneys, massive sulfides, and subjacent alteration zones; Canadian Mineralogist, v. 26, pt. 3, p. 805-826.

Johnson, H.P. and Tunnicliffe, V.
1986: Time-lapse camera measurements of a high temperature hydrothermal system on Axial Seamount, Juan de Fuca Ridge; EOS, Transactions of the American Geophysical Union, v. 67, no. 44, p. 1283.

Jonasson, I.R. and Walker, D.A.
1987: Micro-organisms and their debris as substrates for base metal sulfide nucleation and accumulation in some mid-ocean ridge deposits; (abstract) EOS, Transactions of the American Geophysics Union, v. 68, no. 44, p. 1546.

Juniper, S.K. and Fouquet, Y.
1988: Filamentous iron-silica deposits from modern and ancient hydrothermal sites; Canadian Mineralogist, v. 26, pt. 3, p. 859-870.

Juras, S.J. and Pearson, C.A.
1990: The Buttle Lake Camp, Central Vancouver Island, B.C.; Chapter 9 in Geology and Regional Setting of the Major Mineral Deposits in Southern British Columbia, Guidebook, International Association on the Genesis of Ore Deposits, Field Trip 12, Geological Survey of Canada, Open File 2167, p. 145-161.

Kappel, E.S. and Franklin, J.M.
1989: Relationships between geologic development of ridge crests and sulfide deposits in the northeast Pacific Ocean; Economic Geology and the Bulletin of the Society of Economic Geologists, v. 84, no. 3, p. 485-505.

Kerr, D.J. and Mason, R.
1990: A re-appraisal of the geology and ore deposits of the Horne mine complex at Rouyn-Noranda, Quebec; in The Northwestern Quebec Polymetallic Belt, (ed.) M. Rive, P. Verpaelst, Y. Gagnon, J.M. Lulin, G. Riverin, and A. Simard; The Canadian Institute of Mining and Metallurgy, Special Volume 43, p. 153-166.

Kissin, S.A.
1974: Phase relations in a portion of the Fe-S system; PhD. thesis, University of Toronto, Toronto, Ontario, 234 p.

Klau, W. and Large, D.E.
1980: Submarine exhalative Cu-Pb-Zn deposits, a discussion of their classification and metallogenesis; Geologische Jahrbuch, sec. D, no. 40, p. 13-58.

Knuckey, M.J.
1975: Geology of the Millenbach copper-zinc orebody; (abstract) Economic Geology, v. 70, no. 1, p. 247.

Knuckey, M.J. and Watkins, J.J.
1982: The geology of the Corbet massive sulphide deposit, Noranda, Quebec, Canada; in Precambrian Sulphide Deposits, (ed.) R.W. Hutchinson, C.D. Spence, and J.M. Franklin; Geological Association of Canada, Special Paper 25, p. 296-317.

Knuckey, M.J., Comba, C.D.A., and Riverin, G.
1982: Structure, metal zoning, and alteration at the Millenbach deposit, Noranda, Quebec; in Precambrian Sulphide Deposits, (ed.) R.W. Hutchinson, C.D. Spence, and J.M. Franklin;, Geological Association of Canada, Special Paper 25, p. 255-295.

Lambert, I.B.
1979: Massive copper-lead-zinc deposits in felsic volcanic sequences of Japan and Australia; comparative notes; Mining Geology, v. 29, p. 11-20.

Lambert, I.B. and Sato, T.
1974: The Kuroko and associated ore deposits of Japan: a review of their features and metallogenesis; Economic Geology, v. 69, p. 1215-1236.

Luff, W.M.
1977: Geology of the Brunswick no. 12 mine. The Canadian Institute of Mining and Metallurgy, Bulletin, v. 70, no. 782, p. 109-119.

***Lydon, J.W.**
1984: Volcanogenic massive sulphide deposits. Part 1: a descriptive model; Geoscience Canada, v. 11, p. 195-202.
1988: Ore deposit models #14. Volcanogenic massive sulphide deposits. Part 2: genetic models; Geoscience Canada, v. 15, no. 1, p. 43-65.

Lydon, J.W. and Galley, A.
1986: The chemical and mineralogical zonation of Mathiati alteration pipe, Cyprus, and genetic significance; in Metallogeny of Basic and Ultrabasic Rocks, (ed.) M.J. Gallagher, R.A. Ixer, C.R. Neary, and H.M. Prichard; Institution of Mining and Metallurgy, London, U.K., p. 49-68.

MacGeehan, P.J. and MacLean, W.H.
1980: Tholeiitic basalt-rhyolite magmatism and massive sulphide deposits at Mattagami, Quebec; Nature, v. 283, p. 153-157.

Marquis, P., Hubert, C., Brown, A.C., and Rigg, D.M.
1990: An evaluation of genetic models for gold deposits of the Bousquet district, Quebec, based on their mineralogic, geochemical and structural characteristics; in The Northwestern Quebec Polymetallic Belt, (ed.) M. Rive, P. Verpaelst, Y. Gagnon, J.M. Lulin, G. Riverin, and A. Simard; The Canadian Institute of Mining and Metallurgy, Special Volume 43, p. 383-399.

McConachy, T.F.
1988: Hydrothermal plumes over spreading ridges and related deposits in the northeast Pacific Ocean: the East Pacific Rise near 11°N and 21°N, Explorer Ridge and J. Tuzo Wilson seamounts; PhD. thesis, University of Toronto, Toronto, Ontario, 403 p.

Morton, R.L. and Franklin, J.M.
1987: Two-fold classification of Archean volcanic-associated massive sulfide deposits; Economic Geology, v. 82, p. 1057-1063.

Morton, R.L., Hudak, G., Walker, J., and Franklin, J.M.
1990: Physical volcanology and hydrothermal alteration of the Sturgeon Lake caldera complex; in Mineral Deposits in the Western Superior Province, Ontario; International Association on the Genesis of Ore Deposits, Field Trip Guidebook No. 9, (ed.) J.M. Franklin, B.R. Schneiders, and E.R. Koopman; Geological Survey of Canada, Open File 2164, p. 74-94.

Oftedahl, C.
1958: On exhalative-sedimentary ores; Geologiska Föreningen i Stockholm Förhandlingar, v. 80, p. 1-19.

Ohmoto, H. and Skinner, B.J.
1983: The Kuroko and related volcanogenic massive sulphide deposits: introduction and summary of new findings; in Kuroko and Related Volcanogenic Massive Sulphide Deposits, (ed.) H. Ohmoto and B.J. Skinner; Economic Geology, Monograph 5, p. 1-8.

Osterberg, S.A., Morton, R.L., and Franklin, J.M.
1987: Hydrothermal alteration and physical volcanology of Archean rocks in the vicinity of the Headway-Coulee massive sulfide occurrence, Onaman area, northwestern Ontario; Economic Geology, v. 82, no. 6, p. 1505-1520.

Payne, J.G., Bratt, J.A., and Stone, B.G.
1980: Deformed Mesozoic volcanogenic Cu-Zn sulphide deposits in the Britannia district, British Columbia; Economic Geology, v. 75, p. 700-721.

Perfit, M.R., Fornari, D.J., Malahoff, A., and Embley, R.W.
1983: Geochemical studies of abyssal lavas recovered by DSRV ALVIN from eastern Galapagos rift, Inca transform and Ecuador rift, 3. Trace element abundances and petrogenesis; Journal of Geophysical Research, v. 88, p. 10551-10572.

Petersen, M.D. and Lambert, I.B.
1979: Mineralogical and chemical zonation around the Woodlawn Cu-Pb-Zn ore deposit, southeastern New South Wales; Journal of the Geological Society of Australia, v. 26, p. 169-186.

Piche, M., Guha, J., Sullivan, J., Bouchard, G., and Daigneault, R.
1990: Structure, stratigraphie et implication metallogenique - les gisements volcanogenes du camp minier de Matagami; in The Northwestern Quebec Polymetallic Belt, (ed.) M. Rive, P. Verpaelst, Y. Gagnon, J.M. Lulin, G. Riverin, and A. Simard; The Canadian Institute of Mining and Metallurgy, Special Volume 43, p. 327-336.

Purdie, J.J.
1967: Lake Dufault Mines, Ltd.; The Canadian Institute of Mining and Metallurgy, Annual Meeting, Montreal, Centennial Field Excursion, Northwestern Quebec and Northern Ontario, p. 52-57.

Richards, H.G., Cann, J.R., and Jensenius, J.
1989: Mineralogical zonation and metasomatism of the alteration pipes of Cyprus sulfide deposits; Economic Geology, v. 84, p. 91-115.

Riverin, G., Labrie, M., Salmon, B., Cazavant, A., Asselin, R., and Gagnon, M.
1990: The geology of the Ansil deposit, Rouyn-Noranda, Quebec; in The Northwestern Quebec Polymetallic Belt; (ed.) M. Rive, P. Verpaelst, Y. Gagnon, J.-M. Lulin, G. Riverin, and A. Simard; The Canadian Institute of Mining and Metallurgy, Special Volume 43, p. 2.

Sangster, D.F.
1972: Precambrian volcanogenic massive sulphide deposits in Canada: a review; Geological Survey of Canada, Paper 72-22, 44 p.

Sangster, D.F. and Scott, S.D.
1976: Precambrian stratabound massive Cu-Zn-Pb sufide ores of North America; in Handbook of Strata-bound and Stratiform Ore Deposits, (ed.) K.H. Wolf; Elsevier, Amsterdam, p. 129-222.

Scott, S.D.
1978: Structural control of the Kuroko deposits of the Hokuroku district, Japan; Mining Geology, v. 28, p. 301-311.

***Seyfried, W.E., Jr. and Janecky, D.R.**
1985: Heavy metal and sulfur transport during subcritical and supercritical hydrothermal alteration of basalt: influence of fluid pressure and basalt composition and crystallinity; Geochimica et Cosmochimica Acta, v. 49, p. 2545-2560.

Shegelski, R.I.
1978: Stratigraphy and geochemistry of Archean iron formation in the Sturgeon Lake and Savant Lake greenstone terrains, northwestern Ontario; PhD. thesis, University of Toronto, Toronto, Ontario, 251 p.

Shirozu, H.
1974: Clay minerals in altered wall rocks of the Kuroko-type deposits. Society of Mining Geologists of Japan, Special Issue 6, p. 303-311.

Simmons, B.D.
1973: Geology of the Millenbach massive sulphide deposit, Noranda, Quebec; The Canadian Institute of Mining and Metallurgy, Bulletin, v. 166, no. 739, p. 67-78.

Skirrow, R.G.
1987: Silicification in a semiconformable alteration zone below the Chisel Lake massive sulphide deposit, Manitoba; MSc. thesis, Carleton University, Ottawa, Ontario, 171 p.

Solomon, M., Eastoe, C.J., Walshe, J.L., and Green, G.R.
1988: Mineral deposits and sulphur isotope abundances in the Mount Read volcanics between Que River and Mount Darwin, Tasmania; Economic Geology, v. 83, no. 6, p. 1307-1328.

Spooner, E.T.C.
1977: Hydrodynamic model for the origin of the ophiolitic cupriferous pyrite ore deposits of Cyprus; in Volcanic Processes in Ore Genesis; Geological Society of London, Special Publication 7, p. 58-71.

Spooner, E.T.C. and Fyfe, W.S.
1973: Sub-sea floor metamorphism, heat and mass transfer; Contributions to Mineralogy and Petrology, v. 42, p. 287-304.

Spooner, E.T.C., Bechinsdale, R.D., England, P.C., and Senior, A.
1977a: Hydration ^{18}O enrichment and oxidation during ocean floor hydrothermal metamorphism of ophiolitic metabasic rocks from E. Liguria, Italy; Geochimica et Cosmochimica Acta, v. 41, p. 857-872.

Spooner, E.T.C., Chapman, H.J., and Smewing, J.D.
1977b: Strontium isotopic contamination and oxidation during ocean floor hydrothermal metamorphism of the ophiolitic rocks of the Troodos Masiff, Cyprus; Geochimica et Cosmochimica Acta, v. 41, p. 873-890.

Tatsumi, T. (ed.)
1970: Volcanism and Ore Genesis; University of Tokyo Press, Tokyo, 488 p.

Tatsumi, T. and Watanabe, T.
1971: Geological environment of formation of the Kuroko-type deposits; Society of Mining of Geologists Japan, Special Issue 3, p. 216-220.

Taylor, B.E.
1990: Carbon dioxide and methane in hydrothermal vent fluids from Middle Valley, a sediment-covered ridge segment; EOS, Transactions, American Geophysical Union, v. 71, no. 43, p. 1569.

Thorpe, R.I. and Harris, D.C.
1973: Mattagamite and tellurantimony, two new telluride minerals from Mattagami Lake mine, Matagami area, Quebec; Canadian Mineralogist, v. 12, pt. 1, p. 55-60.

Thorpe, R.I., Pringle, G.J., and Plant, A.G.
1976: Occurrence of selenide and sulphide mineral in bornite ore of the Kidd Creek massive suphide deposit, Timmins, Ontario; in Report of Activities, Part A; Geological Survey of Canada, Paper 76-1A, p. 311-317.

Tivey, M.K. and Delaney, J.R.
1986: Growth of large sulphide structures on the Endeavour segment of the Juan de Fuca Ridge; Earth and Planetary Science Letters, v. 77, p. 303-317.

Urabe, T., Marumo, K., and Nakamura, K.
1990: Mineralization and related hydrothermal alteration in Izena Cauldron (Jade Site), Okinawa Trough, Japan; Geological Society of America, Abstracts with Programs, v. 22, no. 7, p. A9.

van Staal, C.R.
1987: Tectonic setting of the Tetagouche Group in northern New Brunswick: implications for plate tectonic models of the northern Appalachians; Canadian Journal of Earth Sciences, v. 24, no. 7, p. 1329-1351.

von Damm, K.L. and Bischoff, J.L
1987: Chemistry of hydrothermal solutions from the southern Juan de Fuca Ridge; Journal of Geophysical Research, v. 92, p. 11334-11346.

von Stackelberg, U. and Brett, R.
1990: Extended hydrothermal activity in the Lau Basin (southwest Pacific): first results of R.V. Sonne cruise 1990; EOS, Transactions, American Geophysical Union, v. 71, no. 43, p. 1680.

Watkinson, D.H., McEwen, J.H., and Jonasson, I.R.
1990: Mine Gallen, Noranda, Quebec: geology of an Archean massive sulphide mound; in The Northwestern Quebec Polymetallic Belt: a Summary of 60 Years of Mining Exploration; (ed.) M. Rive, P. Verpaeist, Y. Gagnon, J.-M. Lulin, G. Riverin, and A. Simard; The Canadian Institute of Mining and Metallurgy, Special Volume 43, p. 167-174.

6.4 VOLCANIC-ASSOCIATED MASSIVE SULPHIDE GOLD

K.H. Poulsen and M.D. Hannington

INTRODUCTION

Volcanic-associated massive sulphide deposits contain variable abundances of gold (Fig. 6.4-1). There are three ways in which massive sulphide deposits may be considered "gold-rich" (Table 6.4-1). First are those deposits that contain high absolute concentrations of gold: volcanic-associated massive sulphide deposits typically contain 1 to 2 ppm, although a few attain anomalous values of 10-15 ppm or more; some of these are not primary gold producers, but nevertheless have significantly higher than average gold grades (e.g., D'Eldona, Lemoine-Patino; Fig. 6.4-1). Second are those deposits (e.g., Flin Flon, Buchans, Britannia; Fig. 6.4-1) that, by virtue of modest to high gold concentration and large tonnages, have a relatively large total amount of contained gold. Third, a consideration of the relative proportions of contained gold, silver, and base metals (Fig. 6.4-2) shows that volcanic-associated sulphide deposits can be divided into two main compositional groups. The first and largest corresponds to base-metal massive sulphide deposits, including some like Flin Flon and Lemoine with anomalous gold concentrations and significant byproduct gold. The second group corresponds to auriferous sulphide deposits, mainly massive but also as stockworks and disseminations, in which gold is a primary commodity and base metals are of lesser economic importance. They are gold deposits in a strict economic sense (Fig. 6.4-2) and include several important Canadian and overseas deposits (Table 6.4-2).

Poulsen, K.H. and Hannington, M.D.
1996: Volcanic-associated massive sulphide gold; in Geology of Canadian Mineral Deposit Types, (ed.) O.R. Eckstrand, W.D. Sinclair, and R.I. Thorpe; Geological Survey of Canada, Geology of Canada, no. 8, p. 183-196 (also Geological Society of America, The Geology of North America, v. P-1).

Auriferous volcanic-associated sulphide deposits in Canada are exemplified by three main varieties: (1) Archean copper-gold deposits such as Horne, Quebec; (2) Archean pyritic gold deposits such as Bousquet No. 1, Quebec; and (3) auriferous polymetallic sulphide deposits such as the Jurassic Eskay Creek deposit, British

Contents

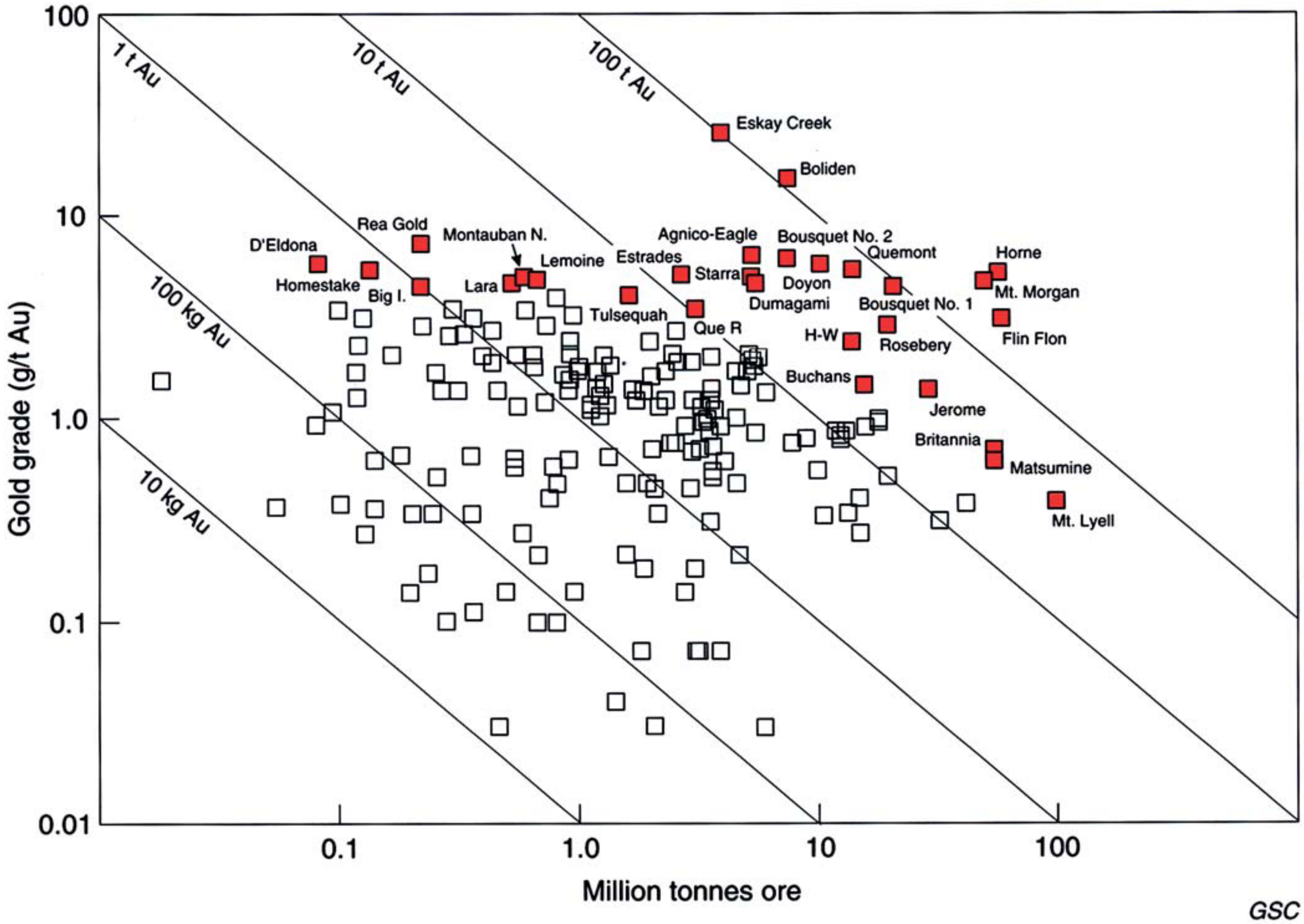

Figure 6.4.1. Plot of tonnage versus gold grade for volcanic-associated massive sulphide deposits, including 184 deposits in Canada and selected gold-rich deposits world-wide. Diagonal lines indicate quantities of contained gold. Open symbols: conventional "gold-poor" base metal-rich massive sulphides. Solid symbol: auriferous volcanic-associated massive sulphide deposits and selected "gold-rich" base metal massive sulphides (see Table 6.4-1 and text for discussion).

Columbia. Other examples that fit into one or more of these categories include the Bousquet No. 2 and Dumagami deposits in the southern Abitibi belt, Quebec; the Agnico-Eagle deposit near Joutel, Quebec; the Proterozoic Montauban North deposit in the Grenville Supergroup; and a variety of Devonian and younger, high-grade polymetallic sulphide deposits in British Columbia. Examples of major gold-producing deposits of this type elsewhere in the world include the early Proterozoic Boliden deposit in the Skellefte district of Sweden and the Paleozoic Mt. Morgan and Mt. Chalmers deposits in metamorphosed volcanic rocks of the Tasman geosyncline, Australia.

Although the auriferous massive sulphide deposits possess many of the geological characteristics of submarine base-metal massive sulphide deposits, many of them are unique in their bulk composition and mineralogy and may have formed under somewhat different geological conditions (Hannington, 1993). The fact that gold deposits of this type co-exist regionally with other base-metal-rich massive sulphides that do not contain anomalous gold is one of their most notable characteristics and implies that their auriferous nature may be due to an enriched source or to a particularly efficient local means of gold precipitation and concentration (e.g., boiling).

IMPORTANCE

Auriferous volcanic-associated massive sulphide deposits account for approximately 5% of Canada's historical gold production and reserves. The giant Horne mine, with a total past production of approximately 330 t Au, has been the largest Canadian producer of this deposit type. Together, the Horne and adjacent Quemont deposits accounted for more than 400 t Au (13 million ounces) and represent fully one-quarter of the total gold production and reserves from deposits of this kind in Canada. Gold-rich pyritic deposits, such as those of the Bousquet district, are also an important type of gold mineralization, and these deposits account for approximately 10% of current Canadian gold output.

Contents

Table 6.4-1. Tonnage and grade statistics for selected "gold-rich" volcanic-associated massive sulphide deposits (see Fig. 6.4-1).

Deposit	Location	Type	Age	Tonnes Ore	Au ppm	Ag ppm	Cu %	Zn %	Pb %	Tonnes Au[1]
Bousquet No. 1	Bousquet district, Quebec	Pyritic gold	Archean	20 737 000	4.5	-	-	-	-	93
Bousquet No. 2	Bousquet district, Quebec	Copper-gold	Archean	7 400 000	6.1	16	0.6	-	-	45
Dumagami	Bousquet district, Quebec	VMS (Cu-Zn-Au)	Archean	5 500 000	4.6	9	-	-	-	25
Doyon	Bousquet district, Quebec	Intrusion-hosted Au	Archean	10 243 000	5.7	-	-	-	-	58
Agnico-Eagle	Joutel, Quebec	Pyritic-gold (I.F.)	Archean	5 279 000	6.4	<10	-	-	-	34
Estrades	Joutel, Quebec	VMS (Cu-Zn-Au)	Archean	2 670 000	5.1	110	0.8	9.6	0.9	14
Horne	Noranda, Quebec	Copper-gold	Archean	54 300 000	6.1	13	2.2	-	-	330
Quemont	Noranda, Quebec	Copper-gold	Archean	13 925 000	5.4	20	1.3	2.4	0.02	75
D'Eldona	Noranda, Quebec	VMS (Cu-Zn-Au)	Archean	90 000	4.1	30	0.3	5.0	-	<1
Louvicourt	Val d'Or, Quebec	VMS (Cu-Zn)	Archean	15 700 000	0.9	30	3.4	2.2	-	14
Montauban North	Grenville, Quebec	Pyritic gold	Proterozoic	600 000	5.0	-	-	-	-	3
Flin Flon	Flin Flon, Manitoba	VMS (Cu-Zn-Au)	Proterozoic	58 416 000	3.1	50	2.3	4.3	-	181
Big Island	Flin Flon, Manitoba	VMS (Cu-Zn-Au)	Proterozoic	220 000	4.5	80	1.0	14.0	-	<1
Eskay Creek[2]	Northeastern B.C.	Auriferous polymetallic	Jurassic	3 968 000	26.0	1000	<1.0	5.0	2.0	103
Tulsequah	Northeastern B.C.	VMS (Zn-Cu-Pb-Au)	Permian	1 620 000	4.0	140	1.3	6.9	1.3	6
Lara	Vancouver Island	VMS (Zn-Cu-Pb-Au)	Devonian	529 000	4.7	100	1.0	5.9	1.2	2
H-W mine	Vancouver Island	VMS (Zn-Cu-Pb)	Devonian	13 818 000	2.4	35	2.2	5.3	0.3	33
Britannia	South central B.C.	VMS (Zn-Cu-Pb)	Cretaceous	55 000 000	0.7	<10	1.1	0.7	0.1	39
Rea Gold	South central B.C.	Auriferous polymetallic	Devonian	134 000	5.4	60	0.7	2.4	2.4	<1
Homestake	South central B.C.	Auriferous polymetallic	Devonian	220 000	7.4	70	0.5	7.3	6.2	1
Buchans	Central Newfoundland	VMS (Zn-Cu-Pb)	Ordovician	15 809 000	1.5	130	1.3	14.6	7.6	24
Rambler Cons.	Central Newfoundland	VMS (Zn-Cu)	Ordovician	399 000	5.1	30	1.3	2.2	-	2
Lemoine-Patino	Chibougamau, Quebec	VMS (Cu-Zn-Au)	Archean	750 000	4.4	90	4.8	10.6	-	3
Boliden	Skellefte district, Sweden	Copper-gold	Proterozoic	8 340 000	15.2	50	1.4	-	-	126
Mt. Morgan	East-central Queensland	Copper-gold	Devonian	50 000 000	4.8	<10	0.7	0.1	0.05	240
Mt. Chalmers	East-central Queensland	Copper-gold	Permian	3 600 000	2.0	15	1.8	1.0	0.2	7
Starra	Mt. Isa Inlier, Queensland	Pyritic-gold (I.F.)	Cambrian	5 300 000	5.0	-	2.0	-	-	26
Mt. Lyell	Mt. Read, Tasmania	Copper-gold	Cambrian	98 574 000	0.4	<10	1.2	<0.1	<0.1	39
Mt. Lyell (Blow)	Mt. Read, Tasmania	Copper-gold	Cambrian	5 600 000	2.0	60	1.3	-	-	11
Rosebery	Mt. Read, Tasmania	VMS (Zn-Cu-Pb-Au)	Cambrian	19 400 000	2.9	160	0.7	16.2	5.0	56
Que River	Mt. Read, Tasmania	VMS (Zn-Cu-Pb-Au)	Cambrian	3 100 000	3.4	200	0.6	13.5	7.5	10

Notes: [1] deposits with greater than 30 tonnes Au are considered to be major gold deposits (i.e., more than 1 million ounces of contained gold)
[2] base metal values quoted for Eskay Creek are approximate grades for the 21B zone
- signifies no data available
I.F. = iron formation
VMS = volcanic-associated massive sulphide

SIZE AND GRADE

Auriferous volcanic-associated massive sulphide deposits are characterized by grades typical of other gold deposits and by tonnages similar to those of other base-metal massive sulphide deposits (Fig. 6.4-1). Their base metal contents and gold/silver ratios are distinct from those of typical massive sulphide deposits (Fig. 6.4-2) and also differ somewhat from other types of gold deposits that occur in greenstone belts (see Fig. 15.4-4). The giant Horne deposit (54.3 Mt grading 6.1 g/t Au) and the much smaller, but high grade Eskay Creek deposit (3.95 Mt grading 26.4 g/t Au) illustrate the range of sizes and gold grades of the individual orebodies.

Many auriferous massive sulphide deposits occur in close proximity to base metal massive sulphides, but few camps contain more than one distinctly auriferous deposit. Of the 22 sulphide deposits at Noranda, the giant Horne and Quemont gold deposits have produced more than 90% of the gold and also account for more than 65% of the total massive sulphide tonnage (Kerr and Mason, 1990). In the Skellefte district of Sweden, the Boliden deposit (7.6 million tonnes grading 15.2 g/t Au) is among the largest of 20 different massive sulphide orebodies, but also has ten times the average gold grade for the district. In contrast, all 14 deposits within the Bousquet district have high gold grades ranging from 4.3 to 9.7 g/t Au (Marquis et al., 1990b). Collectively these deposits contain nearly 60 million tonnes of ore averaging 5 g/t Au.

GEOLOGICAL FEATURES

Setting

Auriferous massive sulphide deposits occur in rocks of dominantly volcanic derivation, typical of host rocks for other volcanic-associated base metal massive sulphide deposits of all ages. In nearly all cases the paleotectonic

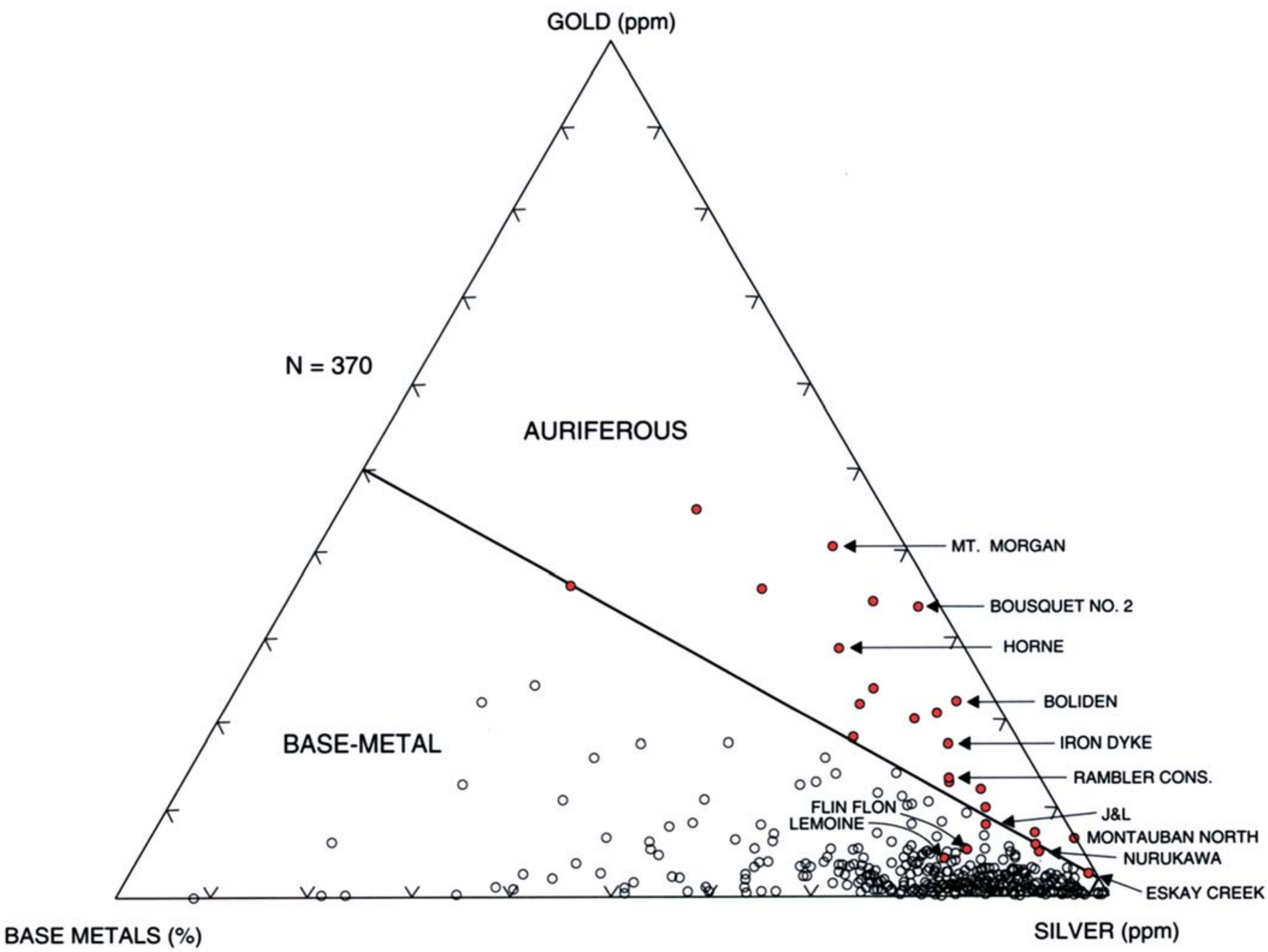

GSC

Figure 6.4-2. Ternary diagram portraying the relative abundance of gold (ppm), silver (ppm), and base metals (total per cent combined) for selected volcanic-associated massive sulphide deposits world-wide. The centrally located diagonal line can be used to make an approximate compositional separation of auriferous and base metal massive deposits. Red dots portray volcanic-associated massive sulphide deposits with high absolute abundances of gold.

Contents

settings are inferred to be those of island arcs, rifted arcs, or back-arc basins and, at regional scales, the gold deposits occur within the same lithological units as base metal deposits. The host sequences typically comprise two contrasting components: a mafic one, in the form of basalt, andesite, or amphibolite, and a felsic one, in the form of tuffs and volcanic breccias.

Archean deposits of this type in Canada include the Horne, Bousquet (No. 1 and No. 2), and Agnico-Eagle deposits, which occur in the 2.7 Ga greenstone belts of the Abitibi Subprovince. The Horne deposit occurs in a sequence of felsic fragmental rocks and flows of the Blake River Group with virtually no mafic volcanic rocks (Kerr and Gibson, 1993). The Bousquet district (Fig. 6.4-3), also within the Blake River Group, hosts important gold

Table 6.4-2. Geological characteristics of selected auriferous volcanic-associated massive sulphide deposits.

Deposit	Host rocks	Metamorphism	Structure	Intrusions	Nature of orebodies	Ore mineralogy/ chemistry	Gangue/alteration
Canadian examples:							
Horne	felsic volcaniclastics and rhyolite flows	lower greenschist	relatively undeformed, E-W cleavage	mafic, felsic dykes subvolc. tonalite	pipe-like mass. and stringer py-cp, mass. py	pyrite-pyrrhotite-chalcopyrite-tellurides-sphalerite	quartz-sericite-chlorite
Quemont	rhyolite breccias	lower greenschist	relatively undeformed, E-W cleavage	mafic, felsic dykes subvolc. tonalite	mass. and dissem. sulphides, multiple lenses	pyrite-pyrrhotite-chalcopyrite-tellurides-sphalerite	quartz-sericite-chlorite
Bousquet No.1	felsic and mafic tuffs	middle-upper greenschist	intense E-W foliation and shearing	none known	pyritic qtz-ser. schists, dissem. sulphides and foliation-parallel stringers	pyrite-chalcopyrite-sphalerite-arsenopyrite-tellurides-gudmundite	quartz-muscovite kyanite-andalusite-chloritoid
Bousquet No. 2	felsic tuffs	middle-upper greenschist	intense E-W foliation and shearing	none known	foliation-parallel stringers mass. py, remob. cp-bn	pyrite-chalcopyrite-bornite-tellurides	quartz-muscovite andalusite-kyanite-paragonite
Dumagami	felsic tuffs	middle-upper greenschist	intense E-W foliation and shearing	none known	mass. pyritic sulphides	pyrite-sphalerite-chalcopyrite-bornite	quartz-muscovite andalusite-kyanite-paragonite
Doyon	felsic tuffs, intrusion	middle-upper greenschist	intense E-W foliation	adjacent tonalite	quartz-pyrite veins	pyrite-chalcopyrite-tellurides	quartz-muscovite andalusite-kyanite-chloritoid
Agnico-Eagle	felsic tuffs and cherty sulphide-carb. iron-fm.	middle-upper greenschist	NW foliation near regional shear zone	postore diabase	chemical and clastic seds., mass. sulphides	pyrite, minor chalcopyrite and arsenopyrite	chert, Fe-carbonate, Fe-silicates
Montauban North	felsic volcanics (quartz-biotite gneiss)	amphibolite	folded N-S foliation	none known	dissem. sulphides	pyrite-sphalerite-chalcopyrite-pyrrhotite±glena	quartz-biotite garnet-cordierite-anthophyllite
Eskay Creek	felsic tuffs, breccias, mudstone at rhyolite-basalt contact	weak	N-S folds	diorite sheets	stockwork and stratiform massive sulphides	sphalerite-tetrahedrite-pyrite-galena, stibnite-realgar-cinnabar-arsenopyrite	quartz-chlorite-sericite
Non-Canadian deposits with similar characteristics:							
Boliden	dacite-rhyolite	greenschist-amphibolite	intense E-W foliation and isoclinal folds	subvolc. tonalite intrusion	multiple mass. py-cp and mass. py-aspy lenses	pyrite-pyrrhotite-arsenopyrite-chalcopyrite-tetrahedrite-tellurides	quartz-chlorite-sericite-rutile-andalusite-corundum
Mt. Morgan	felsic tuffs, siltstones, lavas and porphyries	weak	moderately deformed, intense E-W foliation	subvolc. tonalite intrusion	pipe-like dissem.-stringer py-cp, mass. py-cp	pyrite-pyrrhotite-arsenopyrite-galena-sphalerite	quartz-biotite andalusite-staurolite-sillimanite
Mt. Chalmers	rhyolite-dacite dome, volcaniclastics, siltstone	weak	relatively undeformed	qtz.-feld. porphyry, andesite sills	dissem.-stringer py-cp, minor mass. sulphides	pyrite-chalcopyrite-sphalerite-galena-barite	quartz-sericite-chlorite-dolomite
Mt. Lyell (The Blow)	felsic pyroclastics and flows	lower greenschist	moderately deformed, folded	minor int. and felsic intrusives	dissem.-stringer py-cp-bn, mass. py-cp, mass. sp-gn	pyrite-pyrrhotite-chalcopyrite-bornite± sphalerite±galena	quartz-sericite-chlorite-siderite-hematite-barite
Starra; Trough Tank	oxide facies iron-fm., mafic-felsic tuffs	middle-upper greenschist	multiphase, intense foliation and shearing	none known	iron-formation	quartz-magnetite-pyrite-chalcopyrite±scheelite	chlorite-magnetite-hematite±sericite
Nurukawa, Japan	rhyolite-dacite flows and pyroclastics	unmetamorphosed	relatively undeformed	none known	stockwork and dissem. sulphides	pyrite-chalcopyrite	quartz-sericite± chlorite- kaolinite-pyrophyllite

Abbreviations: carb., carbonate; fm., formation; qtz., quartz; feld., feldspar; mass., massive; remob., remobilized; dissem., disseminated; seds., sedimentary rocks; subvolc., subvolcanic; int., intermediate; py, pyrite; cp, chalcopyrite; bn, bornite; sp, sphalerite; gn, galena; aspy, arsenopyrite; ser., sericite.

deposits of three different types, including Bousquet No. 1 (pyritic gold), Bousquet No. 2 (copper-gold; Fig. 6.4-4A), and the Dumagami mine (auriferous polymetallic). A number of intrusion-related pyritic gold deposits also occur in the vicinity of the Bousquet mines (e.g., Doyon-Silverstack, Ellison) and these may be related to the near-surface exhalative deposits. Although in such a deformed terrane it is difficult to distinguish between volcanogenic deposits and deep-seated intrusion-related deposits, the presence of an extensive Mn-garnet "exhalite" unit and the local stratiform base metal mineralization (e.g., Warrenmac) near Doyon argues for a volcanogenic origin for the Bousquet deposits. The Agnico-Eagle pyritic gold deposit, north of Joutel, is interpreted to sit near the top of the Joutel volcanic complex, which hosts a number of gold-poor base metal deposits (Poirier, Joutel Cu, Consolidated Northern). The host rocks are interpreted to consist of a stratiform carbonate-sulphide-silicate-oxide iron-formation, intercalated with cherty sedimentary rocks and tuffs, and an apparent chloritic footwall (Barnett et al., 1982). Although the nearby base metal massive sulphides at Joutel are gold-poor, the small Estrades Cu-Zn deposit, northeast of Joutel, is anomalously gold-rich (2.67 Mt grading 5.1 g/t Au).

Montauban North is the only notable Canadian example of a Proterozoic deposit of this type, but deposits of this age elsewhere in the world include Boliden, Sweden and Yavapai, U.S.A. Gold-rich pyritic sulphides occur along strike from the Montauban Zn-Pb orebody in Middle Proterozoic gneisses of the Grenville Supergroup in Quebec. The North and South zones of the Montauban deposit produced subequal amounts of gold (0.7 t Au) and silver (0.9 t Ag) from a zone of pyrite-sphalerite-chalcopyrite mineralization associated with cordierite-anthophyllite and quartz-biotite-garnet assemblages within quartz-biotite and quartz-sillimanite gneisses (Morin, 1987). The gold zones contained as much as 30% disseminated suphides, but high gold values appear to have been independent of base metals. Although of high metamorphic grade, the quartz-plagioclase-biotite gneiss adjacent to the Montauban deposit has been interpreted to be derived mainly from felsic volcaniclastic rocks that contained local sedimentary intercalations (Morin, 1987). The Boliden auriferous massive sulphide deposit occurs in the circa 1.8 Ga greenstone belt of the Skellefte district in Sweden. The Boliden orebody consists of two large pyrite-chalcopyrite orebodies (6 Mt), which envelop several smaller arsenopyrite-rich lenses (2 Mt), and crosscutting quartz-tourmaline veins. The deposit is hosted by pyritic quartz-sericite±chlorite and andalusite-rich schists of the Skellefte Volcanics (Fig. 6.4-4B). Likewise, the stratiform pyritic gold occurrences in Yavapai County, Arizona, are of Early Proterozoic age. The Yavapai deposits (e.g., Iron Dyke) consist of gold-bearing disseminated zones and local thin massive sulphide lenses with minor base metals in cherty, quartz-sericite and quartz-chlorite schists (Swan et al., 1981).

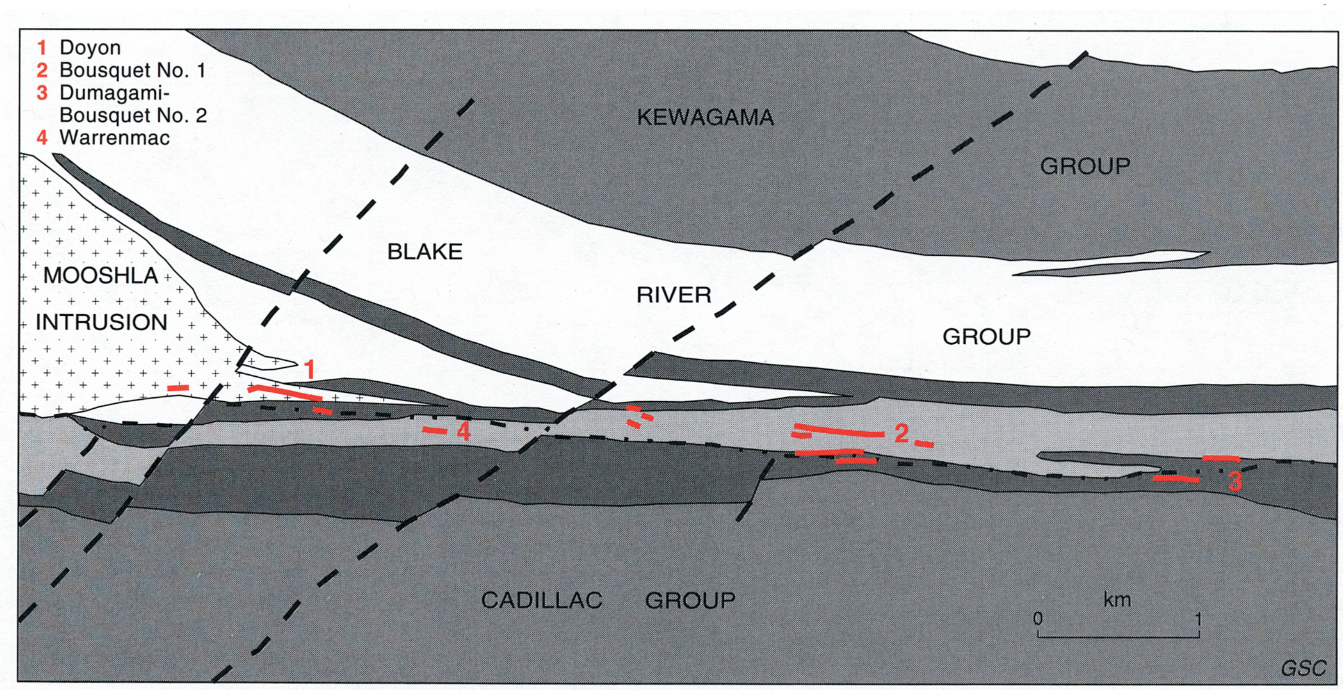

Figure 6.4-3. Regional setting of the gold-rich volcanic-associated massive sulphide deposits in the Bousquet district, Quebec (adapted after Marquis et al., 1990b). The rocks of the Blake River Group include felsic volcanics (light grey); intermediate composition tuffs and epiclastic rocks (dark grey); basalt (uncoloured). Heavy dashed and dash-dot lines represent faults and shear zones respectively, and areas in red represent the surface traces of gold orebodies and showings.

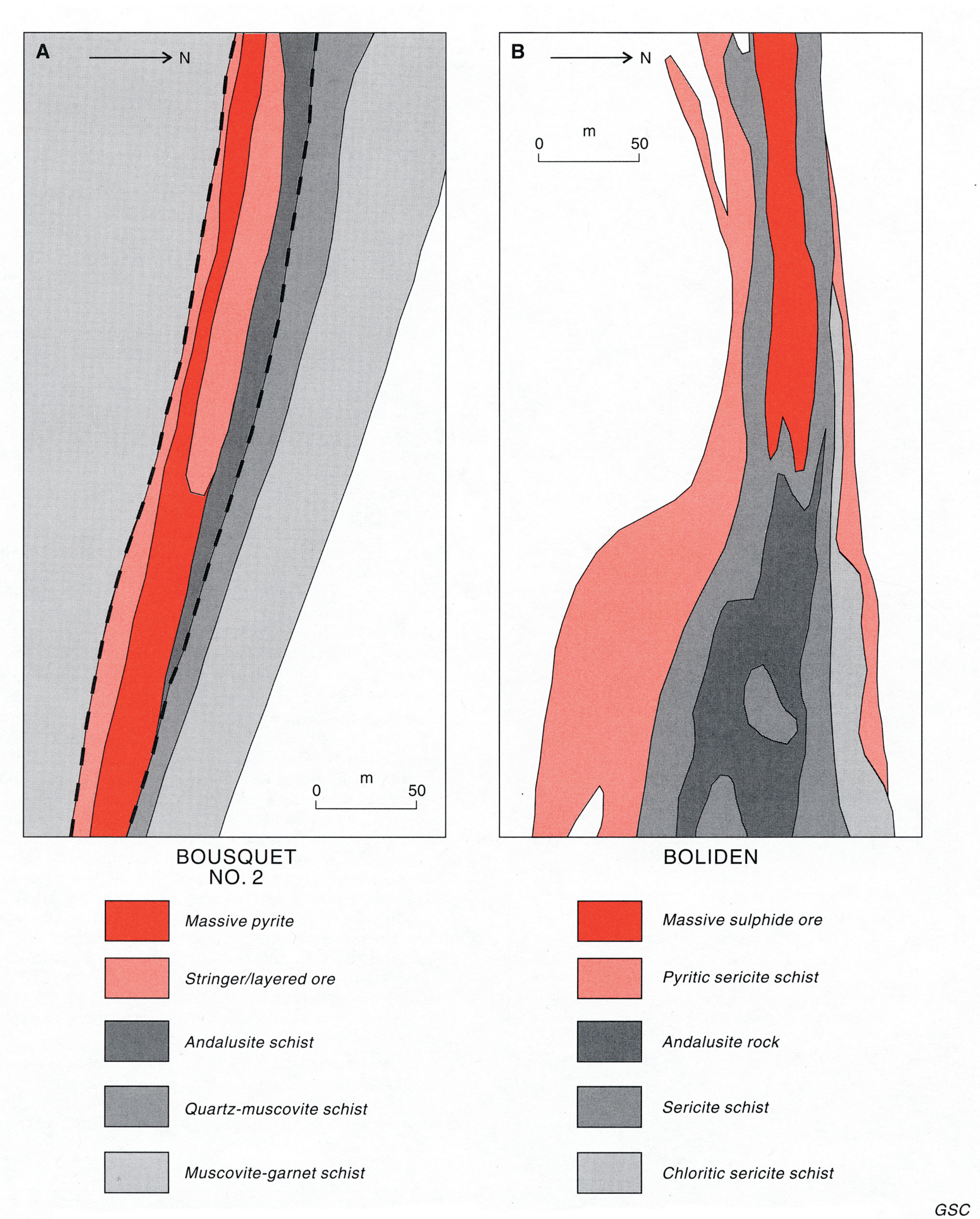

Figure 6.4-4. Distribution of alteration minerals in and adjacent to auriferous massive sulphide orebodies which are shown in red: **A)** cross-section of the Bousquet No. 2 deposit, Bousquet district; dashed lines correspond to faults (adapted after Tourigny et al., 1993); **B)** comparative section through Boliden deposit, Sweden (adapted after Grip and Wirstam, 1970).

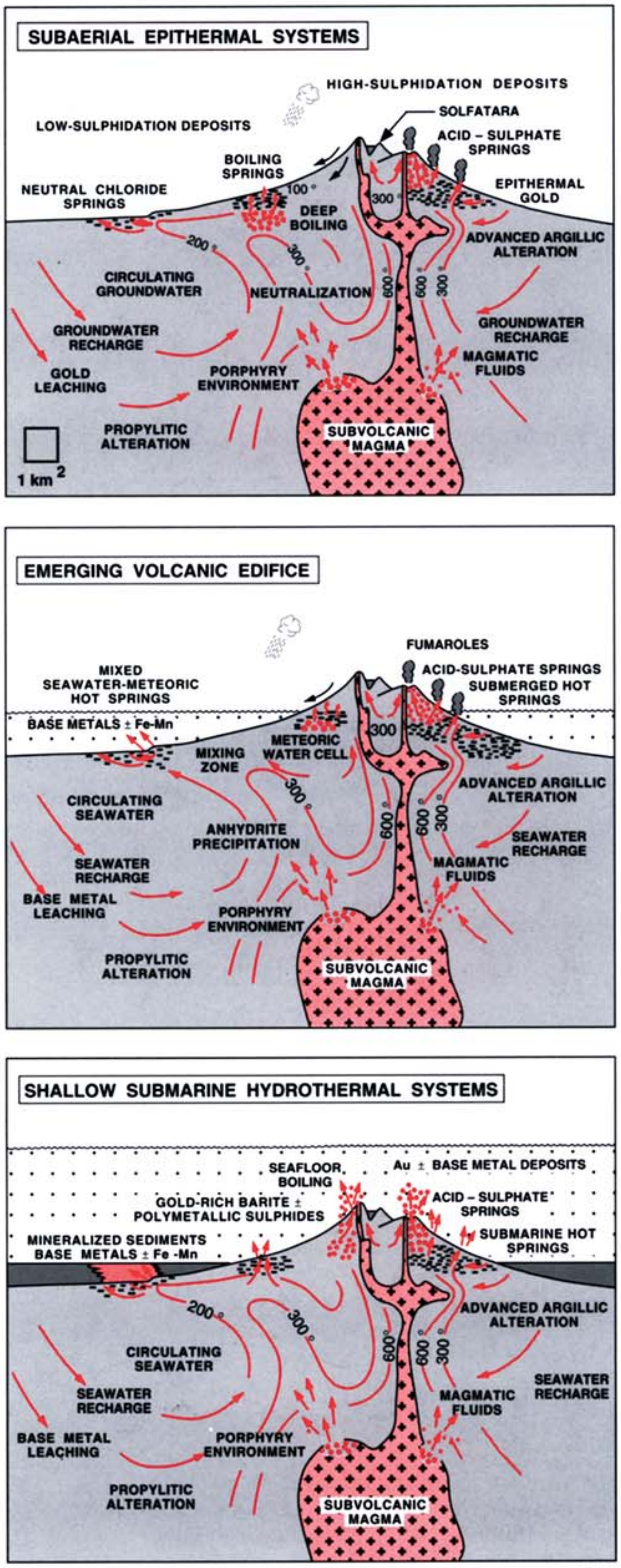

GSC

Volcanic-associated massive sulphide deposits are well known in contemporaneous felsic volcanic rocks of the Jerome area, and the Yavapai Volcanics also host the nearby Iron King base metal massive sulphide deposit (4.97 Mt grading 7.3% Zn, 2.5% Pb, 0.2% Cu, and 4.2 g/t Au).

The only Paleozoic examples of this deposit type in Canada include small, high grade auriferous polymetallic sulphide deposits that are found in volcanic rocks of Devonian age in central British Columbia (e.g., Höy, 1991). Of these, Rea Gold, Homestake, and J&L are the most gold-rich examples, but they are compositionally transitional between typical base metal massive sulphide deposits and truly auriferous deposits (Fig. 6.4-2). Important Paleozoic auriferous massive sulphide deposits do occur, however, in the Tasman Geosyncline. The large Mt. Morgan deposit in the Mt. Windsor volcanic rocks of eastern Australia has been one of the country's largest single lode-gold deposits, having produced nearly 238 t of gold. Mt. Morgan and the nearby Reward deposit are copper-gold deposits hosted by pyritic quartz-sericite schists (Large, 1992). In addition, the Mt. Lyell copper-gold deposit in Tasmania consists of massive, gold-rich pyrite ore (e.g., The Blow), siliceous barite-chalcopyrite-bornite ore (e.g., North Lyell), and disseminated pyrite-chalcopyrite ore (e.g., Prince Lyell and others), all of which are hosted by quartz-sericite and quartz-sericite-chlorite schists. These orebodies were originally worked for gold and remain among the largest gold producers in Tasmania (Large et al., 1990). A number of other uncommonly gold-rich base metal deposits are also known in the Mt. Read volcanic rocks of Tasmania (e.g., Rosebery, Hellyer, Que River, South Hercules, Mt. Charter) and resemble Canadian gold-rich base-metal massive sulphides such as Flin Flon and H.W.

Among Mesozoic and Cenozoic deposits of this age, the best example of this type occurs at Eskay Creek in British Columbia in Jurassic volcanic rocks of the Upper Hazelton Group. The ore zones at Eskay Creek are situated near the contact between rhyolite breccia, tuff, and mudstone and overlying pillowed andesite (Britton et al., 1990). These are distinctive deposits, typically consisting of small, high-grade massive sulphides which resemble the Miocene Kuroko-type, polymetallic Zn-Pb-Cu deposits of Japan. Although these gold-rich deposits are modelled after Kuroko-type massive sulphides, most Kuroko deposits have rather restricted zones of gold enrichment (e.g., Shakanai No. 1-3). A particularly high-grade, Kuroko-type copper stringer zone has recently been documented in the Nurukawa deposit in Japan (Yamada et al., 1987), and this may be analogous to some older, metamorphosed, pipe-like copper-gold deposits.

Intrusions constitute a large proportion of the rocks in most of the above districts and include dykes, subvolcanic sills, and porphyry stocks that range from mafic to felsic in composition and from pre- to post-tectonic in timing.

Figure 6.4-5. Schematic diagram of a hypothetical shallow marine to epithermal transition (after Hannington, 1993). Note the expected progression from marine to emergent epithermal conditions and the possible involvement of shallow subvolcanic intrusions.

Tonalitic subvolcanic intrusions are present at Quemont (Powell pluton) and Horne, Bousquet (Mooshla pluton), Boliden (Jarn granitoids), and Mt. Morgan (Mt. Morgan tonalite). In many cases the intrusions are hydrothermally altered and contain vein- and stockwork-style mineralization that locally constitutes significant gold ore in itself (e.g., Doyon deposit in the Mooshla intrusion).

Regional dynamothermal metamorphism of low to medium grade has affected the rocks in most of the older greenstone belts that contain gold deposits of this type. Middle to upper greenschist metamorphic conditions are inferred at Bousquet and Agnico-Eagle, and metamorphism at Montauban fully attained the amphibolite facies. The Boliden deposit in Sweden occurs in rocks at the transition from greenschist to amphibolite facies. The deposits at Noranda and Eskay Creek are virtually unmetamorphosed.

Structure

Regional metamorphism of the older greenstone belts has resulted in penetrative deformation of many of the deposits and the development of at least one generation of tectonic fabric that overprints the mineralization. In most cases, the degree of deformation and transposition has obscured many of the primary relationships between the ore deposits and their host rocks, and significant remobilization of gold has complicated the paragenetic relationships between gold and sulphide mineralization, leading to considerable debate about possible syntectonic versus synvolcanic origins for much of the gold. The existence of well preserved, relatively unmetamorphosed gold deposits of this type in younger volcanic sequences, and detailed mapping at a number of metamorphosed examples, indicate that a synvolcanic origin for gold in many cases is valid (see "Genetic models" below).

A common feature of older, metamorphosed deposits is a strong foliation, amplified within discrete shear zones, that strikes subparallel to the regional lithological trend. In the Bousquet district, pyritic gold and copper-gold deposits are contained within a zone of intense brittle-ductile deformation known as the Dumagami structural zone (Tourigny, 1991). Here the local structure is dominated by metre-scale anastomosing shear zones in which the transposition of bedding into parallelism with the inherited schistosity is common (Tourigny et al., 1989; Marquis et al., 1990a; Tourigny et al., 1993). Such transposition accounts for the "straightness" of the rock units (e.g., Fig. 6.4-3) and usually obscures any original relationships between the ore deposits and their host rocks. Strong linear fabrics, such as the axes of asymmetric minor folds and mineral and shape lineations, are also characteristic of these areas and are of consistent orientation within a district. Moderate to steep plunges have been noted at Bousquet, whereas fold hinges and lineations of shallow plunge are common at Montauban. The relationship of gold mineralization to the mixed volcanic, chemical, and clastic sedimentary host rocks at Agnico-Eagle is also complicated by the fact that the rocks have a moderate tectonic fabric, and the presence of gold within late carbonate veins and fractured pyrite is evidence for introduction or remobilization of gold during brittle deformation (Wyman et al., 1986). The Boliden deposit is tightly isoclinally folded, and a well developed axial planar schistosity gives the appearance of a shear zone (Grip and Wirstam, 1970; Rickard, 1986).

Orebodies

Auriferous massive sulphide orebodies may have formed directly on the seafloor as massive sulphide accumulations or in the immediate subseafloor as stratiform replacements. However, many of the auriferous volcanic-associated pyritic and copper-gold deposits consist largely of disseminated and stockwork-like vein systems and are, strictly speaking, not massive sulphide ores. These deposits are commonly pipe-like bodies with relatively minor massive stratiform sulphide accumulations (e.g., Mt. Morgan, Boliden). Nevertheless, the presence of minor amounts of exhalative sulphides in most cases argues strongly for a submarine setting. Such deposits are generally considered to be stratabound at the scale of a district (e.g., within or along strike from well-defined lithotectonic packages of rocks), even where transposition has resulted in structural and lithological trends that are parallel to one another. Furthermore, the deposits commonly occur at contacts between distinctive lithological units or solely within a particular unit. The lenticular to tabular shapes of most orebodies is such that they are geometrically concordant with their host rocks, even though the main sources of ore-grade massive sulphides may be discordant (e.g., Bousquet No. 1 and No. 2); where deformation has been extreme, the long axes of orebodies are commonly parallel to other linear fabrics in the district. Where deformation is less severe (e.g., Horne, Eskay Creek) the concordance of orebodies and host rocks is more clearly related to pretectonic processes. Orebody thicknesses, especially for the massive sulphide type deposits, range from 2 m to 60 m, a factor which, along with consistent ore grades, has made many of them amenable to open pit mining methods (Bousquet, Mt. Morgan, Boliden).

Ore composition

Specific deposits in this category display considerable variation in both the distribution and composition of ore types.

The Horne mine was a pipe-like copper-gold deposit (Upper H and Lower H orebodies) capped by a large, lower-grade pyritic massive sulphide lens (No. 5 zone). Most of the ore produced from the mine consisted of massive pyrite-pyrrhotite-chalcopyrite and associated stringer mineralization from the Upper H and Lower H orebodies. Gold was present mainly as Au-Ag tellurides and as native metal.

At Bousquet most ores contain 5-20% pyrite, locally substantial amounts of chalcopyrite, and lesser quantities of other sulphide and telluride minerals. The auriferous suphides are interpreted to be synvolcanic in origin, and subsequent deformation and remobilization of the ore constituents are responsible for many of the veins present (Tourigny et al., 1989). The Bousquet No. 1 mine consists of gold-bearing, pyritic quartz-muscovite schists with multiple, foliation-parallel and foliation-oblique, disseminated and vein-type ore lenses. Bousquet No. 2 has characteristics of both pyritic gold and base-metal-rich deposits. The orebodies consist of foliation-parallel, pyritic stringers, massive pyritic sulphides, sulphide breccias, chalcopyrite-rich layered stringer ore with minor sphalerite and galena, and semimassive remobilized bornite-chalcopyrite veins (Tourigny et al., 1993). This latter ore type accounts for the major part of the gold mineralization in Bousquet No. 2. As in Bousquet No. 1, the mineralization is largely structurally-controlled, but mainly as the result of metamorphic remobilization of a synvolcanic copper-gold protore. The ore mineralogy is also unusually complex, consisting of pyrite, chalcopyrite, bornite, digenite, chalcocite, sphalerite, galena, tennantite, mawsonite, colusite, native gold, and Au-, Ag-, and Pb-tellurides. The Dumagami orebodies consist of massive pyritic suphides, which include abundant sphalerite, chalcopyrite, and bornite, and most closely resemble exhalative massive sulphides (Marquis et al., 1990a, b).

The Agnico-Eagle gold deposit consists of auriferous chemical and volcaniclastic sediments, which contain about 20% disseminated pyrite and local massive to semimassive stratiform pyrite (Barnett et al., 1982; Wyman et al., 1986). Minor amounts of base-metals are also present. Fine grained gold occurs within distinct pyritic laminae and within late carbonate veins and fractures.

The mineralization at Eskay Creek is exceptionally high grade (e.g., 26 g/t Au and 100 g/t Ag) and consists of stockwork and disseminated sulphides in an epithermal-style vein system (21A zone), as well as stratiform, bedded sulphides that include sphalerite, galena, tetrahedrite, stibnite, realgar, cinnabar, and arsenopyrite (21B zone) (Britton et al., 1990; Roth, 1993). The mineralization is hosted in a quartz-sericite-chlorite assemblage derived from altered rhyolite breccias and tuffs.

Mt. Morgan consists of a large pyritic massive sulphide lens capped by stratiform pyritic and cherty horizons (Main Pipe orebody) and a siliceous zone of disseminated and stringer mineralization (Sugarloaf orebody), which together form a pipe-like body, similar to the Horne deposit (Taube, 1986). The ore mineral assemblage is pyrite, pyrrhotite, chalcopyrite, magnetite, and minor sphalerite, together with native gold and gold tellurides. In addition, nearly 72 t of native gold (30% of the total production) was recovered from a 2.4 million tonne gossan cap with an average grade of 30.6 g/t Au. In the Mt. Morgan area, there are also several conventional volcanogenic massive sulphides (Ajax, Upper Nine Mile Creek), as well as porphyry-related mineralization and alteration (Taube, 1990). The nearby Mt. Chalmers copper-gold deposit has a somewhat higher base-metal-to-gold ratio, but also possesses a gold-rich pyritic massive sulphide body and associated copper-stringer zone (Large and Both, 1980).

Boliden ore averaged 15.2 g/t Au from 8.34 million tonnes mined over a 43 year period. Although pyrite is the dominant sulphide, the major ore minerals are chalcopyrite, arsenopyrite, and sphalerite; minor galena, pyrrhotite, and locally abundant sulphosalts are present. Arsenic, silver, cobalt, selenium, and mercury were also enriched in the Boliden ores; the average arsenic grade for the mine was 6.9 wt.% As, making it one of the largest arsenic deposits in the world. Gold occurs mainly as native metal and electrum and shows a positive correlation with arsenic. Bonanza-type gold mineralization also occurred locally in large crosscutting quartz-tourmaline veins, as well as in arsenopyrite-rich ore lenses (e.g., 600 g/t Au over 1 m in the Gold Rise and 200 g/t Au over 2 m in the root zone of the Eastern Ore arsenopyrite lenses).

As a group, deposits of this type are distinguishable mainly by their high gold content relative to base metals (Fig. 6.4-2) and in some cases by their unique mineralogy. However, their variability in bulk composition is broadly similar to that of massive base metal sulphide deposits of similar age and host rock lithology (e.g. subtype 6.3). The pyritic gold (e.g., Bousquet No. 1) and copper-gold (e.g., Horne) deposits typically have much higher Au/Ag ratios than auriferous polymetallic sulphides, the latter sometimes having exceptional silver concentrations (e.g., Eskay Creek). The nature of the ore-bearing material differs from deposit to deposit, with highly variable proportions of sulphide-to-silicate host rock. The ore mineral assemblages commonly show greater complexity than in similar gold-poor massive sulphides and may include a variety of minor minerals such as bornite, arsenopyrite, tellurides, and high-sulphidation minerals (e.g., enargite-tennantite) which are less common in conventional base-metal massive sulphides (e.g., Table 6.4-1). Notable concentrations of massive to semimassive bornite ore, together with abundant and complex assemblages of sulphosalt minerals, are common in many pyritic and copper-gold deposits of this type (e.g., Bousquet No. 2, North Lyell, Boliden) and in some auriferous polymetallic sulphides. High gold grades are also commonly associated with those parts of conventional base-metal massive sulphides with similar high-sulphidation mineral assemblages (e.g., H.W., typical Kuroko-type deposits: Hannington and Scott, 1989b). Auriferous polymetallic sulphides commonly display a wide range of minor and trace minerals, dominated by sulphosalts of silver, arsenic, antimony, lead, and mercury which are typical of epithermal gold deposits. Tetrahedrite, stibnite, realgar, cinnabar, and arsenopyrite are present in both ore types at Eskay Creek, and the 21B zone contains massive, bedded stibnite ore. These deposits are commonly capped by or associated with abundant barite mineralization, and in some cases barite may occur within auriferous stockworks (e.g., Mt. Charter and North Lyell).

Alteration

Aluminous mineral assemblages and distinctly acid alteration (e.g., alunite or pyrophyllite common) are common features of the rocks adjacent to many gold deposits of this type. Pyritic, quartz-sericite schists are the most common hosts, although in some unmetamorphosed and weakly metamorphosed deposits, advanced argillic alteration (quartz, kaolinite, pyrophyllite, and other clay minerals) is well preserved. Numerous Kuroko-type deposits in Japan are characterized by clay-rich alteration minerals, and these assemblages are recognized in a number of the younger auriferous polymetallic sulphide deposits (e.g., Marumo, 1990). The aluminous nature of these rocks is similar, in many respects, to that ascribed to alunite-kaolinite alteration associated with certain porphyry deposits and high-sulphidation epithermal gold deposits (see subtype 15.1). However, the significance of this alteration in relation to gold mineralization in auriferous sulphide deposits is not fully understood, and similar alteration is in some cases found in association with gold-poor massive sulphides (e.g., Mattabi, Bathurst-Norsemines). Typical base-metal sulphide deposits are noted for their distinctive chloritic, footwall alteration "pipes", but many gold-only deposits possess an enveloping alteration halo consisting dominantly of sericite and silica. Nevertheless, some gold-only deposits also have discordant alteration "pipes" that are not noticeably different from those of conventional base-metal massive sulphides and reflect ordinary seafloor hydrothermal activity. For example, the main mine formation at the Horne deposit consists of rhyolite flows and felsic volcaniclastic rocks, and the No. 5 pyritic lens is contained within a well bedded tuffaceous unit. All of the felsic rocks have been altered to quartz-sericite and quartz-chlorite-sericite assemblages.

The alteration in the Bousquet district (Fig. 6.4-4A) is typical of metamorphosed deposits of this type. The altered rocks are strongly foliated quartz-muscovite±andalusite± kyanite schists that locally contain pyrophyllite and diaspore, and are interpreted to be the metamorphosed equivalents of advanced argillic alteration (Valliant et al., 1983; Tourigny et al., 1989). At Dumagami, peraluminous alteration also hosts the massive pyrite and massive sphalerite-galena bodies, and is surrounded by a sericitic envelope (Marquis et al., 1990a). The aluminous nature of the alteration associated with many pyritic gold deposits of this type is also obvious in other metamorphosed Archean and Proterozoic examples. For example, at Boliden, alteration is dominated by quartz-sericite-andalusite in close proximity to the ore, and this core is surrounded by a chloritic outer envelope (Fig. 6.4-4B). The laminated quartz-sericite schists containing abundant andalusite, and local kyanite, that occur on both sides of certain of the Bousquet deposits (Valliant et al., 1983; Marquis et al., 1990a) are remarkably similar in disposition to those at Boliden (Fig. 6.4-4B).

In addition to aluminosilicates, ferromagnesian aluminous minerals, such as chloritoid, staurolite, cordierite, and garnet, are noteworthy in many of these deposits (Fig. 6.4-4). Chloritoid and manganiferous garnets are also notable at Bousquet (Valliant and Barnett, 1982). At Montauban, a unit of sillimanite gneiss envelops the deposit, and cordierite, anthophyllite, and manganiferous garnets are locally abundant (Morin, 1987; Jourdain et al., 1987).

DEFINITIVE CHARACTERISTICS

As a group, auriferous sulphide deposits possess a number of definitive characteristics.

1. The deposits have low contents of base metals relative to gold (i.e., less than one per cent combined base metals for each part per million gold).
2. Layered, stratiform massive sulphides typically contribute to at least some of the ore, although the most gold-rich zones may be restricted to disseminated and stockwork-like feeders.
3. Sulphide ores commonly include a complex assemblage of minor and trace minerals such as bornite, sulphosalts, arsenopyrite, tellurides, and other high-sulphidation minerals, locally with high concentrations of the epithermal suite of elements (e.g., Ag, As, Sb, Hg).
4. Individual orebodies are commonly associated with zones of sericitic alteration and silicification and, in some cases, are enclosed by aluminous, acid alteration zones; the presence of magnesium-rich and manganiferous alteration minerals may be indicative of seafloor hydrothermal alteration, and abundant carbonate may indicate boiling.
5. The deposits typically occur together with conventional base metal massive sulphide deposits and share many of their geological characteristics; they are typically stratabound at the district and deposit scale and commonly occur at or near interfaces between felsic volcanic rocks and either mafic volcanic or clastic sedimentary rocks.

GENETIC MODEL

Currently two genetic models are applied to these deposits:

1. They are viewed to be variants of conventional massive sulphide deposits that are distinguished by inherently anomalous fluid chemistry and/or deposition within a shallow marine to subaerial volcanic setting in which boiling may have had a significant impact on the chemistry of the ore fluids; or
2. They are viewed to be syntectonic sulphide replacement deposits in shear zones or, at least, as massive sulphide deposits that have been overprinted by gold-bearing fluids during regional deformation and metamorphism.

In the first case, gold deposits of this type are seen as transitional between submarine base metal sulphide deposits and terrestrial epithermal gold deposits (Fig. 6.4-5). The Eskay Creek deposit, which is relatively undeformed and possesses unequivocal exhalative affinities, is an example of a distinctly gold-rich massive suphide which likely formed in very shallow water (Britton et al., 1990). For deposits of this kind that have escaped regional metamorphism and significant deformation, the relationship between gold enrichment and massive sulphide mineralization is usually obvious and provides strong evidence for a synvolcanic origin for the gold. The genetic models for these deposits are essentially variations on those for other volcanogenic sulphide deposits, and recent discoveries of gold-rich massive sulphides actively forming on the ocean floor have provided unique opportunities to study the processes of gold mineralization in this environment.

The concept that some pyritic gold deposits are not inherently gold-rich, but were overprinted by auriferous fluids during deformation and metamorphism, is founded in the fact that many of the type localities for these deposits are strongly deformed and that gold and its associated minerals, at the mesoscopic and microscopic scales, exhibit a late textural paragenesis. Features such as sulphide veins that are discordant to regional foliation and ore zones that locally are parallel to foliation, but at a high angle to transposed bedding, are particularly common in the Bousquet district and similar structural complexities have also been identified at Agnico-Eagle. The important structural controls in these districts have led to alternate hypotheses concerning the emplacement of the ore: (1) the deposits are wholly syntectonic in origin – i.e., sulphide replacements in shear zones (note that this same interpretation was applied to the Boliden and Horne deposits earlier in this century); (2) the sulphide ores are pretectonic and synvolcanic, but some or all of the gold has been superimposed on them during regional tectonism (e.g., Wyman et al., 1986; Tourigny et al., 1989; Marquis et al., 1990a); (3) the sulphide ores are pretectonic and inherently auriferous, and the regional metamorphism and deformation served only to modify the deposits and locally remobilize some of the ore constituents into structurally controlled sites (Barnett et al., 1982; Valliant and Barnett, 1982; Valliant et al., 1983; Tourigny et al., 1993). Although the third hypothesis is compelling, it is unlikely that the alternatives can be conclusively excluded in the case of Bousquet and Agnico-Eagle.

In older metamorphosed terranes, the apparent stratigraphic controls on the location of the deposits at a district scale is the strongest point in favour of a volcanic exhalative model. In most districts, pyritic gold deposits that have all of the attributes of volcanogenic massive sulphide deposits occur within the same stratigraphic sequences and adjacent to conventional base metal deposits. The Bousquet gold orebodies occur within the same sequence as the Dumagami Zn-Cu-Au deposit, and the Montauban gold orebodies occur immediately along strike from the Montauban Zn-Pb deposit. In both of these cases the base metal deposits are considered by most geologists to be of volcanogenic massive sulphide type. In a re-examination of the geology of the Horne deposit, Kerr and Mason (1990) offered numerous reasons why late tectonic superposition of gold is unlikely. Foremost among these are the observations that, locally, an unmineralized debris flow deposit has unconformably cut down into the gold-copper mineralization and that otherwise barren pyroclastic tuffs in the stratigraphic hanging wall contain blocks of the underlying gold-rich massive sulphides. It also has been argued that, because inherently auriferous chemical and volcaniclastic sediments are common host rock for some gold deposits of this type and because high gold grades occur in regional chemical sediments away from the deposits, a volcanogenic origin for at least some of the gold is likely. If one accepts a volcanic exhalative origin for some of these deposits, the most relevant inquiry pertains to the controls on mineralization that distinguish them from other volcanic-associated deposits containing relatively little gold.

Some insight on gold in volcanogenic massive sulphide systems has also been gained from an evaluation of data from hydrothermal vents on the modern seafloor (Hannington and Scott, 1989a; Hannington et al., 1991). Analysis of vent fluids and precipitates from the seafloor shows that submarine hydrothermal systems have enormous capacities to transport gold. Large differences in the gold contents of seafloor sulphide deposits can be explained either in terms of gold-enriched sources or in terms of a favourable mechanism by which to effectively concentrate gold from solution. Gold may be precipitated at low temperatures by oxidation of aqueous sulphur complexes during mixing with cold seawater or at higher temperatures from chloride complexes in fluids ascending through the volcanic pile. The locus of mixing, extent of sulphide-sulphate equilibrium, and degree of interaction between the fluid and wall rocks will be important controls on the efficiency and site of gold deposition, and such factors have been used to explain gold enrichment in both modern and ancient seafloor sulphide deposits (e.g., Hannington and Scott, 1989a, b; Large et al., 1989). Boiling is an additional factor that may have a major impact on the nature and efficiency of gold precipitation, but, although the efficiency of gold deposition largely determines whether or not a deposit will be gold-rich, the possibility of gold-enriched source fluids for some deposits cannot be excluded. Some gold-rich seafloor precipitates are characterized by high-sulphidation mineral assemblages in association with advanced argillic alteration and resemble epithermal systems on land. This style of mineralization and alteration is thought to reflect direct input of magmatic volatiles to the hydrothermal fluids, and this input may also be responsible for significant contributions of gold (see "Related deposit types" below).

The above observations suggest that there may be a number of end-member explanations for primary gold enrichment in volcanic-associated sulphide deposits. In the first case, gold enrichment is a consequence of the efficient precipitation of gold from cooling hydrothermal fluids and the continuous hydrothermal reworking of gold into high-grade zones within the sulphide deposits. In the second case, sustained boiling allows for the effective separation of gold from base metals and the deposition of a significantly gold-enriched massive sulphide at the seafloor. The third case is one in which a uniquely gold-rich fluid may be produced by direct contributions from a high-level degassing magma (e.g., a porphyritic subvolcanic intrusion) into the submarine hydrothermal system. When abundant volcanic gases are introduced, a strongly acidic fluid chemistry may evolve which, combined with conditions that are shallow enough for boiling, may promote alteration and mineralization similar to that of subaerial epithermal systems. The proposed conditions that fit this scenario might be those of an emerging (or submerging) volcanic arc (e.g., Fig. 6.4-5). This model is attractive in that it allows for co-existence of gold-rich sulphides with gold-poor varieties, perhaps on the same volcanic edifice but at different water depths.

RELATED DEPOSIT TYPES

Three other distinct classes of gold deposits appear to share many of the attributes of auriferous volcanic-associated sulphide deposits:

1. High sulphidation epithermal Cu-Au and porphyry Cu-Au deposits.

A number of the auriferous volcanic-associated sulphide deposits described above have similarities to high-sulphidation epithermal gold deposits (e.g., acid alteration, a history of boiling, separation of gold and base metals, and possible contributions from magmatic fluids). High-sulphidation epithermal copper-gold deposits, also commonly referred to as being of acid-sulphate-type, alunite-kaolinite-type or enargite-type, are characterized by "high sulphur" mineral assemblages (e.g., enargite-tennantite) and by advanced argillic or acid alteration (e.g., alunite or pyrophyllite common). These conditions are thought to arise from acidic fluids in which SO_2 is contributed directly as a volcanic gas. The associated mineralization is similar to auriferous sulphide deposits in their relative contents of gold, silver, and base metals, although these deposits typically form as subsurface replacements (e.g., in tuffaceous rocks) within subaerial andesitic volcanic complexes. Subaerial examples have also commonly developed above high-level porphyry stocks in a geometric configuration that is virtually identical to that of submarine volcanic-associated massive sulphide deposits and their subvolcanic intrusions (Fig. 6.4-5). In some emerging (or submerging) arc settings, there may be a continuum between subaerial epithermal gold deposits and auriferous submarine massive sulphides, the main variables being water depth and the degree of interaction between evolved seawater and rising magmatic vapours (Hannington, 1993). Recently, a number of high-grade, gold-rich base metal deposits with distinctive epithermal characteristics have been recognized in volcanic arcs of the Pacific Rim. As well, a number of modern analogues of high-sulphidation and Eskay-type deposits may be forming on the modern seafloor in several back-arc basins and submerged volcanic arcs (e.g., Hine Hina vent field, Lau Basin: Herzig et al., 1993; Jade deposit, Okinawa Trough: Halbach et al., 1993).

In some volcanic-associated auriferous sulphide districts, there is a close spatial, and perhaps genetic, relationship between the gold deposits and high-level porphyry systems. The Doyon deposit in the Bousquet district may be an example. Unlike other gold deposits in the area, Doyon possesses most of the features of subvolcanic porphyry gold deposits (e.g., pretectonic stockworks, veins and disseminations in trondhjemite-diorite host). The relationship between subvolcanic intrusions and gold deposits of the type described above is also well illustrated at Mt. Morgan, Australia which has been interpreted to be both a massive sulphide deposit (Taube, 1986 and other authors) and an intrusion-related sulphide replacement deposit (Arnold and Sillitoe, 1989).

2. Disseminated and replacement gold deposits.

Auriferous volcanic-associated sulphide deposits of the type described above also share some characteristics with other disseminated, stockwork, and replacement gold deposits, particularly those that are volcanic-hosted. Deposits such as Hope Brook, Hemlo, and Equity Silver (see subtype 15.4) share moderately aluminous mineral assemblages and comprise mainly disseminated to locally massive sulphides. These deposits occur in moderately to strongly deformed terranes and it may be difficult to distinguish them definitively from other types of sulphide deposits. The absence of distinctive exhalative units and the local primary discordance of the ore zones with respect to stratigraphic units may be important distinguishing criteria.

3. Vein Cu-Au deposits.

The copper-gold deposits of the Chibougamau and Chapais camps are dominantly sulphide-rich veins, many of which are hosted by shear zones in mafic subvolcanic intrusions (i.e., the Dore Lake anorthosite complex and Cummings mafic-ultramafic complex). Although these deposits occur in late tectonic shear zones, the mineralization appears to be close in age to that of the mafic sills and may be partly synvolcanic. In a morphological and compositional sense there is considerable similarity between the sulphide-rich veins at Chapais and Bousquet No. 2. A number of Cu-Zn massive sulphides also occur in the hanging wall volcanic rocks of the Dore Lake anorthosite at Chibougamau (e.g., the Lemoine-Patino that contained 0.75 Mt grading 4.4 g/t Au) and in volcanic rocks adjacent to the Chapais deposit (No. "8-5" zone that contains 50 000 t grading 0.4 g/t Au at the Cooke mine).

EXPLORATION GUIDES

On a regional scale, gold-rich volcanic-associated massive sulphide deposits occur at major lithological contacts that mark distinctive changes in volcanic and sedimentary facies, and that typically host other massive sulphide deposits that may not be particularly gold-rich. The close spatial relationship between deposits of both types at Noranda, Joutel, Bousquet, and Montauban suggest that auriferous deposits may exist in any base metal camp. At the mine scale, the presence of acid alteration and aluminous mineral assemblages in rocks in which they are not normally expected may be a useful exploration guide, as these features are well developed at Bousquet and Boliden. The sulphide contents of many of these deposits are sufficient to produce geophysical responses and, owing to the disseminated to massive nature of the sulphides, induced polarization methods should be the most effective geophysical tools.

SELECTED BIBLIOGRAPHY

References marked with asterisks (*) are considered to be the best sources of general information on this deposit subtype.

Arnold, G.O. and Sillitoe, R.H.
1989: Mount Morgan copper-gold deposit, Queensland, Australia: evidence for an intrusion-related replacement origin; Economic Geology, v. 84, p. 1805-1816.

Barnett, E.S., Hutchinson, R.W., Adamcik, A., and Barnett, R.
1982: Geology of the Agnico-Eagle deposit, Quebec; in Precambrian Sulphide Deposits, (ed.) R.W. Hutchinson, C.D. Spence, and J.M. Franklin; Geological Association of Canada, Special Paper 25, p. 403-426.

Britton, J.M., Blackwell, J.D., and Schroeter, T.G.
1990: #21 Zone deposits, Eskay Creek, northwestern British Columbia; in Exploration in British Columbia 1989, (ed.) B. Grant and J. Newell; British Columbia Geological Survey Branch, p. 197-223.

Grip, E. and Wirstam, A.
1970: The Boliden sulphide deposit; Sveriges Geologiska Undersökning, v. C651, 68 p.

Halbach, P., Pracejus, B., and Marten, A.
1993: Geology and mineralogy of massive sulfide ores from the Central Okinawa Trough, Japan; Economic Geology, v. 88, p. 2210-2225.

Hannington, M.D.
1993: Shallow submarine hydrothermal systems in modern island arc settings; The Gangue, no. 43, p. 6-8.

Hannington, M.D. and Scott, S.D.
*1989a: Gold mineralization in volcanogenic massive sulfides: implications of data from active hydrothermal vents on the modern sea floor; Economic Geology, Monograph 6, p. 491-507.
1989b: Sulfidation equilibria as guides to gold mineralization in volcanogenic massive sulfides: evidence from sulfide mineralogy and the composition of sphalerite; Economic Geology, v. 84, p. 1978-1995.

Hannington, M.D., Herzig, P.M., and Scott, S.D.
1991: Auriferous hydrothermal precipitates on the modern sea floor; in Gold Metallogeny and Exploration, (ed.) R.P. Foster; Blackie, Glasgow and London, p. 249-282.

Herzig, P.M., Hannington, M.D., Fouquet, Y., von Stackelberg, U., and Petersen, S.
1993: Gold-rich polymetallic sulfides from the Lau back arc and implications for the geochemistry of gold in sea-floor hydrothermal systems of the southwest Pacific; Economic Geology, v. 88, p. 2182-2209.

Höy, T.
1991: Volcanic massive sulphide (VMS) deposits in British Columbia; Chapter 5 in Ore Deposits, Tectonics and Metallogeny in the Canadian Cordillera; Ministry of Energy Mines and Petroleum Resources, Paper 1991-4, p. 89-123.

Jourdain, V., Roy, D.W., and Simard, J-M.
1987: Stratigraphy and structural analysis of the North Gold Zone at Montauban-les-mines, Quebec; Canadian Institute of Mining and Metallurgy Bulletin, v. 80, p. 61-66.

Kerr, D. and Gibson, H.L.
1993: A comparison of the Horne volcanogenic massive sulfide deposit and intracauldron deposits of the Mine Sequence, Noranda, Quebec; Economic Geology, v. 88, p. 1419-1442.

Kerr, D.J. and Mason, R.
1990: A reappraisal of the geology and ore deposits of the Horne mine complex at Rouyn-Noranda, Quebec; in The Northwestern Quebec Polymetallic Belt, (ed.) M. Rive, P. Verpaelst, Y. Gagnon, J.-M. Lulin, G. Riverin, and A. Simard; The Canadian Institute of Mining and Metallurgy, Special Volume 43, p. 153-166.

Large, R.R.
1992: Australian volcanic-hosted massive sulfide deposits: features, styles, and genetic models; Economic Geology, v. 87, p. 571-500.

Large, R.R. and Both, R.A.
1980: The volcanogenic sulfide ores at Mt. Chalmers, eastern Queensland; Economic Geology, v. 75, p. 992-1009.

Large, R.R., Huston, D.L., McGoldrick, P.J., McArthur, G., Wallace, D., Carswell, J., Purvis, G., Creelman, R., and Ramsden, A.
1990: Gold in western Tasmania: Australasian Institute of Mining and Metallurgy, Monograph 17, p. 71-82.

Large, R.R., Huston, D.L., McGoldrick, P.J., Ruxton, P.A., and McArthur, G.
1989: Gold distribution and genesis in Australian volcanogenic massive sulfide deposits and their significance for gold transport models; Economic Geology, Monograph 6, p. 520-536.

***Marquis, P., Hubert, C., Brown, A.C., and Rigg, D.M.**
1990a: Overprinting of early, redistributed Fe and Pb-Zn mineralization by late-stage Au-Ag-Cu deposition at the Dumagami mine, Bousquet district, Abitibi greenstone belt, Quebec; Canadian Journal of Earth Sciences, v. 27, p. 1651-1657.
1990b: An evaluation of genetic models for gold deposits of the Bousquet district, Quebec, based on their mineralogic, geochemical, and structural characteristics; Canadian Institute of Mining and Metallurgy, Special Volume 43, p. 383-399.

Marumo, K.
1990: Genesis of kaolin minerals and pyrophyllite in Kuroko deposits of Japan: implications for the origins of the hydrothermal fluids from mineralogical and stable isotope data; Geochimica et Cosmochimica Acta, v. 53, p. 2915-2924.

Morin, G.
1987: Gîtologie de la region Montauban; Ministère de l'Energie et des Ressources, Québec, Report MM-86-02, 59 p.

Rickard, D.
1986: The Skellefte Field; 7th International Association on the Genesis of Ore Deposits Symposium Excursion No. 4, Sveriges Geologiska Undersökning, ser. Ca, v. 62, p. 54.

Roth, T.
1993: Geology and alteration in the 21A zone, Eskay Creek, northwestern British Columbia; MSc. thesis, University of British Columbia, Vancouver, British Columbia, 186 p.

Swan, M.M., Hausen, D.M., and Newell, R.A.
1981: Lithological, structural, chemical and mineralogical patterns in a Precambrian stratiform gold occurrence, Yavapai County, Arizona; in Process Mineralogy, Extractive Mineralogy, Mineral Exploration, and Energy Resources, (ed.) D.M. Hausen and W.C. Park; Proceedings 110th American Institute of Mining, Metallurgical and Petroleum EngineersAnnual Meeting, p. 143-157.

Taube, A.
1986: The Mount Morgan gold-copper mine and environment, Queensland: a volcanogenic massive sulfide deposit associated with penecontemporaneous faulting; Economic Geology, v. 81, p. 1322-1340.
1990: Mount Morgan gold-copper deposit, Queensland, Australia: evidence for an intrusion-related replacement origin - a discussion; Economic Geology, v. 85, p. 1947-1955.

Tourigny, G.
1991: Archean volcanism and sedimentation in the Bousquet gold district, Abitibi greenstone belt, Quebec: implications for stratigraphy and gold concentration - alternative interpretation and reply; Geological Society of America Bulletin, v. 103, p. 1253-1257.

Tourigny, G., Brown, A.C., Hubert, C., and Crepeau, R.
1989: Syn-volcanic and syntectonic gold mineralization at the Bousquet Mine, Abitibi greenstone belt, Quebec; Economic Geology, v. 84, p. 1875-1890.

***Tourigny, G., Doucet, D., and Bourget, A.**
1993: Geology of the Bousquet 2 Mine: an example of a deformed, gold-bearing, polymetallic sulfide deposit; Economic Geology, v. 88, p. 1578-1597.

Valliant, R.L. and Barnett, R.L.
1982: Manganiferous garnet underlying the Bousquet gold orebody, Quebec: metamorphosed manganese sediment as a guide to gold ore; Canadian Journal of Earth Sciences, v. 19, p. 993-1010.

***Valliant, R.L., Barnett, R.L., and Hodder, R.W.**
1983: Aluminous rock and its relation to gold mineralization, Bousquet Mine, Quebec; Canadian Institute of Mining and Metallurgy Bulletin, v. 76, p. 811-819.

Wyman, D.A., Kerrich, R., and Fryer, B.J.
1986: Gold mineralization overprinting iron-formation at the Agnico-Eagle deposit, Quebec, Canada: mineralogical, microstructural and geochemical evidence; in Proceedings of Gold '86, an International Symposium on the Geology of Gold, (ed.) A.J. Macdonald; Toronto, 1986, p. 108-123.

Yamada, R., Suyama, T., and Ogushi, O.
1987: Gold-bearing siliceous ore of the Nurukawa kuroko deposit, Akita Prefecture, Japan; Mining Geology, v. 37, p. 109-118 (in Japanese).

Authors' addresses

J.M. Franklin
Geological Survey of Canada
601 Booth Street
Ottawa, Ontario
K1A 0E8

M.D. Hannington
Geological Survey of Canada
601 Booth Street
Ottawa, Ontario
K1A 0E8

L.J. Hulbert
Geological Survey of Canada
601 Booth Street
Ottawa, Ontario
K1A 0E8

J.W. Lydon
Geological Survey of Canada
601 Booth Street
Ottawa, Ontario
K1A 0E8

K.L. Poulsen
Geological Survey of Canada
601 Booth Street
Ottawa, Ontario
K1A 0E8

Printed in Canada